Understanding the environmental influence of anthropogenic and natural climate forcing on Hamilton Inlet and Lake Melville, Labrador

by

© Nonna Belalov

A thesis submitted to the

School of Graduate Studies

in partial fulfilment of the

requirements for the degree of

Master of *Science*

Environmental Science Program

Memorial University of Newfoundland

August 2016

St. John's Newfoundland

Abstract

Recently, there has been growing interest in the climate variability in Newfoundland and Labrador and its impact on the environment. The warming temperature trend in the past two decades has driven changes in the ice thickness and characteristics of surface inland and coastal ocean waters. In the Hamilton Inlet, these changes are superimposed on the impact of hydroelectric development in Churchill River. Studies of the characteristics of regional climate change and anthropogenic factors are essential for understanding the environmental response. The main objective of this study is to assess the characteristics of climate variability and anthropogenic impact of recent hydroelectric development in Labrador.

The method of the study is based on statistical analysis of observations of atmospheric and river flow characteristics. Decadal shifts in the distributions of the temperature in Newfoundland and Labrador are determined by using Kernel Density estimator. The non-parametric Mann-Kendall trend test and Sen's methods are then applied then to determine the magnitude and significance of the trends.

The first part of the study is focused on characteristics of seasonal, interannual and decadal variability of atmospheric temperature, precipitation, rain, snow and wind speed, and their spatial variations. We found in particular, that the multidecadal trend of atmospheric temperature was negative between 1970 and 1993 and changed to positive in the following period. The magnitude of this trend and its spatial variation across the province is assessed.

The second part of the study presents results from an analysis of extremes of regional climate characteristics. Climate extremes are identified by calculating the

90th/10th percentiles of minimum and maximum daily temperature, which correspond to extreme warm/cold events; the 90th percentile was also calculated for total precipitation, snow and rain, to study extreme precipitation events.

The final part of the study examines the relationship between climate indices and river discharge in Churchill River in Labrador. Here, river discharge volume is analyzed in the context of different climate conditions, before and after hydroelectric development in upper Churchill River.

Acknowledgements

Firstly, I would like to express my gratitude to my advisor, Dr. Entcho Demirov, for his generous support and guidance towards the completion of my thesis. I would also like to thank the professors, staff and colleagues in the Department of Physics and Physical Oceanography and the Department of Environmental Science. My sincere thank you also goes to Dr. Igor Yashayaev, for the continuous encouragement and motivation. I would like to acknowledge the financial support from the Natural Sciences and Engineering Council of Canada (NSERC) and ArcticNet. Finally, I would like to thank my family - my parents Edward and Polina Belalov, and my little brother Baron, for being a constant source of support, guidance and encouragement.

Contents

List of Tables

List of Figures

Chapter 1

Introduction

Anthropogenically driven climate change is one of the global problems of our time, where science is essential for decision making about the future of planetary environmental sustainability. In the past two decades, the earth sciences made significant progress in understanding the observed past climate changes and their causes, scenarios of future climate change, and related risks and impacts on society. Climate studies demonstrated in particular (see [48]) that the rise in anthropogenic CO_2 concentration in the atmosphere since the industrial revolution is a major factor contributing to the climate warming observed in the second half of the past century. The anthropogenically driven changes in ocean, atmosphere and sea-ice characteristics pose challenges to society across Canada and worldwide.

Global Climate change also imposes risks for the planetary environment. In particular, the high atmospheric concentration of CO_2 and intensified air-sea CO_2 exchange contributes to an increase of ocean acidity which can have potentially important implications on biological and biochemical characteristics of the ocean. Understanding

the response of marine ecosystems to variations in physical and biochemical ocean characteristics driven by climate change is essential for understanding the environmental impact of global warming.

The coastal ocean response to climate change involves complex dynamics and interactions of ocean physical, biochemical and biological processes on many time scales from minutes to years and decades. The study of this response is further complicated because of the intensifying anthropogenic stress by the industrial development in coastal areas [5]. The effects of human activities often include soil erosion and sedimentation, over-fishing, drainage and filling of wetlands, eutrophication, and diking or damming for flood control or water diversion [105]. There is a concern that climate warming can potentially interact with this anthropogenic impact and in some cases to amplify it. This thesis focuses specifically on the climate and anthropogenic factors influencing the environment of Newfoundland and Labrador with application to the estuary region of Hamilton Inlet.

1.1 Labrador and Newfoundland - physical geography, inland waters and climate

"God created the earth in six days. On the seventh, He sat back, threw rocks at it and created Labrador." (an old Newfoundland proverb)

Newfoundland and Labrador is the eastern-most province in Canada, located in the country's Atlantic region, from about 46^oN to 60^oN and 67^oW to 52^oW (see Figure 1.1a). Its area is 405,212 km^2, which encompass the island of Newfoundland and mainland Labrador to the northwest. The coast of the province was historically carved by glaciers and continuously modified by exposure to wave action, sea ice, and fluctuating sea levels. The resulting coastline is very irregular and rugged. The shelf is indented with inlets, coves, and bays, many of which house small islands. Coastal elevations range from areas of low relief (i.e. sea level) to steep cliffs exceeding 70 m in height.

Lake Melville (Figure 1.1b) is part of a greater fjord-type estuary system, the Hamilton Inlet on the east coast of Labrador, Canada. The inlet, which consists of Groswater Bay, Lake Melville and Goose Bay, is located at about 54^oN, and between 60.5^oW and 57^oW. Groswater Bay opens to the Labrador shelf; it is approximately 55 km in length. It narrows into a shallow area of 22 km length, 2.8 km width and approximately 30 m depth, known as the Narrows. The Narrows extend to Lake Melville, which is approximately 170 km long, 30 km wide, and has a maximum depth of 180 m. Four major rivers, the Churchill, North West (an extension of the Nauskapi River), Kenamu and Goose rivers, draining a substantial portion of the Ungava Peninsula, enter Lake Melville. The main portion of river discharge comes

from Churchill River and Naskaupi River (via Northwest River), with discharge rates of 56.5 km^3/year and 2.8 km^3/year, respectively. Fresh water is also discharged from the Kenamu River and Goose River, however at much lower rates.

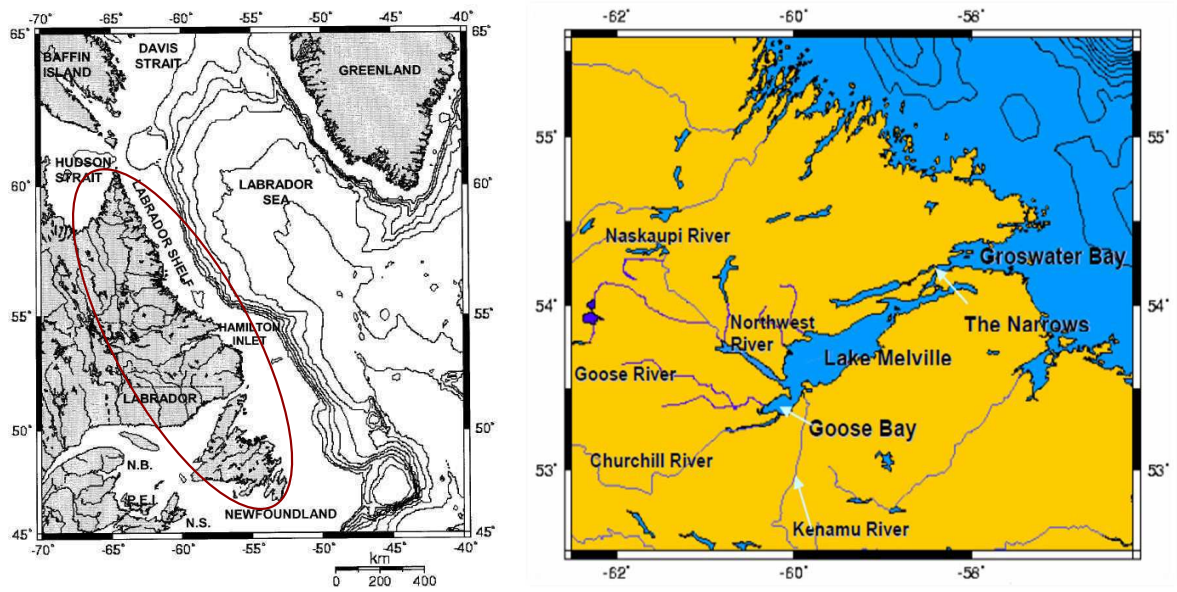

(a) (b)

Figure 1.1: Map of the area of study (a) Newfoundland and Labrador and Labrador Sea; (b) Hamilton Inlet

Newfoundland and Labrador, and the Labrador Sea have typical subarctic climate [77]. The subarctic climate is characterized by long and cold winters and short and cool summers. In winter season, the western coastal region of the Labrador Sea is partly covered by sea-ice whose extension and thickness depends on the severity of the winter cooling in the particular year [25]. Variations in winter surface temperature and precipitation on a synoptic scale over Newfoundland and Labrador are strongly

influenced by the weather disturbances which pass through the region. The storm tracks extend from the US east coast towards the British Isles and Scandinavia, and are associated with strong air-sea exchange of momentum and heat over the SPNA [101]. The position of the storm tracks depends on the phase of the North Atlantic Oscillation, as discussed in Chapter 3. The surface temperature and ocean dynamics over the Labrador Sea shelf additionally contribute the specific characteristics of the local climate of coastal regions of Labrador and Newfoundland [33].

The ocean and atmospheric climate dynamics of the Labrador Sea have important implications for the climate of Labrador and Newfoundland. Some aspects of these dynamics are discussed in in the following two sections.

1.2 The Labrador Sea

The Labrador Sea (Figure 1.1) is a northwestern arm of the North Atlantic Ocean, located between the Labrador Peninsula and Greenland. It is bounded by Davis Strait on the north, a line from Cape St. Francis to Cape Farewell on the East, and the east coast of Newfoundland and Labrador and the northeast limit of the Gulf of St. Lawrence on the west. The Labrador continental shelf is the ocean area with a depth of less than 200 m, and averages 150 km in width. Beyond the continental shelf break of the shelf, lies the continental slope region, rapidly reaching depths of over 3,000 m.

The Grand Banks are relatively shallow underwater plateaus southeast of Newfoundland on the Labrador shelf, ranging from 36 to 185m in depth, and spanning 280,000 km^2. Offshore the Grand Banks is where the cold Labrador Current interacts and mixes with the warm waters of the Gulf Stream. The effects of ocean topography on the dynamics and mixing of these waters bring nutrients to the surface. Consequently, the region is an optimal spawning, nursery and feeding area to a large number of fish and shellfish species, and considered to be among the richest fishing grounds in the world. The mixing of the cold and warm currents also causes fog in the region, which is characteristic of Southeastern Newfoundland.

The Orphan basin lies to north of the Grand Banks. It spans about 160,000 km^2. Positioned on the continental margin of Newfoundland, the Orphan Basin received significant pro-glacial deposits during the late Quaternary period, mostly from ice crossing the continental shelf. The Labrador Current further facilitated the sediment transport, which icebergs and pro-glacial plumes provided from more distant sources.

The dynamics of the basin is similar to that of the Grand Banks, with mean surface temperatures ranging from about -1^{o}C in February and to about 16^{o}C in August. The climate of the region is influenced by weather systems passing through, which trigger high winds and intense buoyancy fluxes.

The Flemish Cap is a region of shallow waters, caused by a wide underwater plateau covering an extended area of 58,000 km^2. The minimum water depth is deeper than the Grand Banks at about 140 m and the average water temperature is generally higher than on the northern Grand Banks. This area is within a region of transition between the cold Labrador Current and warmer Gulf Stream.

The Labrador Sea is an ocean region of intense air-sea exchange of heat, momentum and fresh water. This exchange intensifies during intrusions of cold air masses from continental North America associated with the strong weather disturbances. The buoyancy loss triggered by surface heat and freshwater fluxes drives intense vertical mixing and deep convection in the central Labrador Sea down to depths of about 2000 m (see [68]). This deep convection forms a dense intermediate water mass, the Labrador Sea Water, which then spreads out of the Labrador Sea.

The general ocean circulation of the Labrador Sea is comprised of intense cyclonic boundary current and relatively weak flow in its central part (see [68]). The boundary current in the Labrador Sea consists of three major current systems: the Irminger Current, West Greenland Current, and Labrador Current (see Figure 1.2). The Irminger Current travels at intermediate depths between 500 m and 1000 m along the Greenland Coast, transporting relatively warm and salty Irminger Sea Water (ISW - see Figure 1.2) through the Labrador Sea. The Irminger Current and the ISW originate from the North Atlantic Current which is the northeastward extension

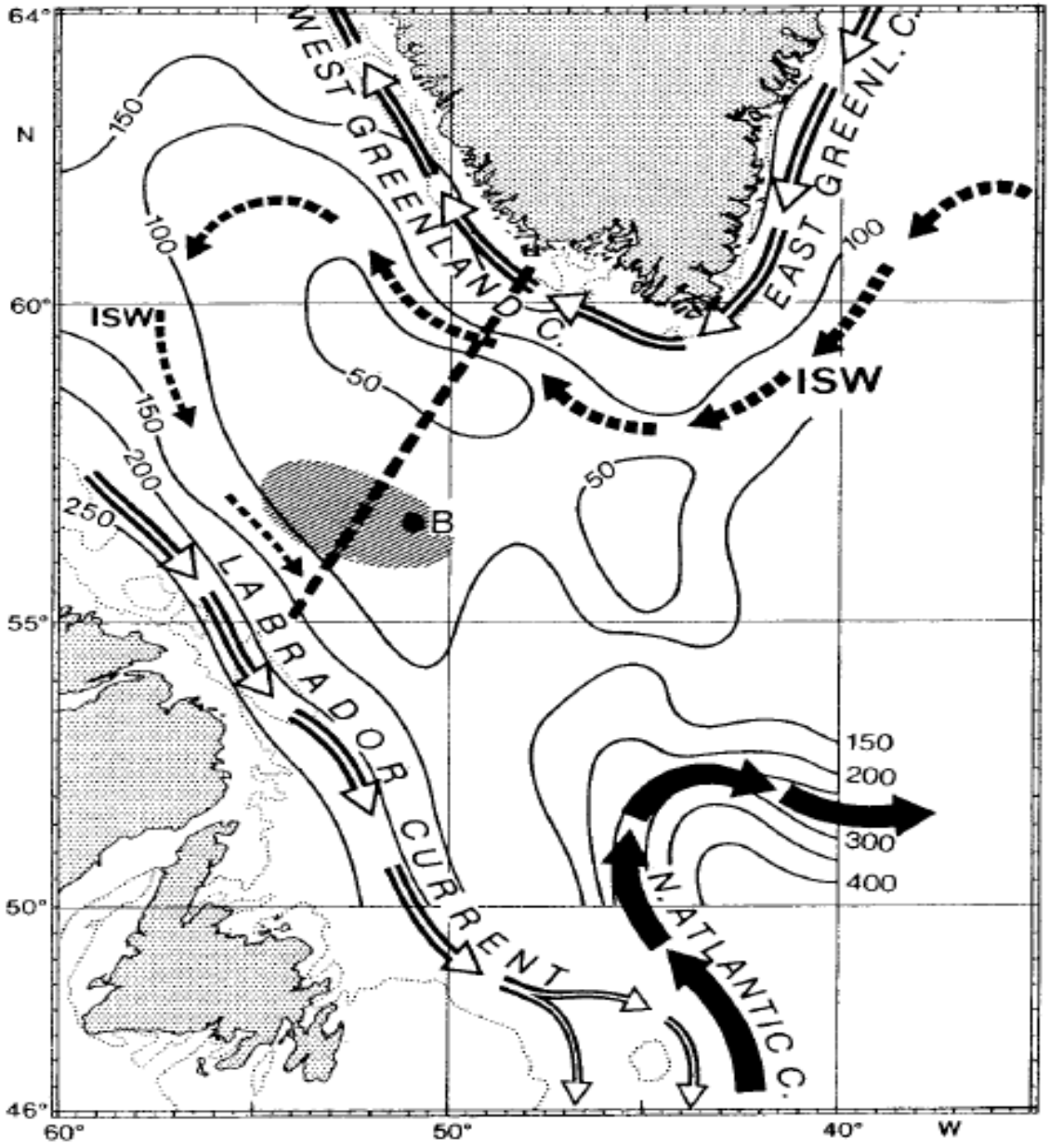

Figure 1.2: Cyclonic circulation of Labrador Sea currents, with the typical early winter depth of 27.6 isopycnal. Solid arrows depict the warm and salty water of the North Atlantic Current, the Irminger Sea Water (ISW) is depicted by dashed arrows, and the near surface, cold and fresh East/West Greenland and Labrador Currents are depicted by open arrows. (Adapted from [67]).

of the Northern branch of the Gulf Stream (see [53]). The Irminger Current flows cyclonically at intermediate depths along the shelf slope of the Labrador and brings ISW to the northernmost part of the basin. The warm and salty ISW is partly transported towards the interior region of Labrador Sea by large eddies called the Irminger Rings. They form due to instability of the Irminger Current along the shelf slope and off the coast of Greenland. They contribute to the restratification of the LSW in spring and summer seasons. The LSW contributes to the lower limb of AMOC which brings cold and fresh waters into the subtropical North Atlantic. Beyond the LSW, this cold component of the AMOC includes the Gibbs Fracture Zone Water (GFZW), and the Denmark Strait Overflow Water (DSOW). Unique physical and chemical properties of these water masses distinguish themselves, which can be derived from vertical sections in the Labrador Sea [108].

The West Greenland Current and Labrador Current are narrow (approximately 100 km) and strong (approximately 40 cm/s at the surface) which travel along the coast of the Labrador Sea (see [53],[54],[13]). The West Greenland Current transports surface low-salinity and cold waters of Arctic Origin northward along the coast of Greenland. The Labrador Current (LC) forms (see [24],[52]) from mixing of the cold southward moving Baffin Land Current, the relatively warm West Greenland waters and the outflow of low salinity waters from Hudson Bay and Fox Basin (see [49]). In western Labrador Sea, the LC develops as a strong barotropic flow which has two branches, one on the shelf slope (300 - 2500 m in isobaths) and the second in the deep part (2500 - 3300 m in isobaths). The volume transport in these two branches are estimated to be 3 Sv and 16 Sv, respectively. [22] found that the nutrients in the LC waters influence the processes of primary production on the Labrador Shelf.

These authors concluded, in particular, that production on the southern part of the Labrador shelf is more supported by the local upwelling, while nutrient concentrations were elevated in the northern shelf due to transport in the LC. The western Labrador shelf is covered with ice seven to ten months of the year. The fjords, bays and a narrow coastal zone are bound in land-fast ice, while pack ice extends 150 - 225 km offshore.

The icebergs which separate from Greenland are initially carried by the West Greenland Current north of 60-70 N and into Baffin Bay [73]. These icebergs are transported southward by the LC, where they are either recirculated within the Labrador Sea or end up melting in the vicinity of the North Atlantic shipping lanes.

Approximately 80% of the flow of the LC on the Labrador shelf is concentrated between the 600 - 800 m in isobaths. This strong flow is parallel to the bathymetry and the shelf slope in this area acts as a barrier for it [53]. The surface heat flux over the Labrador shelf in the summer is positive and dominated by the solar radiation. In winter the net cooling is mainly due to heat loss through turbulent exchange with the cold atmosphere (see [59]). After the cold season a cold intermediate layer water mass (CIL), forms on the shelf during late spring to the fall. This water layer is relatively cold and fresh, and remains isolated from the warmer and saltier water of the continental slope by a frontal region denoted by a strong horizontal temperature and salinity gradients near the edge of the shelf (see [13]).

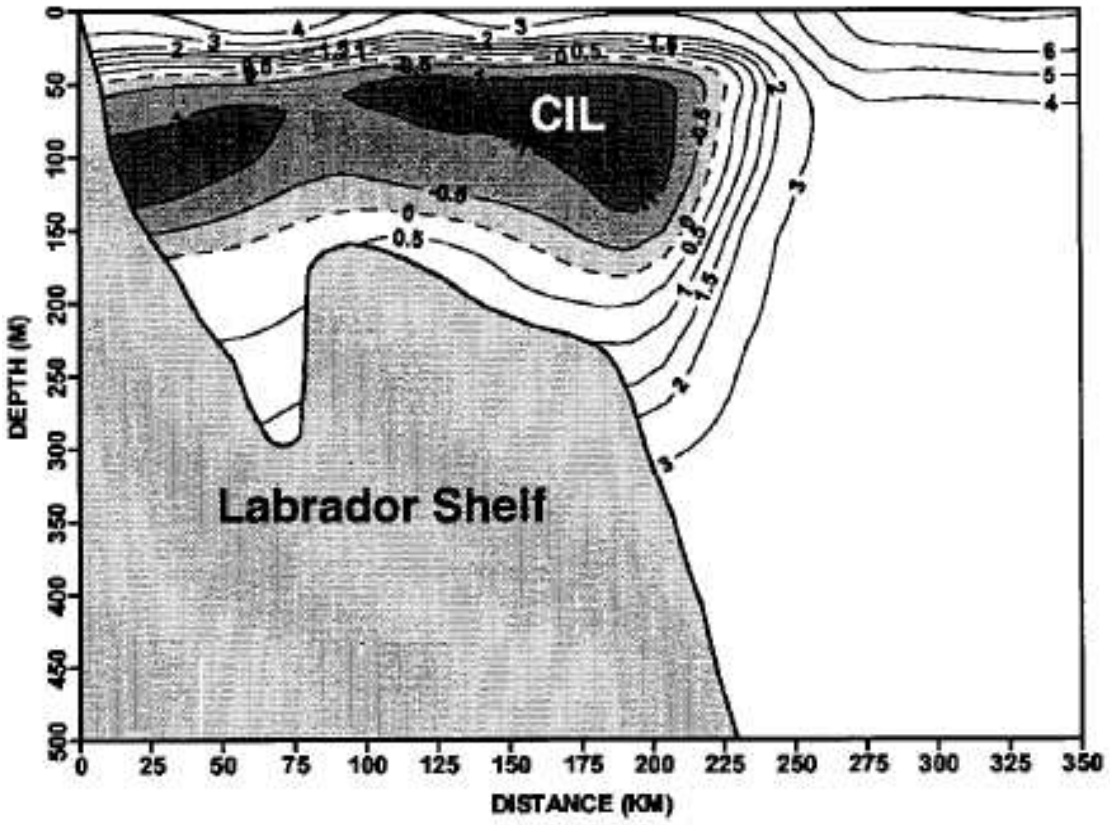

Figure 1.3: Temperature contours along Seal Island, showing the cold intermediate layer (CIL) water in July 2001. (Adapted from [13]).

1.3 The North Atlantic Oscillation and climate variability of the Sub-polar North Atlantic

The interannual and decadal variations in the regional climate of the Sub-polar North Atlantic (SPNA) are dominated by the North Atlantic Oscillation (NAO). The NAO is an atmospheric phenomenon related to the dynamics of the mean atmospheric circulation [95] in the Northern Hemisphere that exhibits natural variability on time scales from sub-seasonal to interannual and decadal [46]. The NAO represents redistribution of air masses between the Arctic and Sub-polar North Atlantic atmospheres, which relates to the strength, frequency, intensity, and paths of storms passing across the North Atlantic ocean with strong implications for the wind speed and the zonal heat and moisture transport between the continents and the oceans [47]. The NAO phase and intensity is measured by the NAO index which is defined as the sea level pressure difference between Iceland and the Azores. The variations in the NAO index are associated with the dynamics of the extratropical jet stream (see Figure 1.4) which approximately follows the path of the major weather disturbances. A positive phase of the NAO index is associated with a shift of the major extra-tropical storm tracks across the North Atlantic. The paths of weather disturbances tend northward (southward) of their climatological positions for positive (negative) NAO. The storm tracks during positive NAO are also tilted in southwestern to northeastern direction which is not observed during periods of negative NAO [98]. A high positive NAO index is associated with stronger than normal westerlies in mid-latitudes and intense and more frequent winter storms over the Labrador Sea. The storm tracks extend from the US east coast towards the British Isles and Scandinavia, and are associ-

ated with strong air-sea exchange of momentum and heat over the SPNA [101]. The negative NAO index is associated with warmer than normal weather and relatively fewer storms passing over the Labrador Sea [101]. This NAO related atmospheric variability is a dominant forcing for the long term variations in the SPNA water mass characteristics and circulation (see [19], [18]). The processes which trigger this variability as well as the ocean response are inherently multiscale and involve variability at all time scales from sub-seasonal to interannual and decadal. [46] rebuked the notion that the persistence of the low frequency NAO index on interannual and decadal time scales implies that the NAO persists in the same phase for long periods. Rather, they found that NAO is highly variable, changing its phase at all time scales, and its longer-term time-average behavior reflects the combined effect of residence time in any given phase and its amplitude therein.

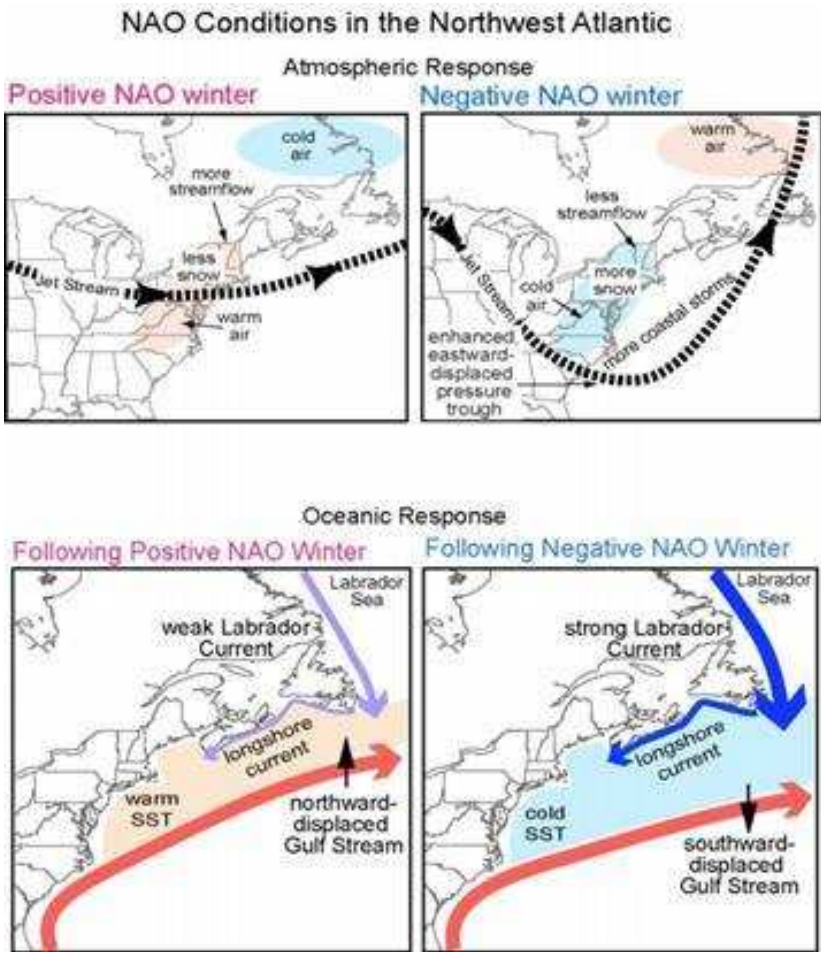

Figure 1.4: Atmospheric and Oceanic response to the NAO. (Adapted from NOAA Airmap, http://airmap.unh.edu/background/nao.html).

1.4 The Hamilton Inlet

While estuaries and continental shelf areas comprise only 5.2% of the earth's surface, and only 2% of the ocean's volume, the coasts of estuaries are among the most heavily populated areas of the world [57]. In the developing world, many estuaries are affected by factors like deforestation, intensified soil erosion and sedimentation, poor farming practices, overfishing, drainage and filling of wetlands, eutrophication, and diking or damming for flood control or water diversion [105]. In particular, the increased soil erosion, resulting from deforestation, poor farming practices and mining, leads to increased sediment loads in estuaries by a factor of 10. As a result, some shorelines change from sandy to muddy. Increased muddiness and turbidity degrades estuarine ecosystems by decreasing the amount of light available for photosynthesis. In many coastal estuaries light attenuation by suspended sediments confines the photic zone to a small fraction of the water column, such that light limitation is a major control on phytoplankton production and turnover rate [10]. The discharge of water into estuaries introduces pollutants from industrial plants and human activities, which propagate downstream or settle in sediments. Estuaries tend to be naturally eutrophic because land runoff discharges nutrients into them. Excess oxygen-depleting chemicals in the water can lead to hypoxia and the creation of dead zones. This can result in reductions in water quality, fish, and other animal populations.

An estuary is characterized as a semi-enclosed coastal area, draining one or more rivers and connected to the open sea. As such, they are subject to influence from the adjacent riverine environment, such as fresh water and sediment input, as well as influence from the open sea, such as tides, waves, and saline water inflow. Conse-

quently, estuarine water is stratified, due to the vertical and horizontal salinity and density gradients caused by the interaction of fresh riverine water and saline ocean water. Estuarine water circulation is dictated by the interaction of freshwater and salt water, as well as tides, wind, and bottom topography. Saline water is denser than fresh water; thus fresh water flowing into the open ocean occupies the upper layer, whereas incoming ocean water sinks to the bottom of the basin (Figure 1.5). The strong stratification resists the exchange of momentum and reduces the vertical mixing. Mixing and entrainment between layers is often the result of internal waves. The influx of fresh water causes further stratification, while vertical mixing due to wind minimizes it; both these factors influence the residence time of estuarine water, and are thus key to estuarine health. Residence time refers to the amount of time water particles remain within the estuary. Naturally, longer residence times allow for nutrient and dissolved oxygen depletion, as well as algal blooms, and are therefore detrimental to estuarine productivity. Conversely, a more frequently flushed estuary with shorter residence time is indicative of a healthier ecosystem. However, residence time is not an independent variable in estuarine circulation, but is rather governed by vertical mixing and therefore the degree of stratification. As aforementioned, vertical mixing decreases the salinity and temperature gradient with depth; whether it occurs at the surface due to wind stress, internally due to tides and waves, or induced by turbulence at the boundary between the estuary and ocean.

Due to the relatively shallow depth, the biological productivity in estaurine regions is highly sensitive to the external stress due to the climate change and anthropogenic impacts. The impact of climate change on estuarine regions has a character that depends on the nature of local climate change and the local geomorphological, bio-

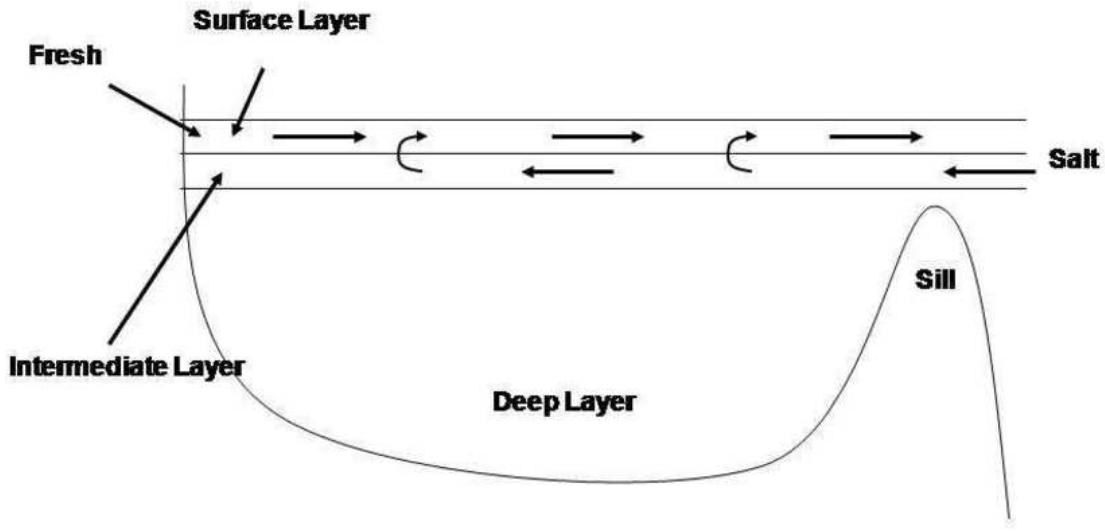

Figure 1.5: Circulation in a fjord-type estuary. Fjords are examples of highly stratified estuaries; they are silled basins that have freshwater inflow that greatly exceeds evaporation. Oceanic water is imported in an intermediate layer and mixes with the freshwater. Mixing and entrainment between layers is often the result of internal waves. The resulting brackish water is then exported into the surface layer. A slow import of seawater may flow over the sill and sink to the bottom of the fjord (deep layer), where the water remains stagnant until flushed by an occasional storm. (Adapted from [105]).

geochemical, ecological and social factors that affect the sensitivity to climate [74]. Long term climate change related decrease or increase in precipitation could also affect the salinity of coastal waters. Droughts reduce fresh water input into tidal rivers and bays, which raises salinity in estuaries, and enables salt water to mix farther upstream [9].

Studies in many geographical regions around the world demonstrated that construction of power generating facilities and erection of control structures can potentially alter the environment, and the extent of these consequences often goes beyond the immediate surroundings [17]. For example, construction of a dam on the Dnieper river, which flows into the Black Sea, caused a significant change to the pattern of seasonal discharge, similar to that in the Hamilton Inlet [97]. Spring discharge rate was reduced and became sporadic through out the year. This resulted in a 3.8 billion dollar loss to the fishery industry. The productivity of a fishery is tied to the health and functioning of the ecosystems on which it depends for nutrients and habitat. Reduced thermal movement of the water also affects water quality by allowing pollutants to accumulate in upper layers of the water and has led to increased levels of mercury and other contaminants in fish. It is worthy to note that concerns over mercury levels in fish were also raised following the impoundment of the Smallwood reservoir (Figure 1.6) in Labrador. The high Mercury levels persisted over 20 years after impoundment [1].

The industrial development in estuarine regions of Atlantic Canada intensified in recent several decades, imposing increasing anthropogenic stress on the marine environment. In particular, Labrador became a major center of hydropower production in Eastern Canada. More than 80 percent of new constructions are run-of-rivers (mostly

Figure 1.6: A spillway on the Smallwood Reservoir. This one is used to vent exess water from the reservoir while other similar structures are also used to manage levels throughout the reservoir. (Adapted from Ryan Arthurs, http://lureoflabrador.blogspot.ca/2012/03/smallwood-reservoir.html).

concentrated in the Western part) while most storage hydro projects are located in the Eastern region. The demand for renewable and clean energy is growing, thus the development of hydroelectric power plants is of high priority. Currently there exists one hydroelectric generating station at Churchill Falls, which was completed in 1971. No dam was constructed; rather, strategically placed dykes regulate the flow of water discharge, while hundreds of existing lakes and bogs in central Labrador were linked to form the Smallwood reservoir. Consequently, this altered the flow of the Churchill River into Lake Melville. A portion of the Churchill River was diverted along a series of lakes parallel to the original riverbed in order to supply water to the power plant, descending 300 m [6]. Water is released from the Smallwood reservoir through control structures, and excess is released through the Jacopie spillway and allowed to flow along the original route. Construction of dykes at Orma and Sail lakes increased the drainage area into the Hamilton Inlet by 11,400 km^2. These dykes divert water from the Naskaupi and Kanairiktok rivers. While Naskaupi river naturally flows into Lake Melville, Kanairiktok river does not. Consequently, diverting water from the Kanairiktok river increased the total amount of freshwater into Lake Melville [6]. Increased freshwater input can potentially alter the circulation dynamics in Lake Melville and therefore the coastal ecosystem.

The examples of anthropogenic impact on the estuary regions in other geographical locations suggest that the recent changes in the freshwater inflow into Lake Melville could influence the dynamics and ecosystem of the lake [6]. Furthermore, this influence can interfere with the impact of climate dynamics and especially in the changes of atmospheric temperature and precipitation. Studies of the anthropogenic effects and recent variations of climate characteristics are essential fur understanding the

changes in external forcing on Lake Melville and the response of its environment. This thesis presents results about the characteristics of climate change and anthropogenic stress to Lake Melville based on observations for the past fifty years. These results contributed to two research projects about Lake Melville response to human induced stress and climate change: (1) Understanding and Responding to the Effects of Climate Change and Modernization in Nunatsiavut, ArcticNet [88] and (2) Lake Melville: Avativut, Kanuittailinnivut (Our Environment, Our Health) [89].

1.5 Objectives

The Upper Churchill Development was accompanied by discussions in the scientific community for its potential alteration to the environment. Although the change in the environment triggered by this development is far from being understood, there are some indications that suggest that there are certain shifts in the ecosystem as a result of Upper Churchill. The northern Atlantic cod fishery, for example, suffered a sever decline in Groswater Bay and Sandwich Bay at the same time as the floe of the Churchill River was altered [84].

Presently, the Lower Churchill Hydroelectric Generation Project is underway. The Project plan is to build hydroelectric generating facilities at Gull Island and Muskrat Falls, and interconnecting transmission lines to the existing Labrador grid. The Gull Island facility will consist of a generating station with a capacity of approximately 2,000 MW, while the Muskrat Falls facility will consist of a generating station that will be approximately 800 MW in capacity.

Understanding the response of the marine environment to these developments

and global warming is essential to the understanding and prediction of future environmental changes that may potentially affect living conditions, off-shore and the fishing industry in the coastal ocean regions of Canada. The focus of this thesis is specifically on studying of past climate variability of Labrador and Newfoundland on interannual, decadal and multidecadal time scales and the impacts that these variations in the regional climate together with the human induced variations in the river discharge have on the physical processes in the Lake Melville estuary. The major objectives of the study are:

(1) to assess the major characteristics of seasonal, interannual, decadal and multidecadal climate changes in Labrador and Newfoundland in the past fifty years. The study focuses specifically on seasonal variations in atmospheric temperature, wind speed and precipitation, dominant periods and magnitude of interannual variability and decadal trends;

(2) to study the spatial variations in extremes of temperature and precipitation across the province and their decadal changes;

(3) To evaluate the variations in the river discharge to Lake Melville in the past fifty years and their link to climate change and anthropogenic impact.

1.6 Organization

Chapter two presents the data and method of the study. Chapter Three describes seasonal, interannual and decadal variations in atmospheric characteristics in Labrador and Newfoundland. Chapter Four presents an analysis of multidecadal trends and extremes. The impact of Upper Churchill on the river discharge into Lake Melville is

discussed in Chapter Five. The last chapter presents conclusions.

Chapter 2

Data and Methods

The data used in this study include atmospheric and river flow observations from stationary observational facilities of Environment Canada in Labrador and Newfoundland.

2.1 Atmospheric Observations

The atmospheric data include temperature, wind speed and precipitation observations. Our preliminary analysis (not shown here) demonstrated that the original, raw hourly data of temperature, precipitation and wind speed from the Canadian Climate Archive of Environment Canada include some inhomogeneities associated with variations of some non-climatic factors, such as changes in instrumentation, changes in local site condition and environment, changes in observing practices and observing time. These inhomogeneities do not allow proper assessment of climate trends and extremes. For this reason, surface observations of daily mean, maximum and minimum temperature, as well as total precipitation, snow and rain were studied based on data

from the Adjusted and Homogenized Canadian Climate Data archive (AHCCD). The AHCCD is maintained by Environment Canada, and offers data from select climate stations in which inhomogeneities associated with non-climate influences have been removed. Fourteen AHCCD locations were used in this study (Figure 3.3b).

Stations were chosen based on the availability, quality and reliability of data. Sixty two years of temperature, precipitation, rain, snow and wind speed data were analyzed, depending on availability. Stations with insufficient historical data for some of the parameters were discarded in the analysis of this parameter. Furthermore, years where data for more than four consecutive months were missing or were inadequate are not included in the calculations of annual mean characteristics. It should be noted that data quality in stations in Northern Labrador (Nain and Hopedale) were neither ideal nor complete due to gaps in the available data sets; however, due to the lack of meteorological stations at higher latitudes, data from these stations was used where possible. The analysis of seasonal cycles of atmospheric parameters is done for winter (DJF), spring (MAM), summer (JJA) and autumn (SON). The correlation with the NAO is assessed for atmospheric characteristics for the long winter season (DJFM).

Wind speed data was also obtained from the AHCCD; monthly means of daily wind speed were analyzed rather than daily wind speed, as this was the highest frequency data set available.

2.2 River flow data

Flowing into Lake Melville in central Labrador are the largest rivers in Labrador, the Churchill and the Naskaupi. During 1971, about 50% of the Naskaupi River, including

Lake Michikamau, was diverted into the Churchill River system for generation of hydroelectricity. Other large rivers entering Lake Melville are the Crooked, Beaver, and Goose, all of which drain the huge, barren plateau of western Labrador. The Kenamu, Kenemich, and English rivers drain the Mealy Mountains which lie south of Lake Melville. North of Lake Melville, the Kanairiktok, Adlatok, and Kogaluk rivers all have drainage areas greater than 5000 km^2. This combined with sharp drops in land elevation occurring near the mouths of these rivers produces high water velocities with numerous falls and rapids. The headwaters of Kanairiktok River have also been diverted into the Smallwood Reservoir prior to 1971.

Daily data for river discharge volume in m^3/s into Lake Melville is available between the years 1954 and 2010 for Churchill River at a site located above Muskrat Falls. This research focused on a comparative analysis between pre- and post-construction river flow into the Lake Melville estuary.

Firstly, the anthropogenic impacts on the seasonal cycle of discharge volume was studied by plotting the seasonal cycle of river discharge prior to and after 1971. While analyzing the daily discharge volume, it was apparent that an adjustment period of approximately a decade took place in altering the seasonal cycle, and the changes did not take place at once. Consequently, histograms were plotted for river discharge volume data for the following periods: 1954-1971, 1971-1980 and 1981-2010. All three histograms were integrated to 1, in order to account for the different number of days in the three sub-periods.

Secondly, the relationship between river discharge volume and precipitation and temperature was studied by plotting the discharge volume against (a) warm, (b) cold, (c) wet and (d) dry years before and after alteration to the river discharge.

2.3 Methods of analysis of atmospheric data

The goal of the analysis of atmospheric observations presented in this thesis is the assessment of characteristics of climate variability in Newfoundland and Labrador. The globally averaged surface atmospheric temperature since 1951 shows a warming trend of about 0.12^oC per decade [48]. Regionally, this trend is superimposed on the variability on interannual, decadal, multidecadal, and interdacadal time scales. These shorter scale variations are normally triggered by natural variability and may have different sign and magnitude from region to region. An example of spatial variability of decadal tendencies of temperature is the general cooling trend on the decadal scale of the Sub-polar North Atlantic in the late 1980s and early 1990s [41]. During the same period the Global Ocean Heat content increased with a rate of 0.4×10^{22} J/yr [56].

The analysis of seasonal, interannual, and decadal variability presented in this thesis is based on seasonal mean characteristics and anomalies. The estimation of longer term multidecadal trends requires more attention because of their relatively small magnitude compared to interannual and decadal variations. These trends also can be expected to change sign over the period of study - from 1951 to 2012. To achieve an accurate estimate of the multidecadal trends, a two step method was applied for each station: (1) find the periods of negative and/or positive trend for each station; (2) assessment of the magnitude and sign of the trend and their statistical significance.

2.3.1 Assessment of multidecadal trends

Step 1: The periods of negative and/or positive multidecadal trends are found by using the so called method of Cumulative Sum (CS) (see [31], [94], [96]). The cumulative sum is defined as a sum of anomalies.

$$CS(n) = \sum_{i=1}^{n} (x_i - \overline{x}) \tag{2.1}$$

where $\overline{x}$ is the long term mean. A segment of the CS(n) curve with an upward slope indicates a period where the values tend to be above average. Likewise a segment with a downward slope indicates a period of time where the values tend to be below the average.

Step 2: The magnitude and sign of the trends are then estimated by using the Mann-Kendall test. Trends were assessed by first calculating temperature anomalies. The Mann-Kendall test was subsequently applied to the calculated anomalies, to identify the presence of long-term trends of precipitation and temperature series in Newfoundland and Labrador.

The Mann-Kendall (MK) test [64], [50], [36] is used to statistically assess the presence of a monotonic upward or downward trend. In this study, it is applied to temperature and precipitation anomalies. A monotonic upward (downward) trend indicates that the variable in question consistently increases (decreases) through time. An important advantage of the MK test is that it is non-parametric and the residuals from the fit need not be normally distributed. Conversely, the often used method of regression analysis requires that the residuals from the fitted regression line be normally distributed. Furthermore, the test capacity is resilient to missing values and values that fall outside the detection limit, skewed distribution [58], [72], and is

more powerful than the equivalent parametric methods. The MK test is a standard recommended by the World Meteorological Organization to assess the monotonic trend in hydro-meteorological time-series.

The original MK test, however, does not account for the serial correlation that very often exists in a climatological time series [40] [110] [72]. The presence of serial correlation in a data set may lead to a misleading interpretation of the results, because it enhances the probability of finding a significant trend when none exits. In order to avoid this drawback of the method, we adopted a modified versions of the MK test based on so called Sen's Method [36] which proved to be suitable for analysis of data with significant auto-correlation [44].

The MK tests for the null hypothesis of trend absence in the vector V, against the alternative of a trend. The result of the test is returned in H = 1 indicates a rejection of the null hypothesis at the alpha significance level. H = 0 indicates a failure to reject the null hypothesis at the alpha significance level. In this study, alpha was set to 5%. If the p-value of a test is less than alpha, the test rejects the null hypothesis. If the p-value is greater than alpha, there is insufficient evidence to reject the null hypothesis.

The original Mann-Kendall test is a rank correlation test for two sets of observations between the rank of the values and the ordered values in the data-set (Mann, 1945; Kendall, 1975). The data set $(x_1, ..., x_n)$ is assumed to be independent and identically distributed [109]. Then the Kendall's Tau is calculated as follows:

(i) Determine the sign of all $n(n-1)/2$ possible differences $x_j - x_k$, where $j > k$. These differences are $x_2 - x_1, x_3 - x_1, ..., x_n - x_1, x_3 - x_2, x_4 - x_2, ..., x_n - x_{n-1}, x_n - x_{n-1}$.

(ii) Calculate the variance S using the equation of Kendall [50]:

$$S = \sum_{k-1}^{n-1} \sum_{j-k+1}^{n} sign(x_j - \overline{x}) \tag{2.2}$$

For positive (negative) values of S, observations obtained later in time tend to be larger (smaller) than observations made earlier.

(iii) Calculate the variance of S using the method outlined in Gilbert ([36]). This method is used for VAR(S) computations where n

$$VAR(S) = \frac{1}{18}\left[n(n-1)(2n+5) - \sum_{p-1}^{g} t_p(t_p-1)(2t_p+5)\right] \tag{2.3}$$

g represents the number of tied groups and t_p is the number of observations in the p^{th} group.

When there are ties in the data due to equal values or non-detects, VAR(S) is adjusted by a tie correction method described in Helsel [43].

(iv) Calculate the standardized test statistic Z_{MK}:

$$Z_{MK} = \begin{cases} \frac{S-1}{\sqrt{VAR(S)}} & if \quad S < 0 \\ = 0 & if \quad S = 0 \\ = \frac{S+1}{\sqrt{VAR(S)}} & if \quad S > 0 \end{cases}$$

A positive (negative) value of Z_{MK} indicates that the direction of trend is upward (downward). The computed Z_{MK} is then compared to the standard normal variate at a chosen level of statistical significance ($alpha$) in order to prove/disprove the null hypothesis.

The Mann-Kendall statistical test has been frequently used to quantify the significance of trends in hydro-meteorological time series [21] [109] [76] [69] [91] [92].

The Sen's slope estimator, often referred to as the TheilSen estimator, is a method for robust linear regression that chooses the median slope among all lines through pairs of two-dimensional sample points. The Sen's slope estimator is a non-parametric statistic, which calculates the magnitude of any significant trends found in a given data set [85] which is done by using the following algorithm:

$$Q_i = \frac{X_j - X_k}{j - k} \quad for \quad i = 1, ..., N$$

where X_j and X_k are the data values at times j and k $j > k$, respectively.

If there is only one datum in each time period, then

$$N = n\frac{n-1}{2}$$

where n is the number of time periods. If there are multiple observations in one or more time periods, then

$$N < n\frac{n-1}{2}$$

where n is the total number of observations.

The N values of Q_i are ranked from smallest to largest and the median of slope or Sen's slope estimator is computed as,

$$Q_{med} = \begin{cases} Q_{\frac{N+1}{2}} & if \quad N \quad is \quad odd \\ Q_{\frac{N}{2}} + Q_{\frac{N+2}{2}} & if \quad N \quad is \quad even \end{cases}$$

The Q_{med} sign reflects data trend reflection, while its value indicates the steepness of the trend. To determine whether the median slope is statistically different than zero, one should obtain the confidence interval of Q_{med} at a specific probability.

The confidence interval about the time slope [45] [36] can be computed as follows:

$$C_\alpha = Z_{1-\frac{\alpha}{2}}\sqrt{VAR(S)}$$

where Var(S) is defined in as in the Mann-Kendall test and $Z_{1-\frac{\alpha}{2}}$ is obtained from the standard normal distribution table. In this study, the confidence interval was computed at the $\alpha = 0.05$ significance level.

2.3.2 Extremes

The Kernel density estimator was used to analyze decadal and interdecadal temperature variability. It is a nonparametric estimate of the probability density function of a random variable, in this study, temperature. The formula is given by

$$\hat{f}_h(x) = \frac{1}{nh}\sum_{i=1}^{n} K\left(\frac{x - x_i}{h}\right) \quad ; \quad -\infty < x < \infty$$

where n is the sample size, the kernel $K(\cdot)$ is a smoothing function, and h is the bandwidth.

The kernel smoothing function defines the shape of the curve used to generate the pdf. It is similar to a histogram, as it builds a function to represent the probability distribution using the sample data. Unlike a histogram however, which places the values into discrete bins, a kernel distribution sums the component smoothing functions for each data value to produce a smooth, continuous probability curve.

In this study, Kernel Density distributions of minimum and maximum daily temperature data were analyzed in order to infer information about long term shifts in extreme temperature. Decadal and bi-decadal plots were constructed for each station and studied.

The extreme warm/cold temperature was calculated as the $90th/10th$ percentile of temperature distribution. Similarly, extreme precipitation was calculated as the $90th$ percentile of the precipitation distribution. Heavy precipitation was considered equal to or greater than 10 mm of daily precipitation. The $90th$ percentile of daily maximum and minimum temperature and precipitation is defined as the upper threshold; conversely, the $10th$ percentile of maximum and minimum daily temperature is defined as the lower threshold.

The number of days with temperature and/or precipitation which surpassed the extreme threshold was calculated for daily maximum and minimum temperature data, and for precipitation. Moreover, the number of days with extreme cold temperature, i.e temperature below the lower extreme threshold, was calculated for maximum and minimum daily temperature data.

Lastly, parameters of extreme temperature and precipitation were analyzed on an inter-annual scale, in addition to the decadal and bi-decadal time scales discussed above. The number of days above/below the upper/lower threshold of daily minimum and maximum temperature were analyzed. Number of days with extreme precipitation, heavy precipitation and number of consecutive days without any precipitation were also calculated and analyzed. Finally, the number of days with extreme precipitation, as well as snow and rain are reported in chapter 4.

Chapter 3

Climate of Newfoundland and Labrador coastal regions

This chapter presents results from an analysis of atmospheric characteristics observed in the past fifty years over Labrador and Newfoundland. Three major characteristics are studied - the near surface atmospheric temperature, wind speed and precipitation. These characteristics are of interest for understanding the dynamical response of inland waters and the coastal ocean to atmospheric climate change as they determine the intensity of surface air-water exchange of momentum, heat and freshwater. The seasonal, interannual and decadal changes in atmospheric temperature, precipitation and wind speed are discussed in this chapter.

One question which is addressed in this chapter is how the large-scale variations in the atmospheric climate, ocean circulation, water and sea-ice characteristics of the Northern Hemisphere influence the climate of Newfoundland and Labrador. Previously [33] found that the North Atlantic Oscillation in the atmosphere and the

Atlantic Ocean Multidecadal Oscillation are the dominant factors influencing the atmospheric climate dynamics in the Sub-polar North Atlantic (SPNA). Our analysis addresses the related question: how the influence of large scale oceanic and atmospheric variability on the regional climate varies geographically across the province and how it is modulated locally by the regional orography, coastline geometry, and the presence of inland waters.

3.1 Impact of large scale atmospheric dynamics on the climate variability of the Subpolar North Atlantic

The North Atlantic Oscillation (NAO) is the dominant mode of atmospheric climate dynamics in the Northern Hemisphere. Although the NAO phase and intensity varies on subseasonal time scales, the past observations exhibit a tendency of NAO to remain in one phase for intervals lasting from several years to decades. These trends influence the climate of the Northern Hemisphere, with direct impacts on mean storm tracks and regional temperature, precipitation, and wind. The NAO related changes in surface temperature, precipitation and storminess, have important impact on both marine and terrestrial ecosystems, and consequently on human activities as well [47].

The phase and intensity of NAO are quantified by the NAO index (see [47]). The NAO index is calculated as a difference in normalized Sea Level Pressure (SLP) between Iceland and the Azores (see Figure 3.1) or as the dominant Principle Component (PC) of the SLP over the North Atlantic [47]. It is indicative of the position

of the jet stream which coincides approximately with the extra-tropical storm tracks across the North Atlantic. Depending on the sign of the NAO, the paths of weather disturbances tend northward of their climatological positions for positive NAO or southward for negative NAO. The storm tracks during positive NAO are also tilted in a southwestern to northeastern direction, which is not observed during periods of negative NAO [98].

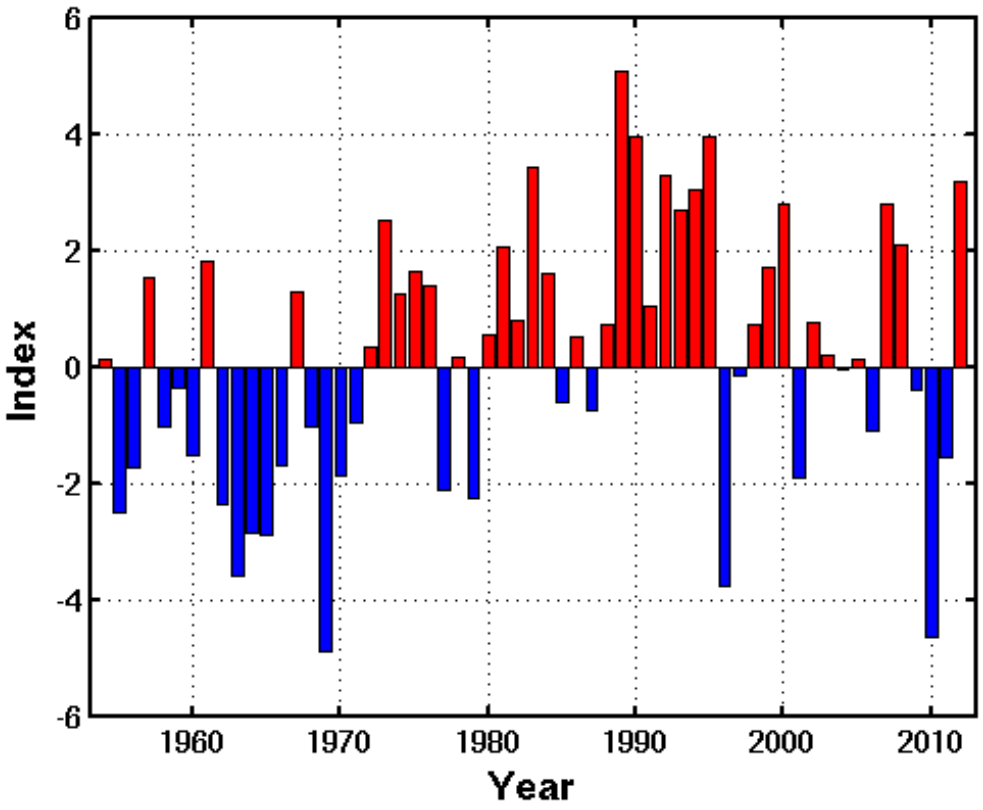

Figure 3.1: Winter mean NAO index. The NAO index was calculated for the long winter (DJFM). Data obtained from [47]

A high positive NAO index is associated with stronger than normal westerlies

in mid-latitudes and intense and more frequent winter storms over the Labrador Sea. The storm tracks extend from the US east coast towards the British Isles and Scandinavia, and are associated with strong air-sea exchange of momentum and heat over the SPNA [101]. The negative NAO index is associated with warmer than normal weather and relatively fewer storms passing over the Labrador Sea [101]. The response to the NAO, however, depends on location. During winters when the NAO is positive, the presence of the strong high-pressure and strong low-pressure systems produces warmer and wetter conditions over northern Europe and most of northeastern North America. This is largely because the jet stream is free of large undulations, and the jet streams westerly winds funnel storms over the Mid-Atlantic states, between the strong North Atlantic pressure cells, and over northern Europe. Colder conditions prevail over parts of Quebec, Newfoundland and Labrador, and western Greenland, and additional sea ice develops in Hudson Bay, Baffin Bay, and off western Greenland during winters when the NAO is positive. A negative NAO index is associated with colder winters in eastern North America and northern Europe due to more-frequent intrusions of Arctic air. North America receives additional snow, while Europe receives less precipitation than normal. Conversely, warmer conditions prevail from Hudson Bay to western Greenland.

This NAO related atmospheric variability is a dominant forcing for the long term variations in the SPNA Ocean water mass characteristics and circulation (see [18], [19], [30], [14], [108], [107], [60], [61] and [113]). The processes which trigger this variability as well as the ocean response are inherently multiscale and involve variability at all time scales from subseasonal to interannual and decadal.

During the 1960s the winters over the Labrador Sea were mild and surface cooling

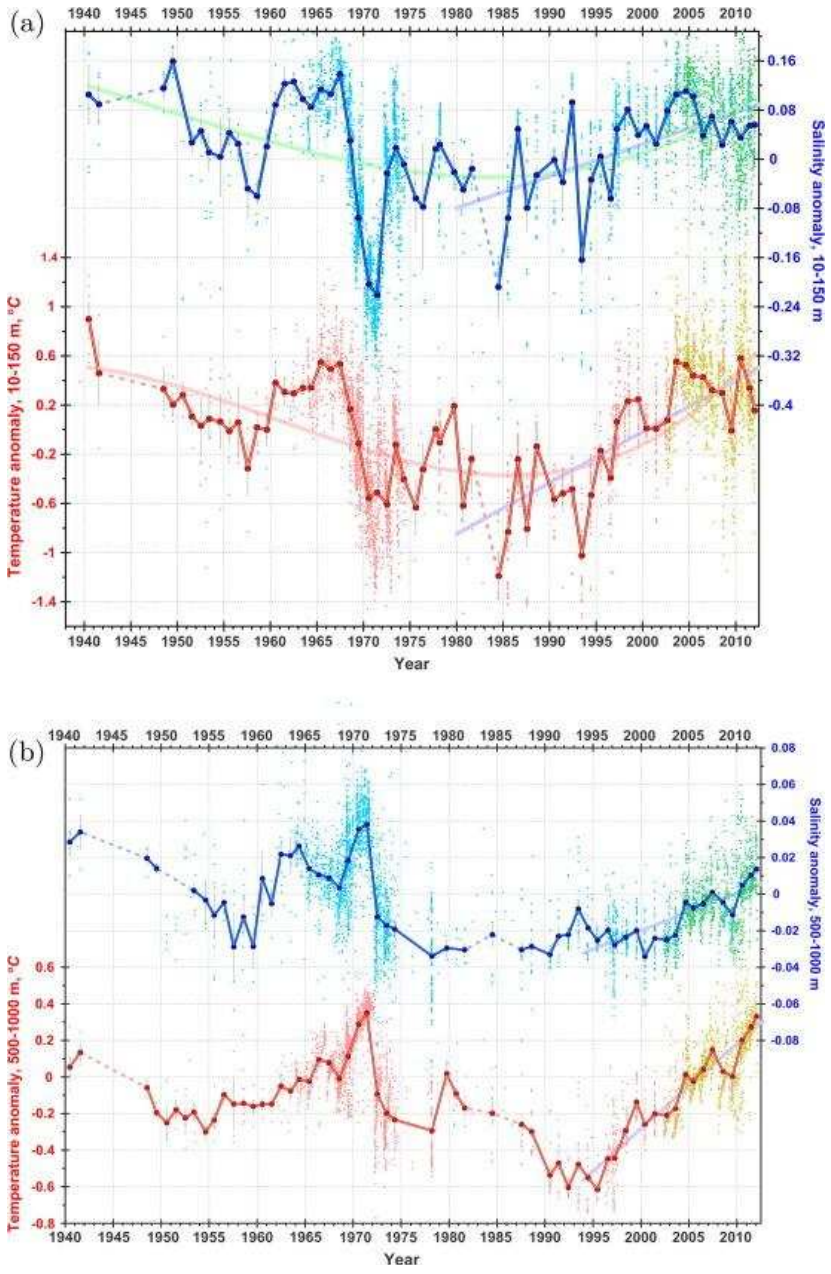

Figure 3.2: (a) Upper layer (10 - 150 m) temperature (red) and salinity (blue) anomalies (upper panel) and (b) Temperature (red) and salinity (blue) anomalies in the Labrador Sea for the 500 - 1000 m layer. (Adapted from [41]).

weaker than average. The deep convection and ocean circulation were less intense than usual [107] and [113]. In the late 1960s a low salinity anomaly in the surface layer was observed to propagate around the Labrador Sea. This phenomena is known as the Great Salinity Anomaly (GSA) [18].

Figure 3.2 shows the major trends in properties of the surface and intermediate water masses in the Labrador Sea over the past fifty years. During the GSA the surface layer salinity dropped by about 0.38 in Central Labrador Sea. This occurred within the period from 1967 to 1971, and is the largest variation in the surface layer salinity for the whole fifty year period. The surface layer temperature anomaly was positive in the 1960s in Labrador Sea, when the NAO was mostly negative in phase and winters warmer than average. The cold winters returned to the SPNA in the 1970s. The associated severe surface winds and cooling triggered intense deep convection [107] and intensified the sub-polar gyre circulation [113]. Since the mid-1990s the SPNA has warmed substantially (see Fig. 17). This warming was initially stronger in the eastern North Atlantic [41]. In the western part of the basin, the warming coincided with a decrease in the intensity of the deep convection [107].

3.2 Impact of large scale atmospheric and ocean dynamics on the climate of coastal regions of Newfoundland and Labrador

The impact of the NAO variability on regional climate of Newfoundland and Labrador is particularly noticeable in the coastal part in winter months [47]. NAO effects are

somewhat muted in the interior portion of Labrador by the prevailing westerly winds, bringing air from the continental interior of North America or Arctic [8]. Positive air temperature anomalies were observed in coastal Labrador in most of the 1950s and 1960s. This warm period coincided with a period of negative NAO index, which persisted from 1950 to 1971. The period between the early 1970s until the mid-1990s was characterized by a cooling surface temperature trend in the SPNA (see [47]).

In Eastern Canada, this cooling trend was predominantly observed over the eastern coast of Labrador, as well as Baffin Bay [71]. Consistent with the cold trend, [66] reported anomalously strong northerly surface winds over the Labrador Sea. They also found an increase in sea-ice extent over the Davis Strait in the month of January from the early 1970s to mid-1990s. The overall cooling trend during this period ranged from -0.5^{o}C per decade off the coast of Newfoundland to a higher rate of -1.3^{o}C per decade over Baffin Bay [87].

The NAO index changed from being steady and high positive before 1995 to low and with variable sign after that. In some years, like 1996 and 2010, the NAO was in a negative phase (see Figure 3.1). In 2010, the NAO index reached a record low for the period of observations. It should be noted that the relationship between the NAO index and the temperature variability in the Labrador and Newfoundland is not always direct [41], suggesting the presence of other climate factors in addition to the NAO that can be held accountable for the climate variability in the region. [33], for instance suggest that the Atlantic Multidecadal Oscillation which impacts the long term variation in the temperature of the Atlantic Ocean has an important impact on the regional climate of Newfoundland and Labrador.

3.3 Climate zones of Newfoundland and Labrador

The climate of Labrador and Newfoundland is of continental subarctic type. This type in the Köppen-Geiger classification [77] refers to a cold and dry climate with long and cold winter seasons. In North America the zone of subarctic climate extends from about 50^o to 70^oN and from Alaska to Newfoundland. In the Köppen-Geiger system, this continental subarctic climate is divided in sub-types. The climate of Newfoundland and Labrador is of subtype Dfc [77] characterized by humid climate with a lot of precipitation and relatively cold summers.

Compared to the continental subarctic climate in central Canada, the climate of Newfoundland and Labrador is additionally influenced by the North Atlantic Ocean. The cold Labrador current, sea-ice and the northern most branches of the North Atlantic Current influence the climate in the region. The character and intensity of this ocean impact on the climate, however, varies across the province. The variations in the significance of large scale atmospheric and oceanic influence contribute to the diversity of the climate characteristics across the province which is divided by [106] into seven climate zones (Figure 3.3a).

The northern most climate zone in Labrador is the **Tundra Climate** zone. The summers in this zone are short and cool. Precipitation in the zone decreases towards the north. The mountains and fjords in northern Labrador have important orographic effect on the regional climate characteristics mostly in the summer season. The part of Labrador south of the Tundra Climate zone is divided into two zones. The **Coastal zone** is the part of Labrador exposed to the influence from the Labrador Sea while the **Interior Labrador** includes the continental part of the province (see Figure 3.3a).

The winters in Interior Labrador are lengthy and cold with deep snow cover. Coastal Labrador is exposed to stormy weather from the Labrador Sea, strong winds and heavy precipitation. Extreme temperatures are observed in this region during intense offshore winds in summer and winter. While geographically Lake Melville is part of this zone (see Figure 3.3a), it is exposed through the Hamilton inlet to the influence of the Labrador Sea. Hence, some previous studies (see [106]) suggest that Lake Melville's climate is characterized by shorter and warmer winters and sunnier summer than in the rest of the Interior Labrador zone. This makes some of the climate characteristics of Lake Melville similar to those of the Coastal Labrador zone.

The Island of Newfoundland is divided in four climate zones: the West Coast, Western Mountains and Central Uplands, Northeast Coast and Central Lowlands, South Coast and Avalon [106] The **West Coast** zone is exposed to influence from the Gulf of St. Lawrence, which normally reduces temperature extremes but causes increased precipitation. The snow falls are especially frequent and intense in this zone during autumn and early winter. The **Western Mountains and Central Uplands** zone is characterized by low temperatures, greater cloudiness and precipitation and stronger winds. The winter snow accumulations are especially heavy toward the west.

The **Northeast Coast and Central Lowlands** is the driest area on the island. Occasional very low winter temperatures are observed in the valleys. The springs are cool and late near the coast. The summers are sunny and warm. The winters in the **South Coast and Avalon** are relatively mild with high variation in snow cover. Heavy rainfalls occur in late autumn and early winter. Summers are cool with low clouds and fogs near the coast and warmer inland.

The present study uses data from atmospheric observations in Newfoundland and

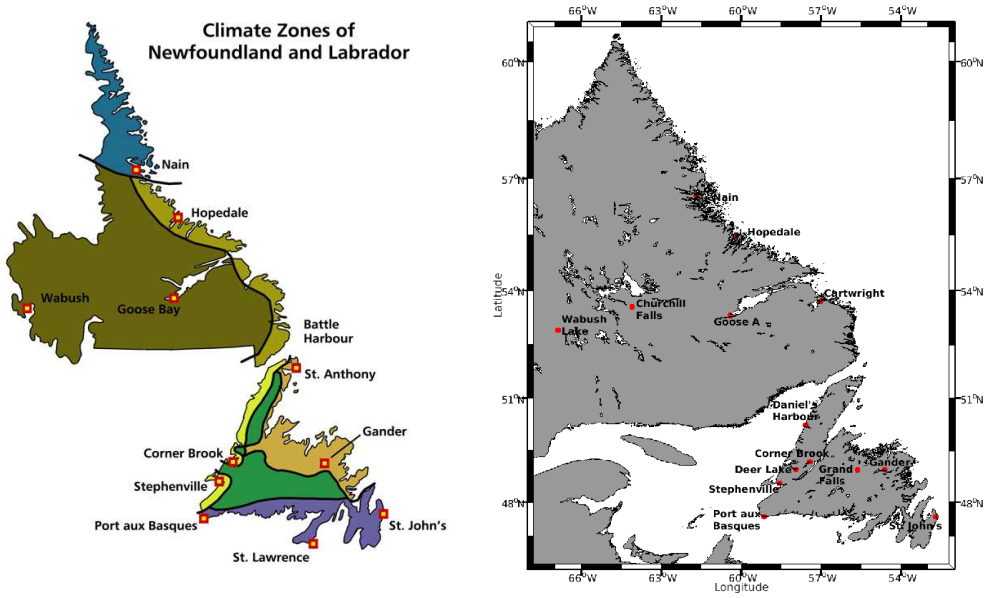

(a) (b)

Figure 3.3: (a) Climate zones of Newfoundland and Labrador. After [106]; (b) observational stations used in the present study.

Labrador (see Figure 3.3b) in six of the seven climate zones. There are no observations available for the Western Mountains and Central Uplands climate zone.

3.4 Seasonal variability

Monthly mean temperature, total precipitation, rain, and snow for Newfoundland and Labrador are shown in Figure 3.4. The Labrador climate is of typical subarctic type with monthly mean temperatures (blue curve in Figure 3.4a) remaining below the freezing temperature for about six months during the year. Summer is cool with a maximum monthly mean temperature in July of about 14^{o}C. One specific

characteristic of subarctic climate is the large amplitude of the seasonal cycle. It is larger than the amplitude of the seasonal cycle in all other climate types in the Köppen-Geiger classification [77]. In Labrador it is of about 32^oC. For comparison, the seasonal cycle in Newfoundland is about 23^oC. While the climate of Newfoundland is also of subarctic type, the ocean impact modifies and makes it milder and more humid especially during early winter when the ocean surface is still warm. During this part of the year the temperature in most parts of Newfoundland remains above the freezing temperature. The annual minimum of surface atmospheric temperature over the island is reached in February when the ocean surface is cooled down.

The seasonal cycles of rain, snow and total precipitation are also different in Labrador (blue curves) and Newfoundland (red curves) (Figures 3.4 b,c,d). In general, the subarctic climate is dry with little precipitation [78]. Labrador and Newfoundland, however, lie on the main path of weather disturbances propagating from continental North America towards the Atlantic Ocean and Europe. These storms bring cold air and intense snow in winter (Figure 3.4 c), and rain during the warm part of the year (Figure 3.4 d). In the April and May when the snowfall and rainfall reach their lowest level, the total precipitation in Labrador is below 3 mm/day. In July it reaches its maximum of about 3.5 mm/day. During the rest of the year, the monthly mean precipitation remains close to a level of 3 mm/day. The total precipitation in Newfoundland has a larger seasonal cycle with intense precipitation in winter and minimum in the summer. Both snow and rain contribute to the high precipitation in Newfoundland in the winter season. The rain contribution to the total precipitation is highest in late autumn and early winter, while the snow contribution is strong from December to March.

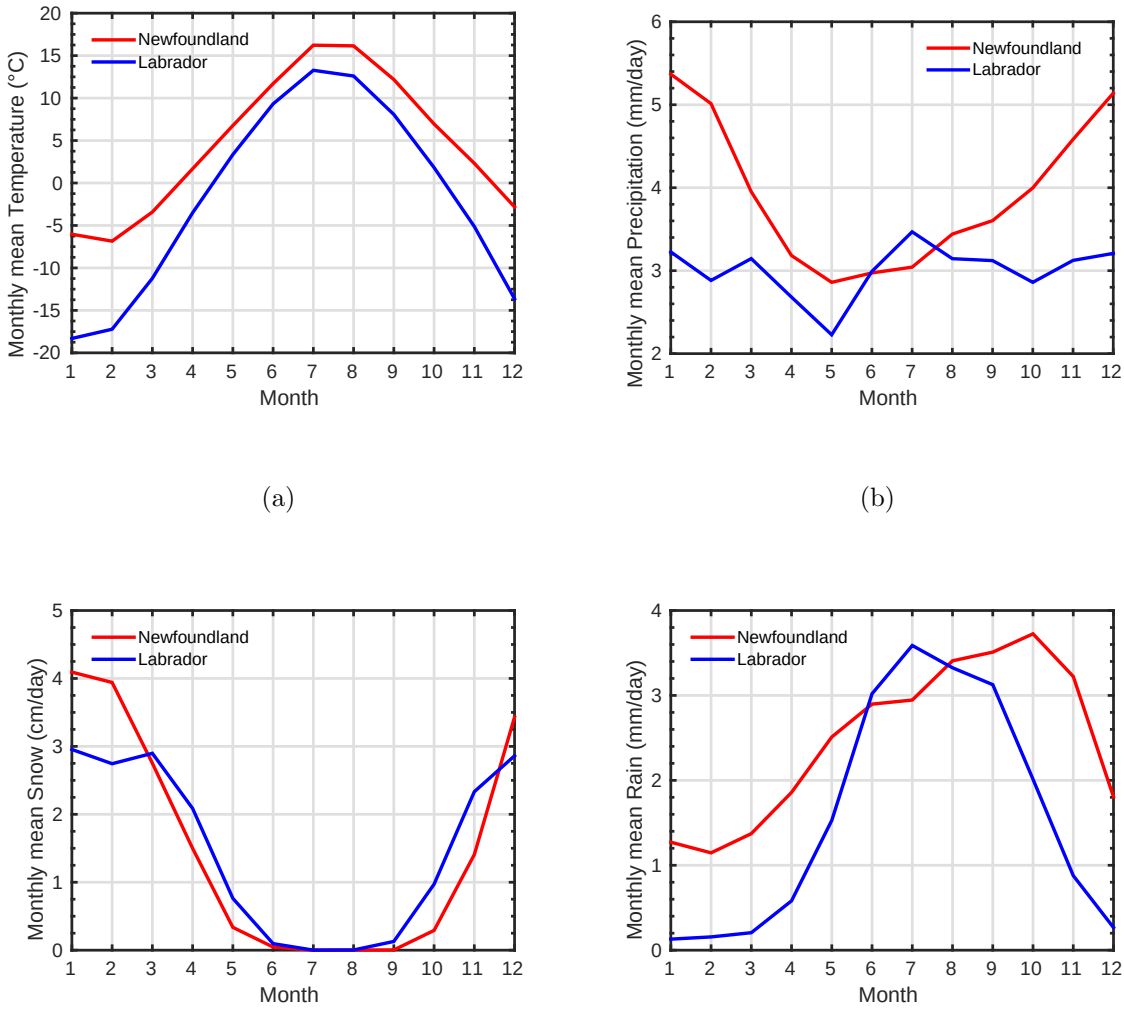

Figure 3.4: Monthly mean (a) temperature, (b) total precipitation, (c) snow fall, and (d) rain in Labrador (blue curves) and Newfoundland (red curves). Mean values were calculated over a 30 year period, between 1970 and 2010.

The monthly mean temperatures across all meteorological stations (Figure 3.5) further demonstrate the spatial differences in the seasonal cycle across Labrador and Newfoundland. These differences are mostly between the coastal and internal stations

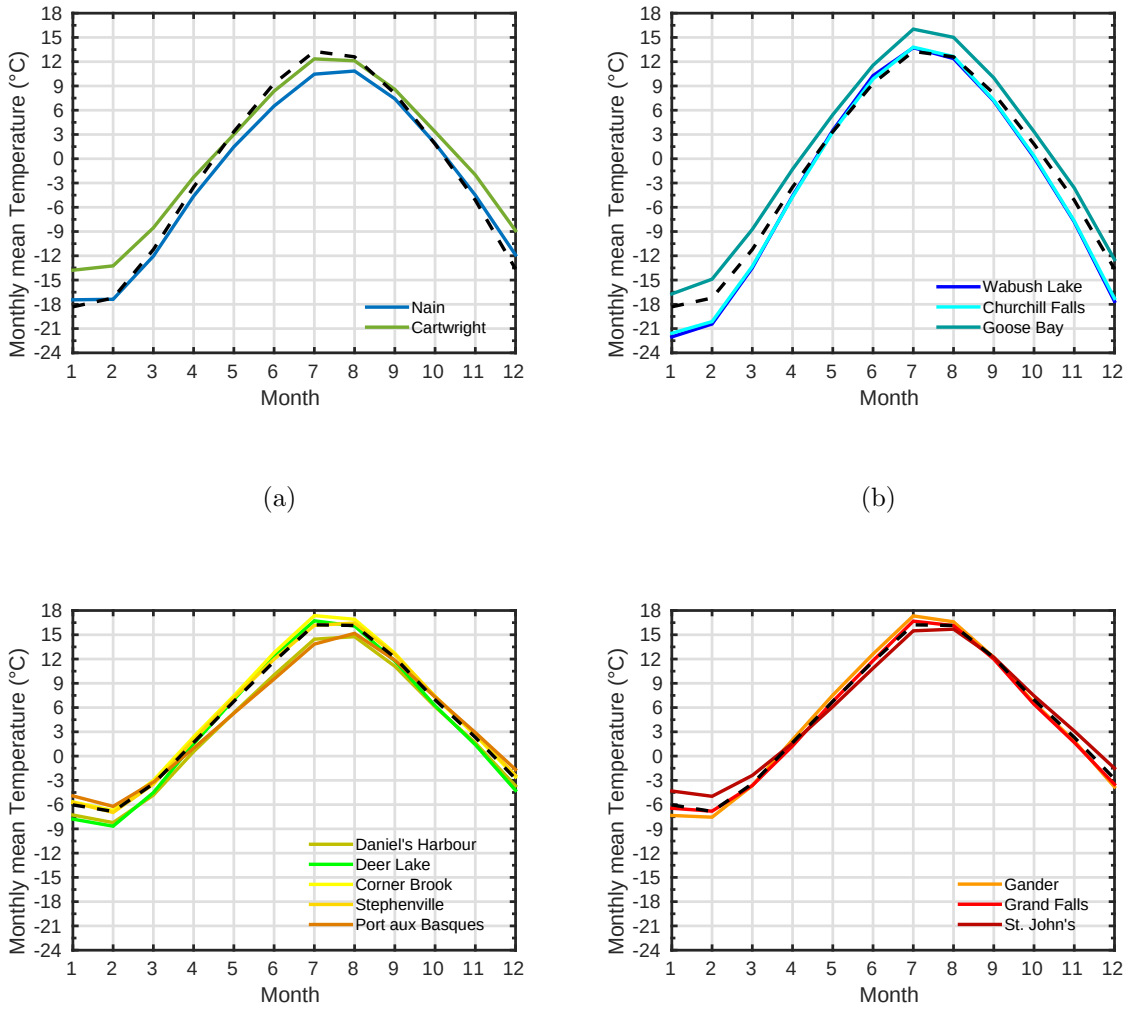

Figure 3.5: Monthly mean temperature in (a) Northern and Coastal Labrador; (b) Interior Labrador; (c) West and Southwest Newfoundland; (d) East and Central Newfoundland. The dashed lines on (a) and (b) show the monthly mean temperature in Labrador and on (c) and (d) the monthly mean temperature in Newfoundland.

of the island. The winters in coastal stations are on average 2^oC to 3^oC warmer and summers - two to three degrees colder than in the interior area. The contrast between

coastal and interior stations in Labrador is much stronger than in Newfoundland. In general the winters in interior Labrador are much colder (see Figure 3.5 b) and the annual cycle in temperature much larger than in the coastal area (see Figure 3.5 a). The seasonal cycle in Cartwright (minimum temperature -13.8^oC and maximum temperature 12.4^{o}C, Table 3.1), is smaller compared to the -21.6^oC minimum and 13.8^oC maximum in Churchill Falls and -22.0^oC minimum and 13.7^{o}C maximum in Wabush Lake. The difference in the magnitude of seasonal variation is related to the weakening of the ocean's moderating impact and the increase of continental influence. Seasonal contrast of temperature variability decreases from the Northern Labrador toward Newfoundland.

This contrast is mainly due to the large range in winter temperature minima, ranging from -17.3^{o}C in Nain, -16.7^{o}C in Hopedale, -13.8^{o}C in Cartwright, and -5.0^{o}C in St. John's. Comparatively, summer temperatures vary within a more restricted range, between 11.4^{o}C, 11.6^{o}C, 12.4^{o}C and 15.7^o in Nain, Hopedale, Cartwright and St. John's, respectively. A similar pattern is observed in the western part of the study region, with temperature minima ranging from -6.7^{o}C, -7.0^{o}C, -8.2^{o}C and -22.0^{o}C in Corner Brook, Stephenville, Daniel's Harbour and Wabush Lake, respectively. In contrast, temperature maxima range between 13.73^{o}C and 17.37^{o}C in Wabush Lake and Corner Brook, respectively.

Table 3.1: Extrema of monthly mean temperature and seasonal cycle amplitude. (The amplitude of the seasonal cycle in the last column is calculated as the difference of the fourth and third columns)

Climate Zone	Station	Winter minimum	Summer maximum	Amplitude of seasonal cycle
Tundra	Nain	-17.3^{o}C	11.4^{o}C	28.7^{o}C
Coastal Labrador	Cartwright	-13.8^{o}C	12.4^{o}C	26.2^{o}C
Interior Labrador	Goose Bay	-16.7^{o}C	16.0^{o}C	32.7^{o}C
Interior Labrador	Churchill Falls	-21.6^{o}C	13.8^{o}C	35.4^{o}C
Interior Labrador	Wabush Lake	-22.0^{o}C	13.7^{o}C	35.7^{o}C
West Coast	Daniel's Harbour	-8.2^{o}C	14.7^{o}C	22.9^{o}C
West Coast	Corner Brook	-6.7^{o}C	17.4^{o}C	24.1^{o}C
West Coast	Stephenville	-7.0^{o}C	16.5^{o}C	23.5^{o}C
North Coast	Grand Falls	-7.6^{o}C	17.3^{o}C	24.9^{o}C
Northeast Coast	Gander	-6.8^{o}C	16.7^{o}C	23.5^{o}C
Northeast Coast	Deer Lake	-8.7^{o}C	16.7^{o}C	25.4^{o}C
South Coast & Avalon	Port aux Basques	-6.2^{o}C	15.2^{o}C	21.4^{o}C
South Coast & Avalon	St. John's	-5.0^{o}C	15.7^{o}C	20.7^{o}C

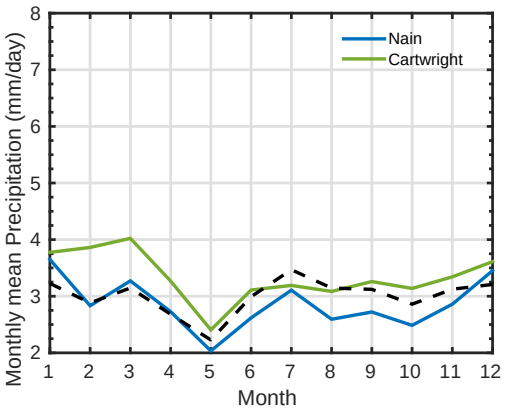

(a)

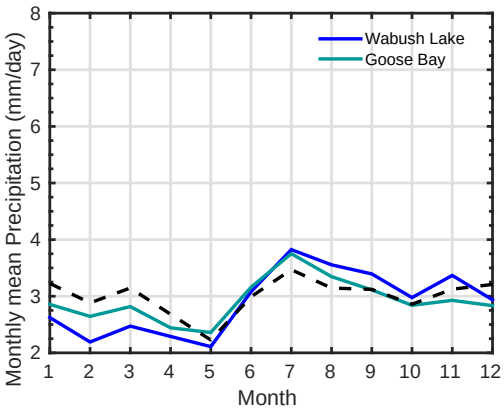

(b)

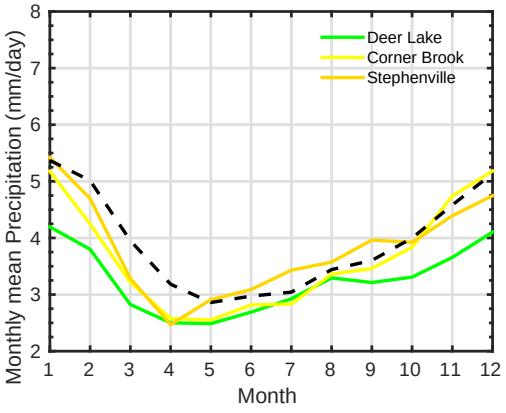

(c)

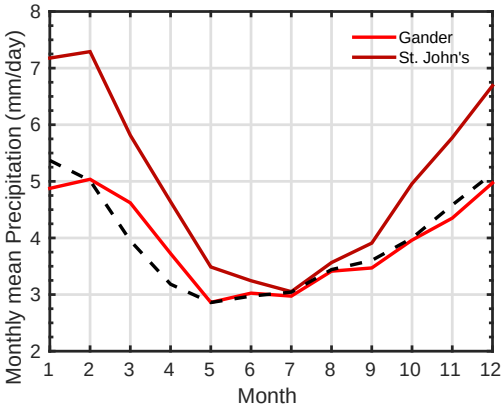

(d)

Figure 3.6: Monthly mean total precipitation in (a) Northern and Coastal Labrador; (b) Interior Labrador; (c) West and Southwest Newfoundland zone; (d) East and Central Newfoundland. The dashed lines on (a) and (b) show the monthly mean total precipitation in Labrador and on (c) and (d) the monthly mean total precipitation in Newfoundland.

The seasonal cycle of precipitation for the available stations clearly falls in two groups. The first group includes the stations in Newfoundland (Figures 3.6cd) and coastal Labrador (Figure 3.6a) which receive maximum precipitation in the cold part of the year, in winter and late fall. The interior regions of Labrador get the largest amount of precipitation in summer(Figure 3.6b). The minimum precipitation in most of the stations is observed in May. Only in St. John's does this minimum occur in July. In general, the magnitudes of seasonal cycles and maxima in precipitation are much larger in Newfoundland than those in Labrador.

While we observe these differences in the seasonal cycle of precipitation across the province, we should also mention that the amount of rain in the summer season is quite stable and close at all stations. The monthly mean precipitation in all stations in Newfoundland from June to August is between 2.5 and 3.5 mm/day. The corresponding amount for most of the stations in Labrador is between 3.0 and 3.5 mm/day, with the exception of Nain, where mean monthly precipitation ranges from 2.5 to 3.3 mm/day.

The general tendency of wind speed (Figure 3.7) is to decrease towards the interior part of Labrador and Newfoundland. The strongest monthly mean winds are observed along the coast of Newfoundland, and the weakest in Wabush Lake and Churchill Falls. In Labrador, wind speeds are highest at the coast, and considerably lower in interior Labrador, ranging from 6.7 m/s in Cartwright to 4.5 m/s in Goose Bay, 4.25 m/s in Churchill Falls and 4.2 m/s in Wabush Lake. In the coastal regions, the peaks of monthly mean winds are observed in winter months (DJF). In interior Labrador, the wind speed variations have smaller magnitudes, as seen from the amplitude of the seasonal cycle, with maximum wind speed in the transient seasons (spring, autumn).

In Newfoundland, the highest wind speeds are observed in St. John's, and the lowest in Deer Lake, at 7.2 m/s and 4.1 m/s in St. John's and Deer Lake, respectively. This is because Deer Lake is partly isolated from the influence of the Gulf of St. Lawrence, compared to Daniel's Harbour, which is also on the west coast but sees higher wind speeds more similar to those in St. John's.

3.5 Interannual and decadal variability

This section presents results from an analysis of the annual mean temperature and precipitation anomalies, defined as averaged differences between the instantaneous quantities and their seasonal mean values. This difference is calculated first as daily means and then averaged for each year. The time series of temperature anomalies for the period from 1951 to 2012 are shown in Figure 3.8. Due to limitations in available observations, the series at some stations are shorter and do not cover the whole period between 1951 - 2012.

The series of temperature anomalies provide (Figure 3.8) an insight into the spatial variability of climate and its temporal variations. Temperature anomalies have large magnitudes in winter (Figure A.1), with departures from the mean winter temperature ranging from -5.87^{o}C to +7.75^{o}C while the magnitudes of summer temperature (Figure A.3) anomalies are much smaller. Temperature anomalies show also significant spatial variability and are most pronounced in coastal and interior Labrador while having smaller magnitudes in Newfoundland. Spring season temperatures (Figure A.2) exhibit a more pronounced interannual variability than summer (Figure A.3) and autumn (Figure A.4), however, not as significantly pronounced as the winter

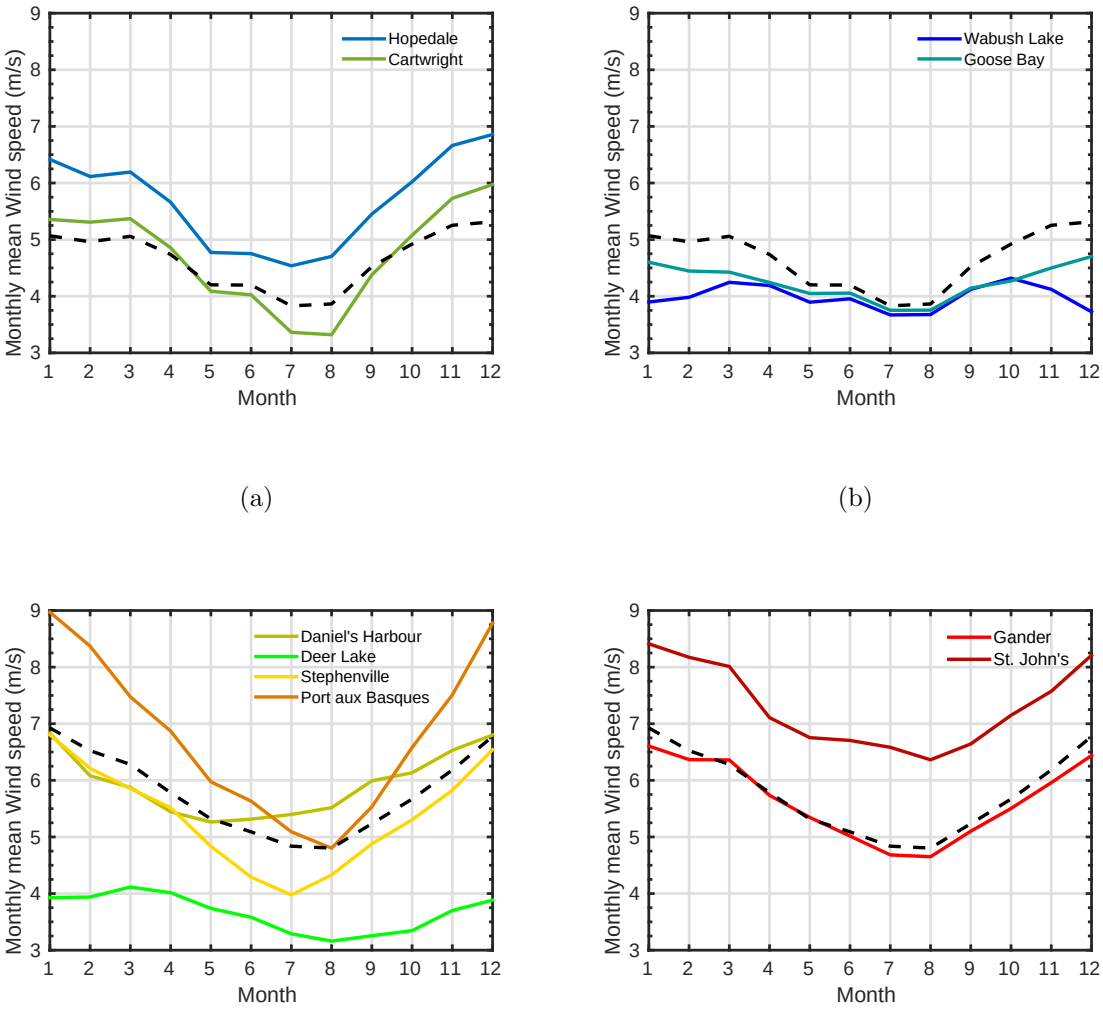

Figure 3.7: Monthly mean wind speed in (a) Northern and Coastal Labrador; (b) Interior Labrador; (c) West Newfoundland zone; (d) East Newfoundland. The dashed lines on (a) and (b) show the monthly mean wind speed in Labrador and on (c) and (d) the monthly mean wind speed in Newfoundland.

months. Spring is a transient season, and considering the long lasting winter period, spring in Labrador is rather cold. Consequently, temperature anomalies are

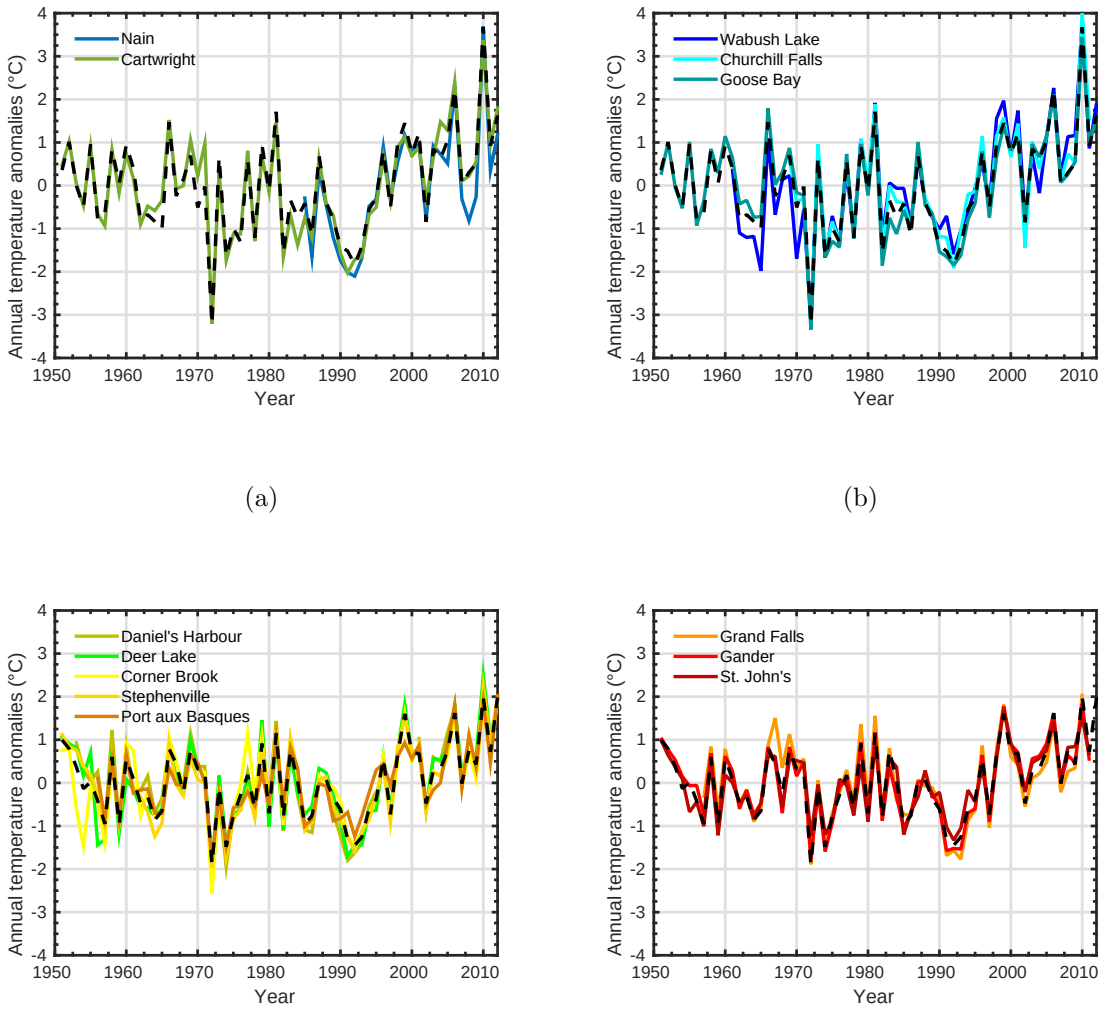

Figure 3.8: Annual mean temperature anomalies in (a) Northern and Coastal Labrador; (b) Interior Labrador; (c) West Newfoundland zone; (d) East Newfoundland. Dashed lines show annual mean temperature anomalies in Labrador (a,b) and Newfoundland (c,d).

pronounced during the spring months, particularly in the region of interior Labrador that is removed and sheltered from the ocean's moderating influence. Overall, win-

ter and spring temperatures show a slight decrease from 1972-1992, whereas summer and autumn show no change in temperature. All seasons show a general warming (Figure 3.8) from the mid-1990s until present, with a general plateauing over the last decade; however, 2010 had the warmest winter, spring and summer in the region, while fall temperature departures were insignificant. The departure from the mean temperature in 2010 varied in each climate zone. The annual temperature anomaly was highest in higher latitudes, ranging from 3.37^{o}C in Cartwright and 4.03^{o}C in Churchill Falls. Comparatively, temperature anomalies on the island ranged from 1.51^{o}C in St. John's to 2.49^{o}C in Deer Lake.

The timing of these trends differ from season to season. There was an especially strong shift from a cold period to a warm period in the mid-1990s. Spring, summer and autumn mean temperatures began to rise in the early 1990s; winter temperatures remained cold until the mid - 1990s. Winters and autumns of the 1950s and 1960s were relatively warm; conversely, spring and summer temperatures were cooler than normal during that period, and did not exhibit a significant warming until the onset of the 1990s. The long term trends of temperature are further evaluated and studied in the following section.

Three major periods of temporal temperature variability are presented on Figure 3.8: (a) interannual with a time scale of two to three years, (b) decadal with periods close to a decade and (c) multidecadal, which appear as long term trends for approximately two decades. The visual inspection of Figure 3.8 suggest that the interannual variations were persistent in the first part of the period until the early 1980s. The temperature anomaly variations after 1980 are dominated by oscillations with periods between five and fifteen years. The analysis of long term trends on time

scales longer than a decade are studied in the following chapter.

Interannual variations of precipitation anomalies are less uniform across the province (Figure 3.9). While the precipitation in all stations exhibits intense variation at the interannual scale from one to three years, the longer term variations are very small or impossible to identify on Figure 3.9.

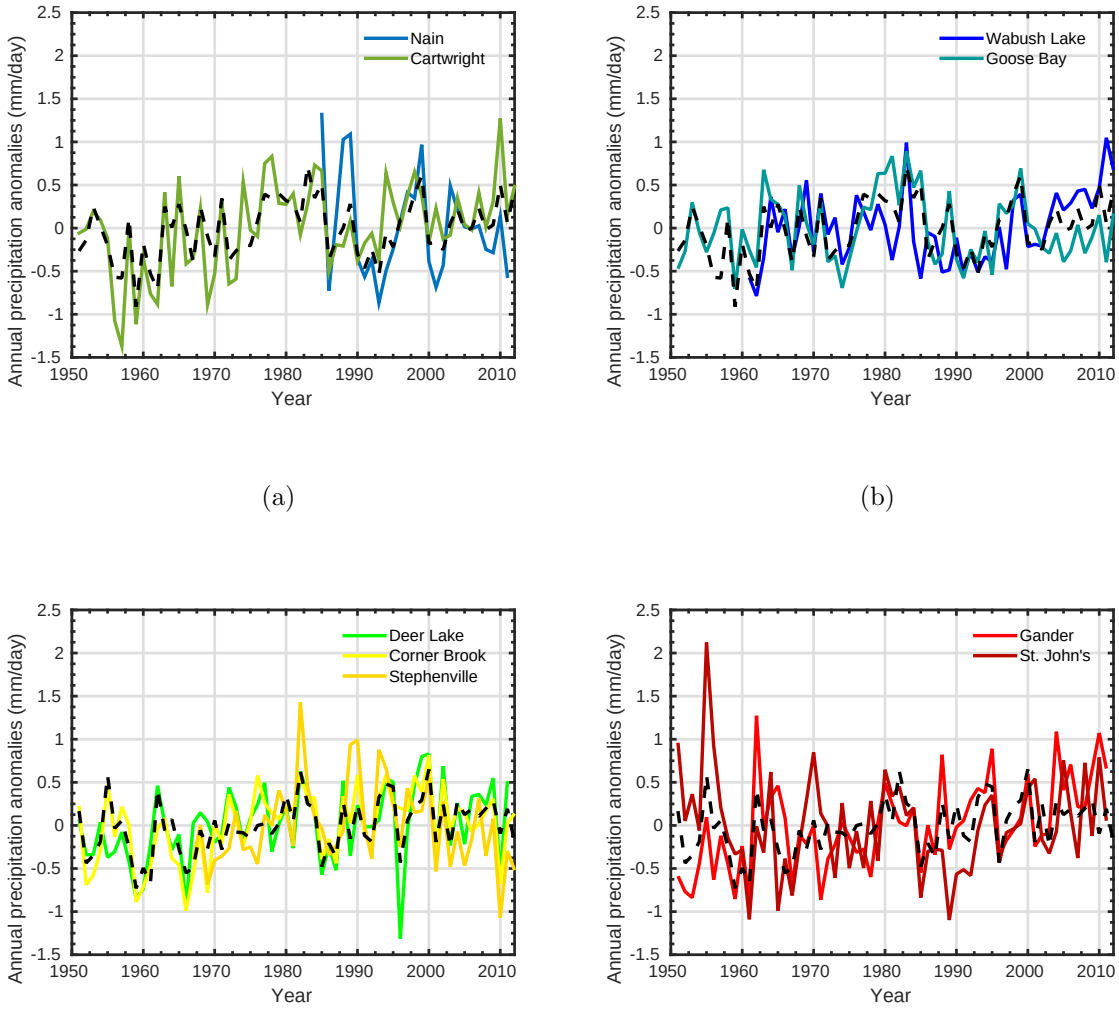

(a) (b)

(c) (d)

Figure 3.9: Annual mean anomalies of total daily precipitation in (a) Northern and Coastal Labrador; (b) Interior Labrador; (c) West Newfoundland zone; (d) East Newfoundland. Dashed lines show annual mean anomalies of total daily precipitation in Labrador (a,b) and Newfoundland (c,d).

Chapter 4

Multidecadal trends and extremes of atmospheric characteristics

The globally averaged combined land and ocean surface temperature data as calculated by a linear trend show a warming of 0.85^{o}C over the period 1880 to 2012 [48]. Locally, however, the temperature trends may vary depending on the regional climate dynamics. The magnitude of regional natural atmospheric variability on multidecadal and interdecadal time scales, which exceeds the long term centennial trends [48], is essential for understanding the climate dynamics and its influence on the environment. In this section, the characteristics of the multidecadal temperature trends, their character and magnitudes are estimated for all of the stations by using the Mann-Kendall trend test. The multidecadal trends are defined as variations with periods longer than a decade. We also study how variations in extreme temperatures are associated with the multidecadal trends.

4.1 Multidecadal trends

D'Arrigo et al. [16] conducted spectral analysis of climate in Labrador by using data from tree ring-widths of white spruce *Picea glauca*. These authors (Figure 4.1)

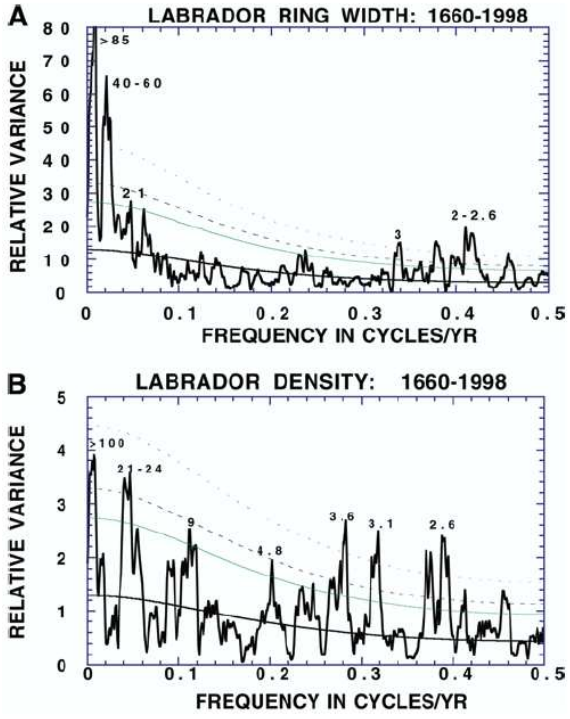

Figure 4.1: (A) Multi-taper method (MTM) spectral analysis of Labrador ring width composite over the period 1660 - 1998. (B) MTM analysis of density series for 1660 - 1998. Thick curve is level of red noise representing null hypothesis. Thin lines indicate 90, 95 and 99% confidence levels. Significant peaks are labeled. (Adapted from [15]).

identify three statistically significant dominant periods in the interannual, decadal and multidecadal variability of Labrador: 21-24 years, 9 years and 2-8 years. They also found that the variability within such periods generally correlates well with the

variability within the same period in the NAO index. Our focus in this section is on periods longer than a decade.

As discussed in the previous section, the past observations of temperature (Figure 3.8) reveal multidecadal periods of positive and negative trends in temperature. The intense interannual and decadal variability, however, precludes exact determination from Figure 3.8 of the characteristics of the trend, in particular (i) the period of time when they are present, and (ii) their sign and magnitude. These two types of characteristics are defined here by using statistical methods described in Chapter 2.

The method of cumulative difference is used here to identify the periods of persistent trends. This method is often used (see [96]) for determining the time when long term trends change sign. The accumulated difference curves for temperature in all climate areas of Newfoundland and Labrador (Figure 4.2) show that 1997 is the point at which the trend reverses from a long cold period to a warm period that still persists today. For comparison, a transition point for the Northern Hemisphere was previously found to be 1993 [62].

As mentioned in the previous chapter the decadal and multidecadal changes in precipitation have much smaller magnitude than in those of temperature. The method of cumulative differences (see Figure 4.3) does not show long term trends which are consistent across the province.

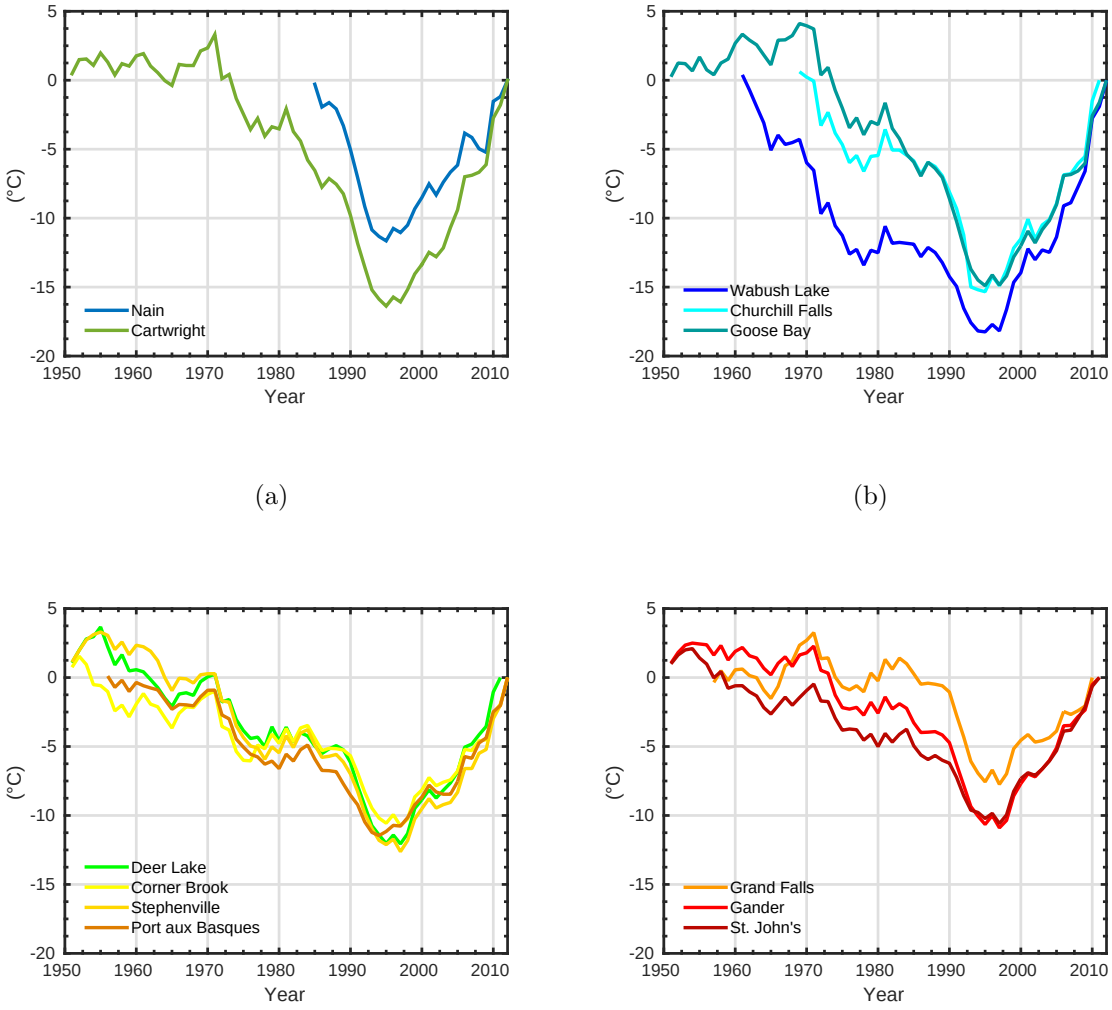

(a) (b)

(c) (d)

Figure 4.2: Cumulative Differences of temperature in (a) Northern and Coastal Labrador; (b) Interior Labrador; (c) West Newfoundland zone; (d) East Newfoundland

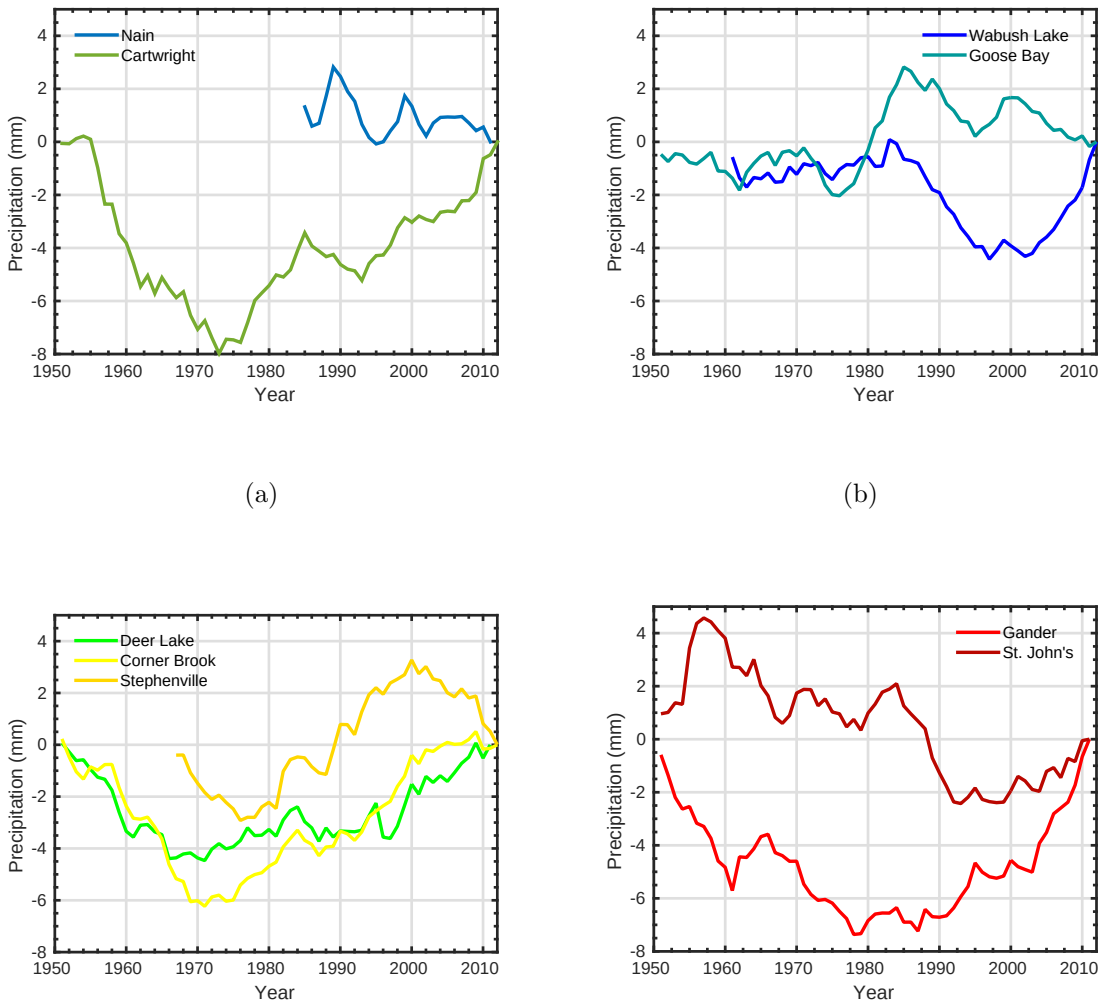

Figure 4.3: Accumulated Differences of total precipitation in (a) Northern and Coastal Labrador; (b) Interior Labrador; (c) West Newfoundland zone; (d) East Newfoundland

The Mann-Kendall test is applied for the annual mean temperature for two periods of time (i) 1973-1992 and (ii) 1993-2012 (Table 4.1). Results from the Mann-Kendall test for seasonal mean temperatures are presented in appendix A.

A cooling trend for the period between 1973 and 1992 was observed in all climate regions, but it was not uniform across the province. In Labrador, the negative trend was more pronounced than in Newfoundland, with the strongest decreasing trend observed in Churchill Falls in interior Labrador (-0.0592^{o}C/year), and weakest in St. John's in the Avalon (-0.0125^{o}C/year). The decreasing trend also varies with latitude - the trend is more pronounced in higher latitudes, as can be seen between St. John's and Cartwright (-0.0415^o/year). This is also observed on the west coast of Newfoundland, where the strongest negative trend was observed in Daniel's Harbour (-0.0588^{o}C/year), and decreased southward to Port aux Basques (-0.0224^o/year). In interior Newfoundland (Grand Falls and Gander), trends are more pronounced further inland, and become less pronounced toward the coast (-0.0341^{o}C/year and -0.0296^{o}C/year in Grand Falls and Gander, respectively), compared to the weakest trend in St. John's. Although a general pattern of trends is evident, the cooling trends in the region are not statistically significant at the 5% significance level.

In the mid-1990s, a warming trend ensued. Contrary to what was observed in the cooling period, the increasing annual temperature was statistically significant in seven climate regions. The strength of warming trends in Newfoundland weakens from west to east, as observed in Deer Lake (+0.0728^{o}C/year), Grand Falls (+0.0692^{o}C/year) and Gander (+0.0588^{o}C/year). In general, the strength of warming trends is stronger in continental Labrador than in Newfoundland, with four of the seven statistically significant trends observed in Labrador (Cartwright, Goose Bay, Churchill Falls and

Climate area	**Station**	**H 73-92**	**Sen's slope 73-92**	**H 93-12**	**Sen's slope 93-12**
Tundra	Nain	—	—	0	0.0687
Coastal Labrador	Cartwright	0	-0.0415	1	0.1255
Interior Labrador	Goose Bay	0	-0.0299	1	0.1190
Interior Labrador	Churchill Falls	0	-0.0592	1	0.1028
Interior Labrador	Wabush Lake	0	-0.0411	1	0.1142
West Coast	Daniel's Harbour	0	-0.0588	0	0.0646
West Coast	Deer Lake	0	-0.0366	0	0.0728
West Coast	Corner Brook	0	-0.0442	1	0.0901
West Coast	Stephenville	0	-0.0282	1	0.1151
Northeast Coast	Grand Falls	0	-0.0341	0	0.0692
Northeast Coast	Gander	0	-0.0296	0	0.0588
South coast & Avalon	Port aux Basques	0	-0.0224	1	0.0812
South Coast & Avalon	St. John's	0	-0.0125	0	0.0628

Table 4.1: Trends in annual temperature anomalies for the periods 1973-1992 and 1993-2012. H_0 and Sen's slope are presented for each period. (If H_0=1, the null hypothesis is rejected; if H_0=0, there is not enough evidence to reject the null hypothesis). Sen's slope calculated at the 5% significance level.

Wabush Lake), and the west coast of Newfoundland (Corner Brook, Stephenville and Port aux Basques). None of the trends in eastern and central Newfoundland were statistically significant, though St. John's fell just outside the significance score of +1.96 with a score of +1.91.

Unlike the warming trends observed in annual temperature; winter temperature trends (Table B.1) were statistically significant in all stations in Newfoundland except Daniel's Harbour, but only the trend in Churchill Falls was found to be statistically significant in Labrador. In general, warming trends were stronger in western Newfoundland than in eastern Newfoundland and the Avalon, although warming was most pronounced on the island in Grand Falls (+0.1776^{o}C/year), which is located in central Newfoundland and furthest away from the ocean's moderating influence. Conversely, no coherent pattern was observed in warming trends of winter temperature in continental Labrador. The same general patterns apply to the cooling trends in winter. It is worthy to note that cooling trends are less spatially variable than warming trends, by approximately one tenth of a degree C.

Cooling trends in summer temperature (Table B.3) were only significant in interior Labrador (Goose Bay and Wabush Lake), where cooling trends were also most pronounced. Temperature decreases of -0.0851^{o}C/year and -0.0741^{o}C/year were found in Wabush Lake and Goose Bay, respectively. In Newfoundland, cooling was muted compared to Labrador (-0.0203^{o}C/year in Deer Lake and -0.0241^{o}C/year in Gander), with the exception of Grand Falls in Central Newfoundland (-0.0480^{o}C/year). Warming in summer temperature was significant in three of the 5 stations in Labrador and three of the eight stations in Newfoundland, all of which are located on the west coast.

Finally, neither of the transient seasons of spring and autumn (Tables B.2; B.4), exhibited statistically significant cooling trends. Warming trends in autumn were statistically significant in the majority of the stations (approximately 70%). Conversely, no statistically significant warming trends were calculated for spring temperature.

4.2 Temperature distribution and climate extremes

Extreme atmospheric characteristics have an important and direct impact on everyday lives, communities and the environment. For these reasons, detection of changes is an important area of current climate studies. In particular a number of climate change indices based on daily temperature and precipitation observations have been developed to provide insights into regional extreme events [79]. They can be obtained from simple climate statistics to describe extremes such as very warm daily temperatures or heavy rainfall amounts. These indices are also valuable for studying the impact of climate change on regional activities, agriculture and the economy. They are also helpful for monitoring climate change itself and are used as benchmarks for evaluating climate change scenarios [35].

During the past few years, the regional trends in extreme temperature and precipitation indices garnered much interest. Overall, the findings have suggested a significant decrease in the number of days with extreme cold temperatures and an increase in the number of days with extreme warm temperatures [99]. A recent analysis over Europe, for instance, has revealed the occurrence of fewer cold nights, more warm days and an increase in the number of extreme wet days from 1946 - 1999, although the spatial coherence of the trends was low for precipitation [93]. Similar

findings were observed in some regions of Africa, though these were over a shorter period, from 1961 - 1990 [26]. The number of cold nights significantly decreased in China for the period from 1961 - 2000. As a result, a significant decrease in the diurnal temperature range was observed [82]; for precipitation, the number of rain days has decreased throughout most parts of China, while the intensity has increased [111]. In Australia, the number of warm days and nights has increased while the number of cold days and nights has decreased since 1961; heavy rainfall has also increased in some areas although these trends were not significant [81]. The length of the frost-free season has substantially increased over the past five decades in Russia, while a slight increase in heavy precipitation events was also observed [38], [99].

In the Americas, similar patterns have been observed. In South America, significant increasing trends were identified in the number of warm nights, while no consistent changes were found in the indices based on daily maximum temperature [100]; rainfall indices indicate a change to wetter conditions during the last four decades [42]. In the Caribbean region, the increase in heavy precipitation events has not been significant, the percentage of days with very warm daytime and night-time temperatures has increased since the late 1950s [80]. In the United States, the frequency of frost days decreased slightly from 1910 - 1998, although a small downward trend was also observed in the number of warm days [27]. The same study indicated increasing trends in the number of heavy precipitation events [99].

Specifically in Canada, [7] analyzed annual and seasonal characteristics of temperature extremes from 1900 - 1998. The results exhibited significant increasing trends in both the lower and higher percentiles of the daily minimum and maximum temperature distributions in southern Canada. They found fewer days with extreme low

temperatures during winter, spring and summer and more days with extreme high temperatures during the winter and spring; however, no consistent trends were found in the number of extreme hot days during the summer. Spatial and temporal characteristics of heavy precipitation events were also examined in southern Canada for the same period of time [112]. The findings revealed no consistent trends in either the number or intensity of precipitation extremes during the last century [99]. In a different study, using different data sets, an increase in heavy and very heavy precipitation events was found for British Columbia south of the 55^{o}N from 1910 - 2001 [37].

4.2.1 Decadal shifts in the temperature distribution

In this section, the decadal variability of winter temperature distributions is presented. The long winter season (DJFM) is considered in this section, and in the remainder of this chapter. Figure 4.4 and Figure 4.5 show the KS density probability distribution for daily minimum (Tmin) and maximum (Tmax) temperature in Labrador and Newfoundland.

A statistically significant warming trend is observed at most of the stations during the last decade (Table 4.1). This warming trend implies an increase both in mean and extreme temperature values. Overall, the range of the distribution is larger in Labrador than it is in Newfoundland. The range of temperature distributions is also smaller in coastal regions, i.e in Cartwright and Goose Bay. Shifts in the tails of the distribution could be due to changes in the intensity of the extremes or in the frequency of occurrence.

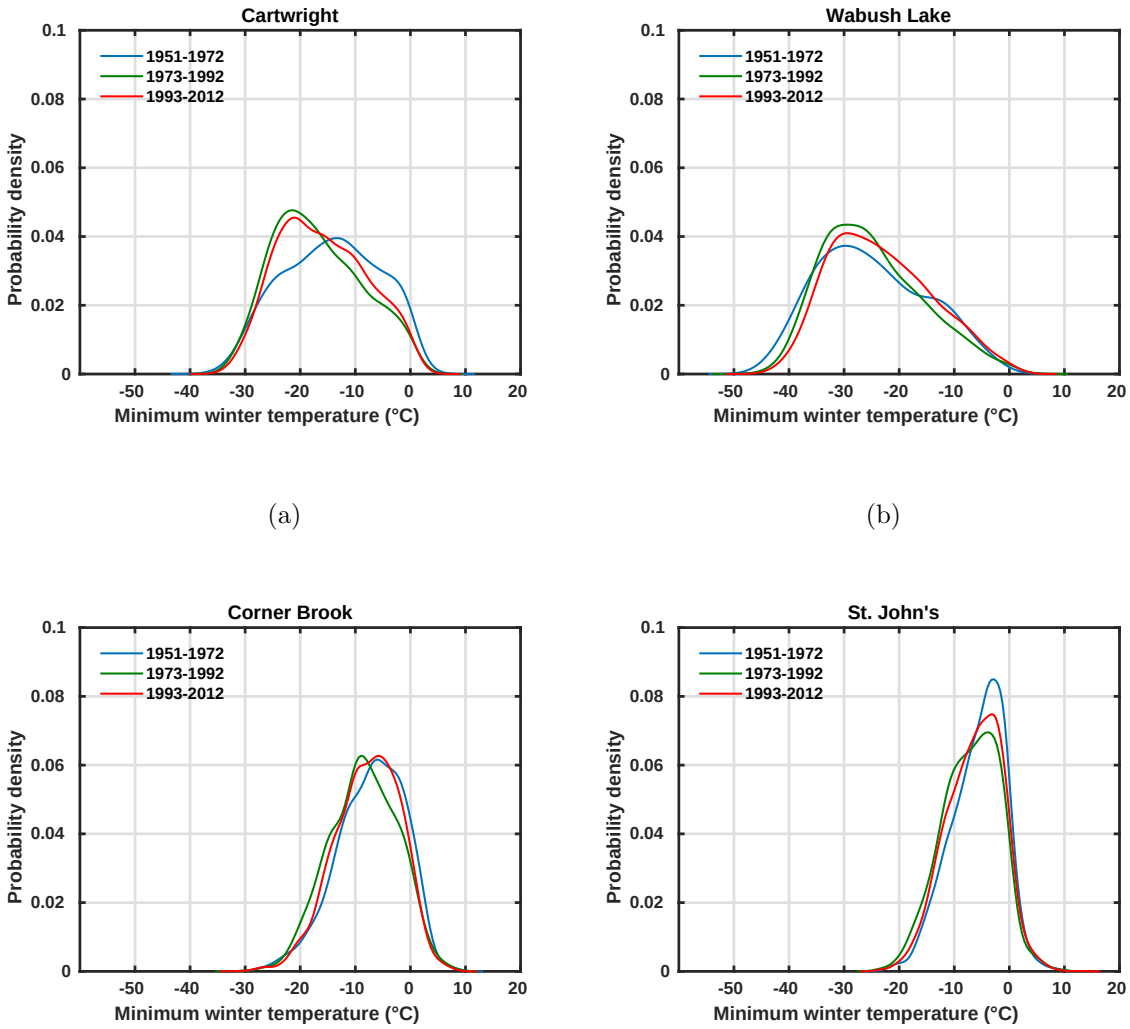

(a) (b)

(c) (d)

Figure 4.4: Kernel Density of minimum winter temperature in (a) Northern and Coastal Labrador; (b) Interior Labrador; (c) West Newfoundland zone; (d) East Newfoundland

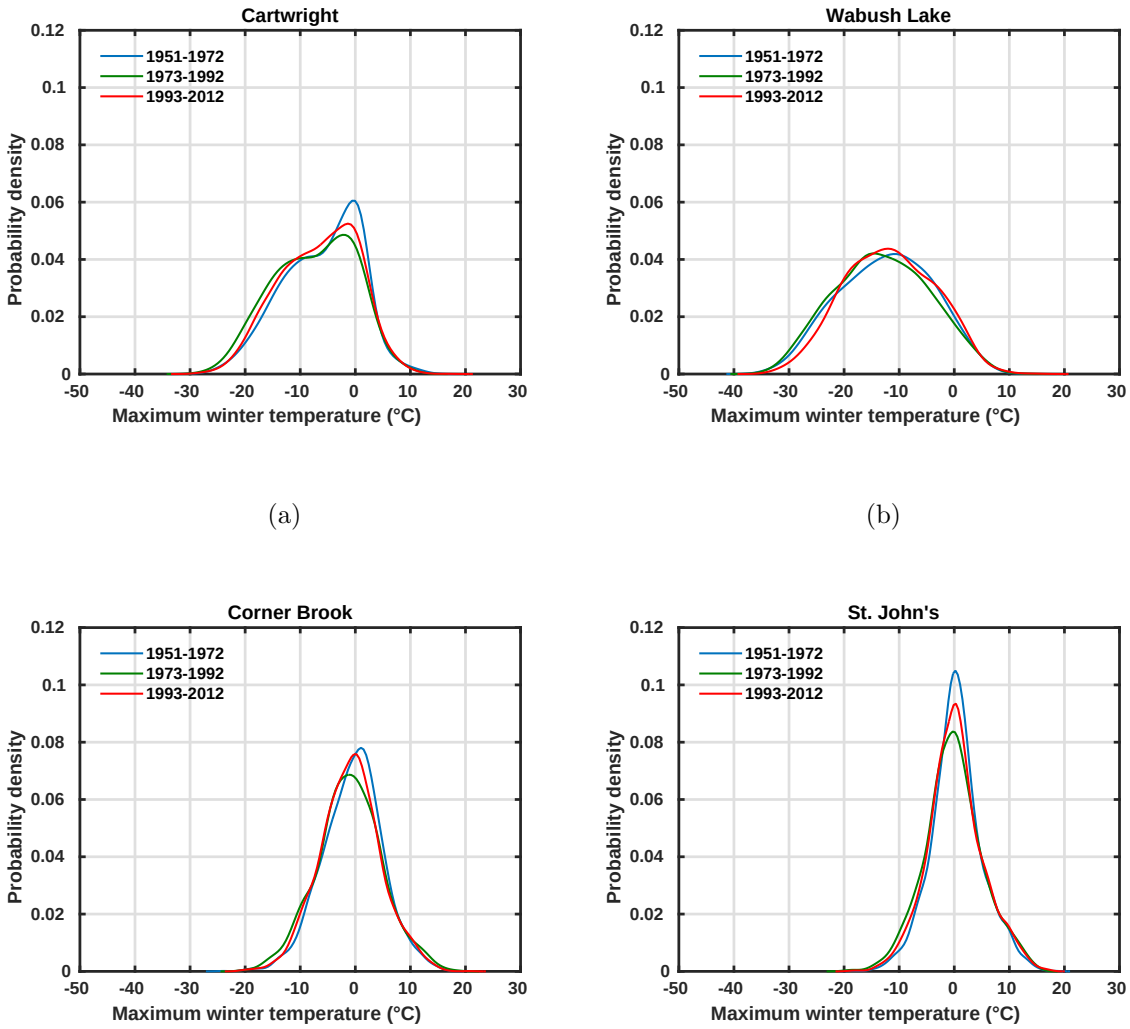

(a) (b)

(c) (d)

Figure 4.5: Kernel Density of maximum winter temperature in (a) Northern and Coastal Labrador; (b) Interior Labrador; (c) West Newfoundland zone; (d) East Newfoundland

4.2.2 Climate Extremes

The extremes are statistically infrequent events for which the atmospheric characteristics have anomalously high or low values. Therefore, we study the statistical distributions of key climate indicators, and identify observations that are well beyond the norm. In this chapter the $10th$ and $90th$ percentile calculated for daily minimum and maximum temperature distributions respectively are analyzed. For precipitation, the $90th$ percentiles for total daily precipitation, rain and snow are calculated to establish the upper threshold. All events that fall below the lower threshold for daily minimum of temperature or above the upper threshold values of daily maximum of temperature are treated as extremes (See Chapter 2).

The number of days with daily maximum temperatures above the 90% threshold are shown by the red curves on Figures 4.6, 4.7. On the same figures, the number of days with daily minimum temperatures below the 10% threshold are shown by the blue curves. Overall, warm (cold) extreme events in maximum temperature have increased (decreased) in the past two decades in Labrador and the west coast of Newfoundland, but not in St. John's and Gander. The overall warming in this period resulted in decreasing number of extreme cold days, particularly in the west coast of Newfoundland and interior Labrador (Wabush Lake and Goose Bay). An interesting observation was made pertaining to the intensity of cold extremes: prior to the continuous decline from the 1990s, the intensities of cold extremes exhibited a decadal oscillation, with the exception of the 1950s, where 1-2 year oscillations were more dominant (Figures 4.6, 4.7). This is interesting because warm extremes did not follow such a coherent pattern, but were rather more stochastic. In all stations, the

extreme cold year of 1972 was caused by a sharp increase in the intensity of extreme cold events.

Figure 4.8 show percentiles for cold and warm extremes of the temperature for different stations, sub-periods and variables. Cold extreme events in maximum temperature show greater changes in eastern Newfoundland (St. John's and Gander), with a decrease of over 3^oC in the first three sub-periods, followed by a period of relatively unchanged extreme cold events in maximum temperature in the following two sub-periods, and an increase in the last sub-period. Warm extreme events in maximum temperatures in the same region oscillated within a lower range of approximately 1^oC. This was also true in stations in Western Newfoundland, where warm extreme events in maximum temperature oscillate within 1^oC, compared to cold extreme events, which are more variable. In all meteorological sites in Newfoundland, the fifth sub-period, which is represents the years 1991-2000 has the highest occurrence of warm extreme events.

Cold extreme events in maximum temperature in Labrador vary within approximately 4^oC between the sub-periods, in Goose Bay and Wabush Lake. In Cartwright, the interdecadal oscillations are muted in comparison with those for Goose Bay and Wabush Lake, with the $10th$ percentile of temperature ranging between -17.7^{o}C and -14.5^{o}C in the third and 6th sub-period, respectively. A notable difference between the island and continental parts of the region is that in continental Labrador, extreme cold temperature events in maximum temperature in the $5th$ sub-period exceeded that of the first sub-period, as seen in Figure 4.5. Comparatively, although warming is observed in the last three sub-periods on the island as well, extreme cold temperatures in maximum temperature events do not warm substantially enough to encompass the

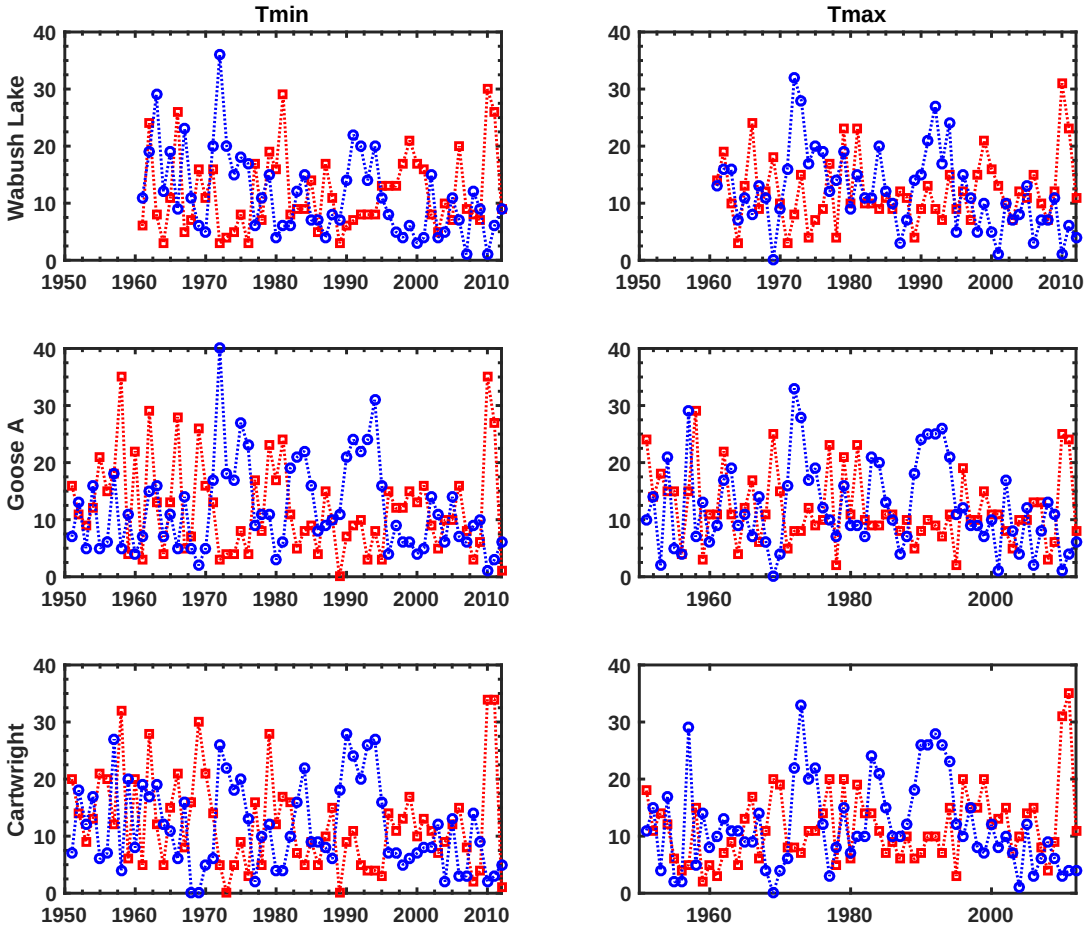

Figure 4.6: Number of annual extreme warm (red) and cold (blue) temperature events in Labrador

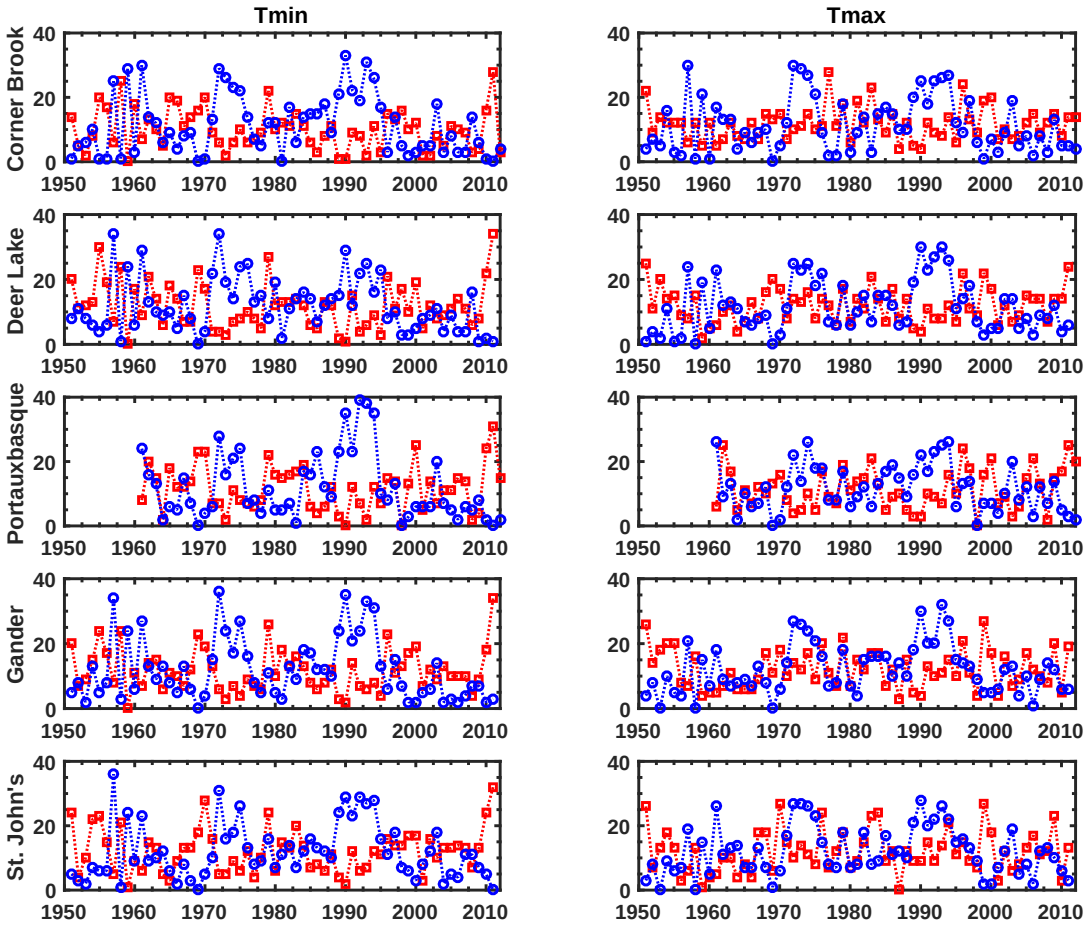

Figure 4.7: Number of annual extreme warm (red) and cold (blue) temperature events in Newfoundland

warm temperature events observed in the 1950s.

Minimum temperature events show an opposite pattern, with extreme warm events in minimum temperature varying within a higher range in Goose Bay and Cartwright, but not in Wabush Lake. In all regions in Newfoundland, variations in extreme warm minimum temperature events are insignificant, while extreme cold events in minimum temperature vary within 1-2^{o}C.

Since the $10th$ ($90th$) percentile indicates the magnitude of the lower (upper) tail of the distribution, an increase (decrease) in this value implies an increase(decrease) in the intensity of cold (warm) extremes. Changes in warm extremes of minimum temperature (Figure 4.8) do not show important changes throughout the period, although a general increase in the $90th$ percentile is seen in minimum temperature at all stations, especially during the last sub-period, indicating an increase in the intensity of warm events. Changes in the $10th$ percentile of maximum temperature depend on the station. The diurnal variations in the atmospheric temperature are shown on Figure C.1.

Similar to the annual mean precipitation time series discussed in Chapter 3, the precipitation extremes vary from year to year but do not show significant decadal or multidecadal changes. The characteristics of extreme precipitation events for all stations are presented in Appendix C.

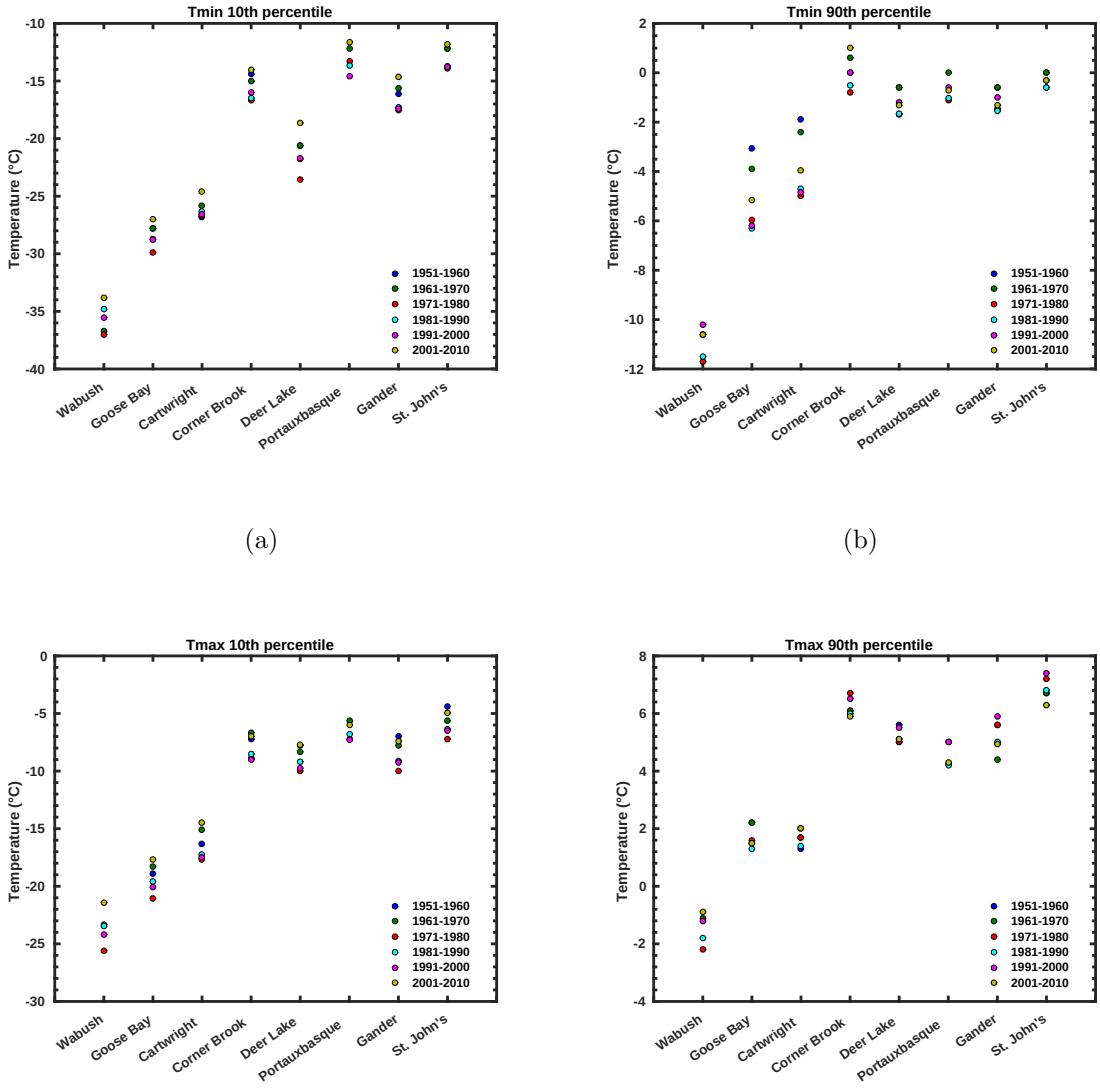

(a) (b)

(c) (d)

Figure 4.8: Regional upper and lower threshold temperatures, calculated as 90th and 10th percentiles respectively, for minimum and maximum daily temperature data.

Chapter 5

River Discharge: anthropogenic and climate impacts

Regime characteristics of rivers are of major importance for freshwater ecosystems of estuarine and coastal regions and water use. The amount of river discharge and water properties affect water quality [23] [39] [75], and the growth rate and distribution of freshwater organisms [28] [29] [70]. In addition, rivers are economically important, for example, for thermoelectric power production [34] [51] [65], drinking water production [83] [86], fisheries [4] [12] [32] and recreation [90] [103]. Due to climate change, regime characteristics of rivers are expected to change. This may have consequences for freshwater ecosystems, water quality and water use in estuarine regions where the rivers flow in. Data and model stuides are often used to assess the impact of climate change and anthropogenic stress on lakes and estuaries at continental [3] [55] and global scales [2] [20] [104] [102]. Understanding variations of river discharge and the impact of climate and human factors on these variations are essential for studies of

environmental dynamics of estuaries. This chapter focuses on analysis of inflow from rivers entering Lake Melville and impact of long term climate change and human activities on the volume of the fresh water discharge.

Lake Melville is an estuarine basin with circulation and dynamics which are strongly influenced by tidal currents [63]. It has a complex topography with depths reaching 180 m in the central part of the basin, combined with a sill which separates the lake from the open ocean. Lake Melville is often classified (see [6]) as a landlocked fjord, due to the large area of the lake compared to the much smaller area of the Narrows, which enclose Lake Melville. This fjord-type estuary is highly stratified; the surface layer consists of fresh water, while the intermediate layer and bottom layers consist mainly of salty waters originating from the Labrador Sea. The surface river discharge into Lake Melville varies seasonally and is an important factor which drives estuarine circulation. The river discharge rates are highest in the springtime, and lowest in the wintertime. At the sill, incoming water from the ocean is flowing in the opposite direction to the surface fresh outflow, thereby transporting salt water into the deep part of the lake. This results in renewal of the intermediate and bottom layers of the estuary. In the winter season when the lake is covered by ice, estuarine circulation is dominated by ocean tides [6].

The demand for renewable and clean energy is growing and development of hydroelectric power plants is of high priority for Newfoundland and Labrador. However, hydroelectric development often has environmental consequences, as the construction of these power generating facilities significantly alters the characteristics of river discharge, and the extent of these consequences often goes beyond the immediate surroundings [17]. One such case is the Upper Churchill Development, which was ac-

companied by much criticism for its considerable alteration to the environment upon its completion in 1971. The constructed dykes serve to regulate the flow of water discharge, while lakes in central Labrador were linked to form the Smallwood reservoir. Consequently, this altered the flow of the Churchill River into Lake Melville. Although the direct causality has not been established with certainty, there are indications that the northern Atlantic cod fishery suffered a severe decline in Groswater Bay and Sandwich Bay at the same time that the flow of Churchill River was altered [84].

The North West River and Churchill Rivers are the biggest rivers entering Lake Melville. The Northern River originates from the Grand Lake which receives its discharge from the Naskaupi River [11]. Northern River inflow into Lake Melville is much smaller than inflow from the Churchill River. The discharge of the two rivers differ seasonally by one to two orders of magnitude during the year. The Churchill River is the largest river in Labrador which drains a major portion of the Labrador Plateau. Therefore, the main focus of this study is the freshwater discharge related to this river only.

The Churchill River is approximately 856 km long from its headwaters near the western Labrador boundary to Lake Melville, and drains a basin of approximately 92,500 km^2. The lower Churchill River and Lake Melville formed in a trough aligned in a northeast-southwest direction, and the river runs in a general west to east orientation (Figure 1.1). The Mealy Mountains are directly adjacent to the trough on its southeastern side.

[11] described the seasonal pattern of the Lake Melville Estuary fresh water inflow based on measurements taken between 1948 and 1953. Winter flows for the Churchill

River ranged from 566 to 708 m^3/s to a summer flow of approximately 3540 to 4240 m^3/s . In winter the fresh water entering the western end of the estuary is of temperature close to 0^oC. The salty bottom water found at the entrance to Lake Melville is of Labrador Sea origin. Reduced fresh water inflow in winter is noted by a salting of the surface layers.

5.1 Seasonal cycle of river discharge

The hydrology of the Churchill River basin reflects the regional climate; runoff is strongly seasonal with high flows in the spring (typically peaking in May or June) and low flows in late winter (blue curve on Figure 5.1). The average annual flow at Churchill Falls is 1,390 m^3/s. At Gull Island it is 1,780 m^3/s and at Muskrat Falls it is 1,840 m^3/s. Flows in the Churchill River are moderated by the operation of the Churchill Falls Generating Station which has been in place for more than 30 years. As an illustration of downstream flow effects, the highest average monthly flows at Muskrat Falls have decreased and the lowest monthly flows have increased, compared to flows before the Churchill Falls Generating Station became operational (red curve on Figure 5.1). Moreover, the peak in the seasonal cycle of river discharge shifted from June to May. After the construction of the Upper Churchill facilities, the river flow into the Lake Melville became steadier in time. The river discharge after 1971 remains close to 1800 m^3/s throughout the year with the exception of the peak in April - May. The differences between the high values in autumn and low values in winter observed before 1971 (blue curve on Figure 5.1), are not present after 1971 (red curve on Figure 5.1), when the amplitude of the seasonal cycle of river discharge

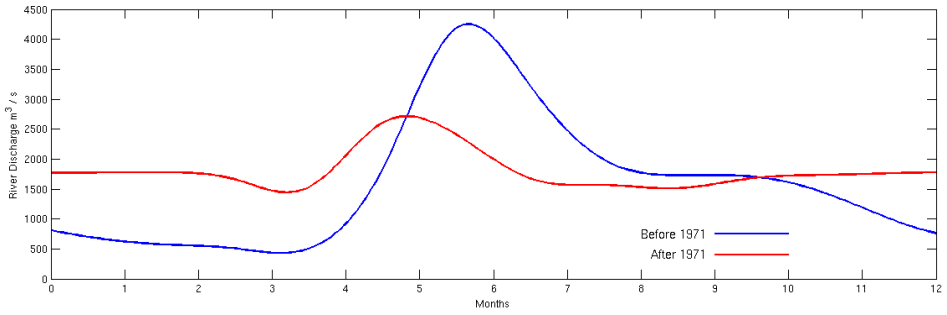

Figure 5.1: Mean seasonal cycle of Churchill River discharge at Muskrat Falls

is significantly smaller than before 1971.

These changes result from the fact that since 1971, the river discharge significantly increases in the winter season (by 1301 m^3/s) when the hydropower facility is working more actively, thus resulting in a less pronounced seasonal cycle. At the same time the annual mean river discharge after 1971 remains almost the same as the annual mean river discharge before 1971 and is about 1800 m^3/s.

A further insight into the impact of the Upper Churchill hydropower facilities on the seasonal cycle of river discharge is provided by the distribution of daily river inflow by Churchill River before 1971, between 1972 and 1980, and after 1981 (Figure 5.2). The distribution of river discharge volume after the Upper Churchill development is based on observations for the period after 1981. This is done because our analysis (not shown here) demonstrates that there is a transition period between typical river discharge volume prior to 1971 and after 1971, which lasted for approximately eight to nine years.

The distribution of river discharge before 1971 has two dominant modes - the first is the winter low levels with a distribution maximum at about 500 m^3/s. The second

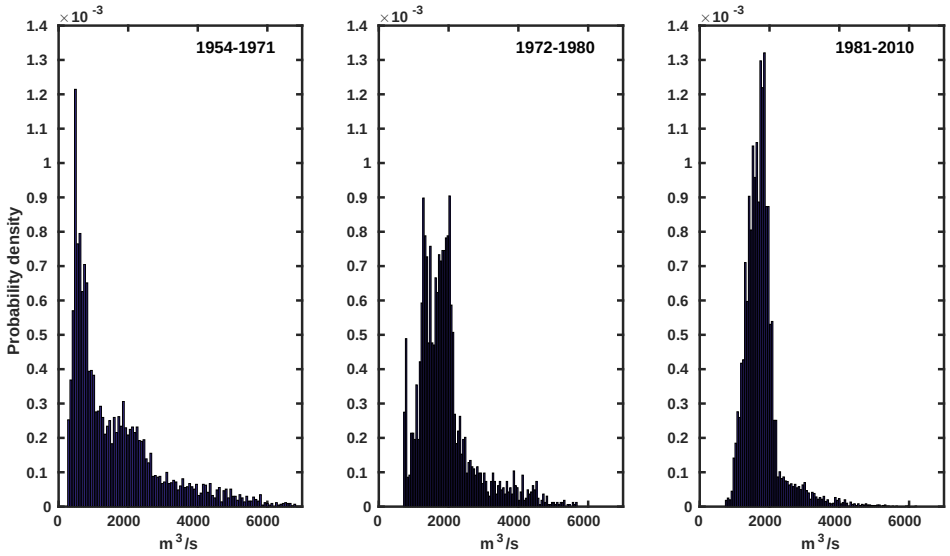

Figure 5.2: Distribution of daily mean river discharge (a) before 1971 and (b) from 1971-1980 and (c) after 1981. River discharge measured at site in Churchill River above Muskrat Falls.

mode is associated with the autumn typical discharge, which corresponds to a local distribution maximum at about $2000m^3/s$. The large spring maximum (blue curve on Figure 5.1) corresponds to the tail of the discharge volume distribution with values larger than 3000 m^3/s.

The predominantly steady river discharge through the year after 1981 (red curve on Figure 5.1) results in a uni-modal distribution with a maximum at about $1800m^3/s$. This is the typical value of the discharge during most of the months through the year. The tail associated with the spring maximum in the river inflow is much smaller than observed before 1971, suggesting that the spring flow maximum significantly decreased in magnitude and in duration.

The specific impact of the reduction of the amplitude of the seasonal cycle of the river discharge also depends on the fact that it is localized in the western part of Lake Melville. The dynamics of this region are essential for the formation of the basin estuarine circulation. The seasonal variations of freshwater input and associated changes in surface salinity in the lake influence the thermodynamic process of sea-ice formation and melting. The preliminary model study of [89] suggests that these effects can cause changes in the surface with magnitude of about 10 - 20 cm which can change sign across the lake.

One important question about these anthropogenically driven variations in the river discharge and their environmental impact is how they interact with the changes driven by climate change. Here this question is studied based on comparison of river discharge for anomalously warm and cold years before and after 1971. Similarly, the river discharge before and after 1971 is compared for years with anomalously high and low total precipitation volumes.

5.1.1 Impact of climate dynamics on river discharge

Figures 5.3, 5.4 show the river discharge before and after 1971 for cold and warm years. For comparison, the dashed red and blue lines show the seasonal cycle of river discharge before and after 1971 from Figure 5.1. We observe that the river discharge after 1971 remains close to the seasonal mean values with minor fluctuations in some of the months. The only significant difference is the relatively low river discharge in the winter months of cold 1992 (Figure 5.4). The anomalies in the river discharge before 1971 have larger magnitudes than before 1971. The largest deviation from the

seasonal cycle in cold and warm years is present in summer months (June, July and August). This anomaly is positive in warm years and negative in cold years.

These anomalies in the river discharge before 1971 can be associated with the intensity of melting of ice and snow in Labrador. As mention in Chapter 3 the summer in Labrador is relatively short. The temperature in the warm season is important for the melting of ice and snow after the long winter. When this temperature is higher, the greater than normal melting process provides higher contributions to the rivers. The presence of the dam after 1971 regulates the flow and practically removes the increased/decreased temperature effects.

The differences in the river discharge for wet (with higher than normal precipitation) and dry (with lower than normal precipitation) years are less pronounced than the differences between warm and cold years. The major differences between wet and dry years after 1971 occur in the spring months of April and May, with a sharp maximum being observed for the river discharge in 1999.

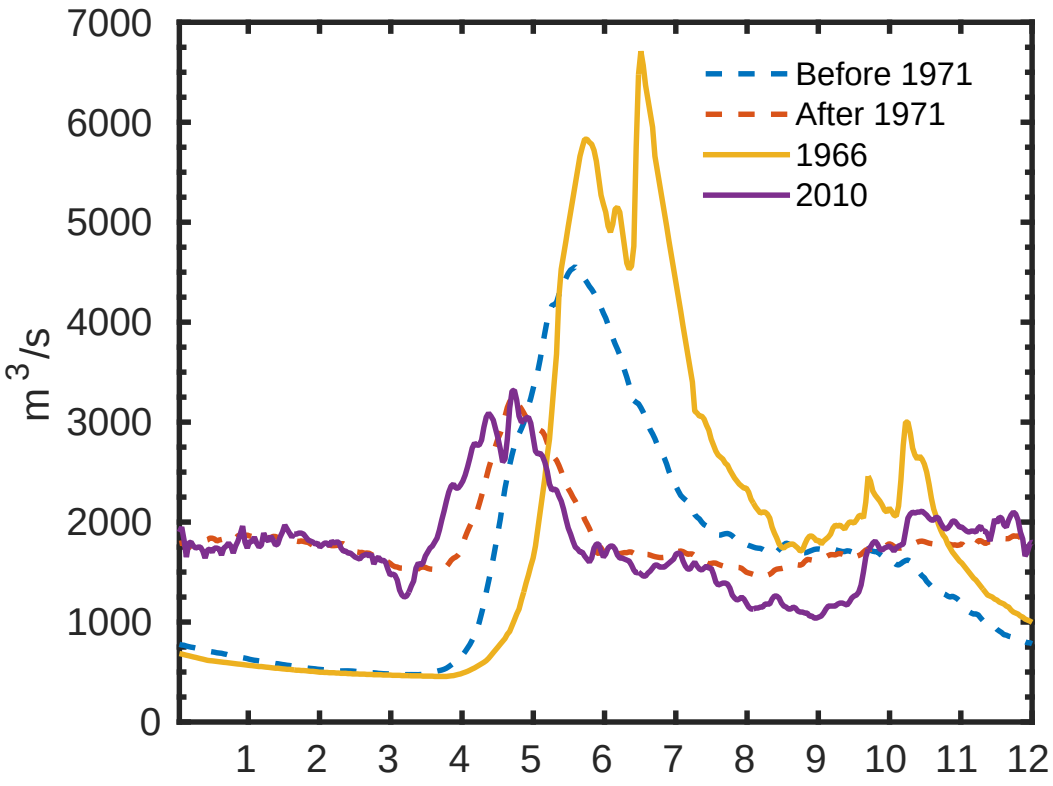

Figure 5.3: River discharge during warm years, before and after hydroelectric construction. Mean discharge volume prior to and post development is presented in dashed lines.

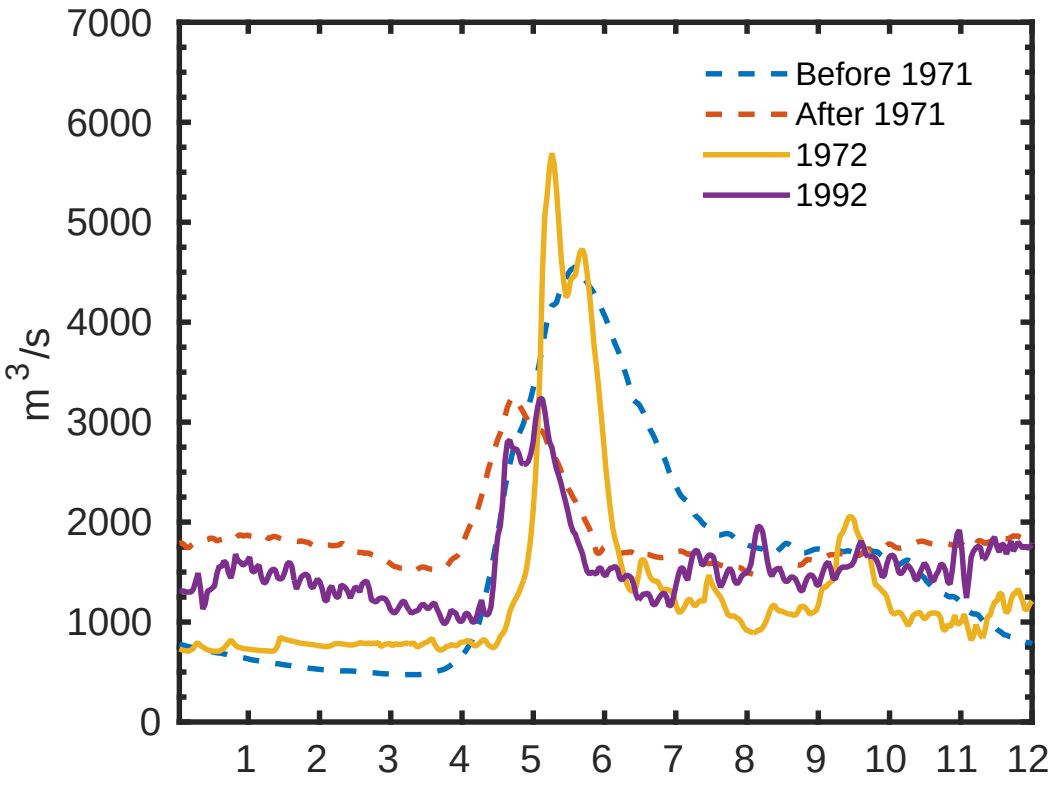

Figure 5.4: River discharge during cold years, before and after hydroelectric construction. Mean discharge volume prior to and post development is presented in dashed lines.

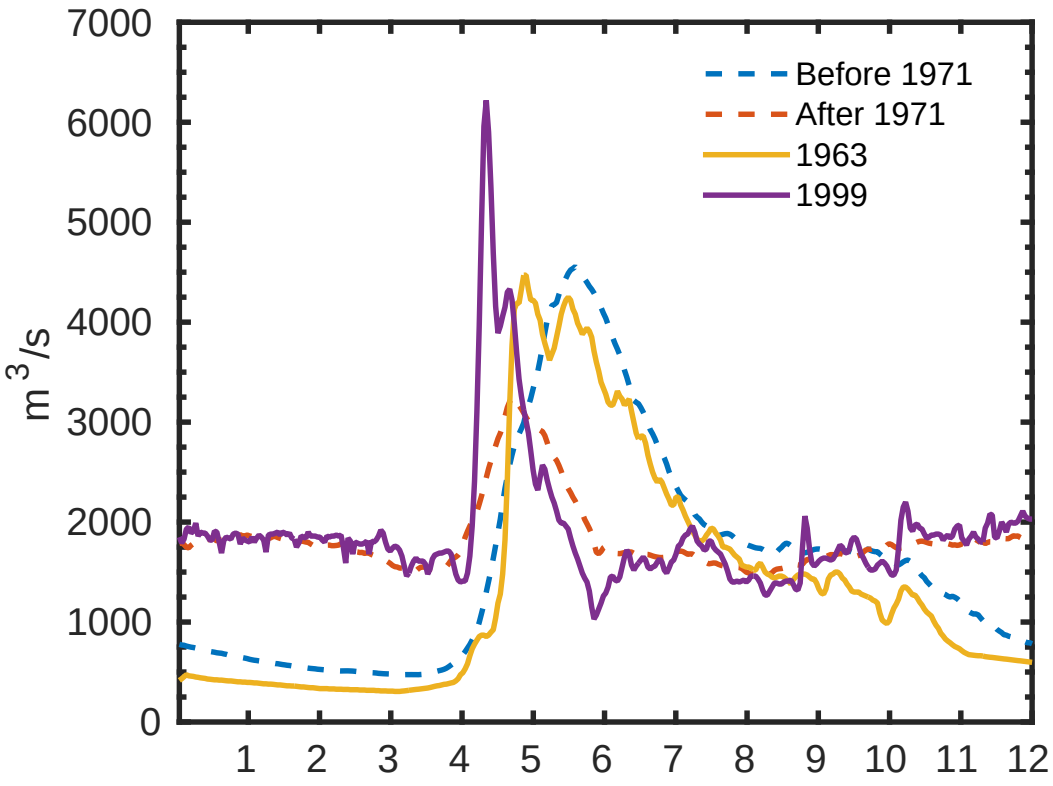

Figure 5.5: River discharge during wet years, before and after hydroelectric construction. Mean discharge volume prior to and post development is presented in dashed lines.

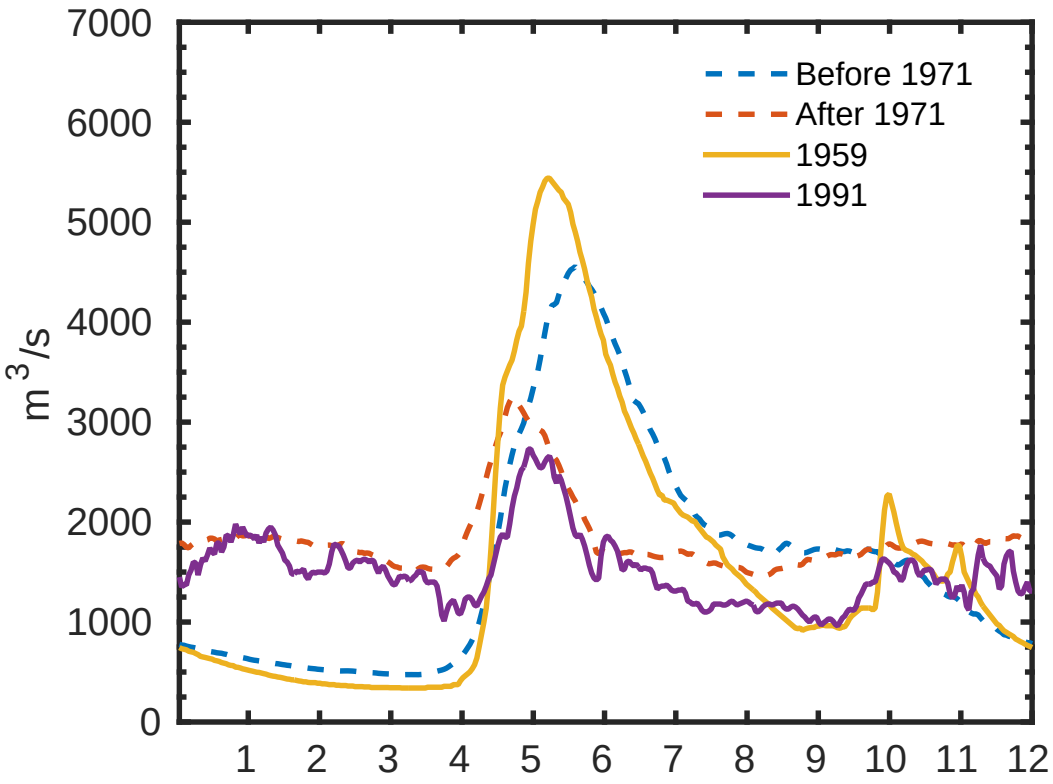

Figure 5.6: River discharge during dry years, before and after hydroelectric construction. Mean discharge volume prior to and post development is presented in dashed lines.

Chapter 6

Conclusions

The results from this study demonstrated that:

- There are two periods longer than a decade that can be distinguished in the variations of surface atmospheric temperature trends in Newfoundland and Labrador. These two dominant periods are between 1972 and 1992 and between 1993 and 2012.

- The cold trend in the first period was found to vary between -0.01^{o}C/year in St. John's to about -0.06^{o}C/year in Daniel's Harbor and Churchill Falls. The warm trend in the second period varies between 0.06^{o}C/year in Eastern and Central Newfoundland and Nain and 0.11^{o}C/year in interior and coastal Labrador.

- The multidecadal trends during the two periods were superimposed on much more intense decadal, interannual and seasonal variations. As a result, the cold trend in the first period was found to be statistically non-significant in all of the stations across the province. The warming trend in the second period is statistically significant only in the stations of West Newfoundland, Interior and Coastal Labrador.

- The warming trends in the second period were found to be associated with a

reduced number of days with extremely cold temperatures rather than an increase of warm extremes.

- No significant trends on multidecadal periods in precipitations were found in the data. This suggests that the most important elements of long term variability of precipitations are the interannual and decadal time intervals.

- The anthropogenic impact which resulted from the hydroelectric development had important effects on the seasonal cycle of river discharge into Lake Melville. These effects were studied by analyzing the change in the river discharge after the construction of Upper Churchill hydropower facilities.

- The impact of Upper Churchill caused "flattening" of the seasonal cycle, i.e. reduction of the intense spring peak of river inflow to the lake and an increase of steady river discharge during the rest of the year. River discharge in the winter after 1971 increased by 1301 m^3/s. The total annual river discharge did not change significantly before and after the construction of Upper Churchill.

Chapter 7

Future work

The results from this thesis beg important research questions about the response of the environment of Lake Melville to climate change and local anthropogenic stress. Answering these questions requires research into three major areas:

- Study of the response of the physical environment of Lake Melville to the alteration in river discharge due to the Upper Churchill development. This research would provide answers about how the circulation, sea-ice, vertical stratification and mixing changed following the construction of the Upper Churchill hydropower facility.

- Study how the impact of climate change affects this response.

- Study of the response of biochemistry and the ecosystem of Lake Melville to the anthropogenically driven changes in the river discharge.

These studies would require continuation and expansion of the existing observational network across the lake (see also [89], [63]) and model simulations of the Hamilton Inlet. A great impact on future studies of Lake Melville would be the availability of regular observations of sea-ice, sea surface temperature and sea surface

salinity along the coast.

Bibliography

[1] M. R. Anderson, D. A. Scruton, U. P. Williams, and J. F. Payne. Mercury in fish in the smallwood reservoir, labrador, twenty one years after impoundment. *Water, Air, and Soil Pollution*, 80(1-4):927–930, 1995.

[2] N. W. Arnell. Climate change and global water resources. *Global Environmental Change*, 9(1):S31–S49, 1999.

[3] N. W. Arnell. The effect of climate change on hydrological regimes in Europe : a continental perspective. *Global Environmental Change*, 9(1):5–23, 1999.

[4] J. M. Bartholow. A modeling assessment of the thermal regime for an urban sport fishery. *Environmental Management*, 15(6):833–845, 1991.

[5] S. Bernal, L. O. Hedin, G. E. Likens, S. Gerber, and D. C. Buso. Complex response of the forest nitrogen cycle to climate change. *Proceedings of the National Academy of Sciences*, 109(9):3406–3411, 2012.

[6] J. Bobbitt and S. Akenhead. *Influence of controlled discharge from the Churchill River on the oceanography of Groswater Bay, Labrador*. Research and Resource Services, Department of Fisheries and Oceans, 1982.

[7] B. R. Bonsal, X. Zhang, L. A. Vincent, and W. D. Hogg. Characteristics of daily and extreme temperatures over canada. *Journal of Climate*, 14(9):1959–1976, 2001.

[8] N. R. Catto, of Fisheries, C. Dept., Oceans. Science, Oceans, Branch, and Environment. *The coastline of eastern Newfoundland*. St. John's, Nfld.: Fisheries and Oceans Canada, 2003.

[9] M. Chin, R. A. Kahn, and S. E. Schwartz. Atmospheric aerosol properties and climate impacts. a report by the us climate change science program and the subcommittee on global change research. Technical report, National Aeronautics and Space Administration, Washington, DC, 2009.

[10] J. E. Cloern. Turbidity as a control on phytoplankton biomass and productivity in estuaries. *Continental Shelf Research*, 7(11):1367–1381, 1987.

[11] L. K. Coachman. River flow and winter hydrographic structure of the hamilton inlet–lake melville estuary of labrador: Blue dolphin labrador expedition–winter project 1953: Hanover, new hampshire, dartmouth college museum, 19 p, 1953.

[12] K. Cochrane, C. D. Young, D. Soto, and T. Bahri. Climate change implications for fisheries and aquaculture. *FAO Fisheries and aquaculture technical paper*, 530:212, 2009.

[13] E. B. Colbourne and C. Fitzpatrick. Physical oceanographic conditions in nafo sub-areas 2 and 3 on the newfoundland and labrador shelf during 2001. *NAFO SCR Doc*, 41, 2002.

[14] R. G. Curry and M. S. McCartney. Ocean Gyre Circulation Changes Associated with the North Atlantic Oscillation. *Journal of Physical Oceanography*, 31(12):3374–3400, 2001.

[15] R. D'Arrigo, B. Buckley, S. Kaplan, and J. Woollett. Interannual to multidecadal modes of labrador climate variability inferred from tree rings. *Climate Dynamics*, 20(2-3):219–228, 2003.

[16] R. D. D'Arrigo, G. C. Jacoby, and R. M. Free. Tree-ring width and maximum latewood density at the North American tree line: parameters of climatic change. *Canadian Journal of Forest Research*, 22(9):1290–1296, 1992.

[17] B. Denes and B. A. Roberts. Environmental Impact of Flooding in the Main (Smallwood) Reservoir of the Churchill Falls Power Plant, Labrador, Canada. I. Background and descriptions of flooded conditions related to vegetation and land cover types. *Journal of Water Resource and Protection*, 2011, 2011.

[18] R. R. Dickson, J. Meincke, S. Malmberg, and A. J. Lee. The great salinity anomaly in the northern north atlantic 1968-1982. *Progress in Oceanography*, 20(2):103–151, 1988.

[19] R. R. Dickson, T. J. Osborn, J. W. Hurrell, J. Meincke, J. Blindheim, B. Adlandsvik, T. Vinje, G. Alekseev, and W. Maslowski. The arctic ocean response to the north atlantic oscillation. *Journal of Climate*, 13(15):2671–2696, 2000.

[20] P. Döll and J. Zhang. Impact of climate change on freshwater ecosystems: a global-scale analysis of ecologically relevant river flow alterations. *Hydrology and Earth System Sciences*, 14(5):783–799, 2010.

[21] E. M. Douglas, R. M. Vogel, and C. N. Kroll. Trends in floods and low flows in the united states: impact of spatial correlation. *Journal of Hydrology*, 240(1):90–105, 2000.

[22] K. Drinkwater and G. C. Harding. Effects of the hudson strait outflow on the biology of the labrador shelf. *Canadian Journal of Fisheries and Aquatic Sciences*, 58(1):171–184, 2001.

[23] A. Ducharne. Importance of stream temperature to climate change impact on water quality. *Hydrology and Earth System Sciences*, 12(3):797–810, 2008.

[24] M. J. Dunbar. *Eastern Arctic Waters: A Summary of Our Present Knowledge of the Physical Oceanography of the Eastern Arctic Area, from Hudson Bay to Cape Farewell and from Belle Isle to Smith Sound*. Fisheries Research Board of Canada, 1951.

[25] M. A. C. E., Demirov, and J. Zhu. A model study of the relationship between sea-ice variability and surface and intermediate water mass properties in the labrador sea. *Atmosphere-Ocean*, 52(2):142–154, 2014.

[26] D. R. Easterling, L. V. Alexander, A. Mokssit, and V. Detemmerman. CCI/CLIVAR Workshop to Develop Priority Climate Indices. *Bulletin of the American Meteorological Society*, 84(10):1403–1407, 2003.

[27] D. R. Easterling, J. L. Evans, P. Y. Groisman, T. R. Karl, K. E. Kunkel, and P. Ambenje. Observed variability and trends in extreme climate events: A brief review*. *Bulletin of the American Meteorological Society*, 81(3):417–425, 2000.

[28] J. G. Eaton and R. M. Scheller. Effects of climate warming on fish thermal habitat in streams of the United States. *Limnology and Oceanography*, 41(5):1109–1115, 1996.

[29] J. L. Ebersole, W. J. Liss, and C. A. Frissell. Relationship between stream temperature, thermal refugia and rainbow trout Oncorhynchus mykiss abundance in arid-land streams in the northwestern United States. *Ecology of Freshwater Fish*, 10(1):1–10, 2001.

[30] C. Eden and T. Jung. North Atlantic interdecadal variability: oceanic response to the North Atlantic Oscillation (1865-1997). *Journal of Climate*, 14(5):676–691, 2001.

[31] P. Ellaway. Cumulative sum technique and its applicatoin to the analysis of peristimulus time histograms. *Electroencephalography and Clinical Neurophysiology*, 45:302–304, 1978.

[32] A. D. Ficke, C. A. Myrick, and L. J. Hansen. Potential impacts of global climate change on freshwater fisheries. *Reviews in Fish Biology and Fisheries*, 17(4):581–613, 2007.

[33] J. Finnis and T. Bell. An analysis of recent observed climate trends and variability in labrador. *The Canadian Geographer/Le Géographe canadien*, 59(2):151–166, 2015.

[34] H. Förster and J. Lilliestam. Modeling thermoelectric power generation in view of climate change. *Regional Environmental Change*, 10(4):327–338, 2009.

[35] P. Gachon, A. St-Hilaire, T. B. M. J. Ouarda, V. T. V. Nguyen, C. Lin, J. Milton, D. Chaumont, J. Goldstein, M. Hessami, T. D. Nguyen, et al. A first evaluation of the strength and weaknesses of statistical downscaling methods for simulating extremes over various regions of eastern canada. *Final report, Sub-component, Climate Change Action Fund (CCAF), Environment Canada, Montréal, Québec, Canada*, 15, 2005.

[36] R. O. Gilbert. *Statistical methods for environmental pollution monitoring*. John Wiley & Sons, 1987.

[37] P. Y. Groisman, R. W. Knight, D. R. Easterling, T. R. Karl, G. C. Hegerl, and V. N. Razuvaev. Trends in intense precipitation in the climate record. *Journal of climate*, 18(9):1326–1350, 2005.

[38] P. Y. Groisman, B. Sun, R. S. Vose, J. H. Lawrimore, P. H. Whitfield, E. Førland, I. Hanssen-Bauer, M. C. Serreze, V. N. Razuvaev, and G. V. Alekseev. 4.8. CONTEMPORARY CLIMATE CHANGES IN HIGH LATITUDES OF THE NORTHERN HEMISPHERE: DAILY TIME RESOLUTION. In *14th Symposium on Global Change and Climate Variations*, 2003.

[39] I. Haag and B. Westrich. Processes governing river water quality identified by principal component analysis. *Hydrological Processes*, 16(16):3113–3130, 2002.

[40] K. H. Hamed and A. R. Rao. A modified mann-kendall trend test for autocorrelated data. *Journal of Hydrology*, 204(1):182–196, 1998.

[41] T. Hauser, E. Demirov, J. Zhu, and I. Yashayaev. North atlantic atmospheric and ocean inter-annual variability over the past fifty years-dominant patterns and decadal shifts. *Progress in Oceanography*, 132:197–219, 2015.

[42] M. R. Haylock, T. C. Peterson, L. M. Alves, T. Ambrizzi, Y. M. T. Anunciação, J. Baez, V. R. Barros, M. A. Berlato, M. Bidegain, G. Coronel, et al. Trends in total and extreme south american rainfall in 1960-2000 and links with sea surface temperature. *Journal of climate*, 19(8):1490–1512, 2006.

[43] D. R. Helsel. More than obvious: better methods for interpreting nondetect data. *Environmental science & technology*, 39(20):419A–423A, 2005.

[44] R. M. Hirsch and J. R. Slack. A nonparametric trend test for seasonal data with serial dependence. *Water Resources Research*, 20(6):727–732, 1984.

[45] M. Hollander and D. A. Wolfe. Nonparametric statistical analysis. *Wiley & Sons, New York*, pages 27–74, 1973.

[46] J. W. Hurrell and C. Deser. North atlantic climate variability: the role of the north atlantic oscillation. *Journal of Marine Systems*, 79(3):231–244, 2009.

[47] J. W. Hurrell, Y. Kushnir, G. Ottersen, and M. Visbeck. An overview of the north atlantic oscillation. *Geophysical Monograph. American Geophysical Union*, 134:1–36, 2003.

[48] IPCC. *Climate Change 2014: Synthesis Report. Contribution of Working Groups I, II and III to the Fifth Assessment Report of the Intergovernmen-*

tal Panel on Climate Change, R. K. Pachauri and L. A. Meyer (eds.). IPCC Geneva Switzerland, 2014.

[49] W. H. S. Jr, R. H. Loucks, K. F. Drinkwater, and A. R. Coote. Nutrient Flex onto the Labrador Shelf from Hudson Strait and its Biological Consequences. *Canadian journal of fisheries and aquatic sciences*, 40(10):1692–1701, 1983.

[50] M. Kendall. *Multivariate analysis*. Charles Griffin, 1975.

[51] H. Koch and S. Vögele. Dynamic modelling of water demand, water availability and adaptation strategies for power plants to global change. *Ecological Economics*, 68(7):2031–2039, 2009.

[52] R. C. Kollmeyer, D. A. McGill, and N. Corwin. Oceanography of the Labrador Sea in the vicinity of Hudson Strait in 1965. Technical report, DTIC Document, 1967.

[53] J. R. N. Lazier. Seasonal variability of temperature and salinity in the labrador current. *J. Mar. Res*, 40:341–356, 1982.

[54] J. R. N. Lazier and D. G. Wright. Annual velocity variations in the Labrador Current. *Journal of Physical Oceanography*, 23(4):659–678, 1993.

[55] B. Lehner, P. Döll, J. Alcamo, T. Henrichs, and F. Kaspar. Estimating the Impact of Global Change on Flood and Drought Risks in Europe: A Continental, Integrated Analysis. *Climatic Change*, 75(3):273–299, 2006.

[56] S. Levitus, J. I. Antonov, T. P. Boyer, R. A. Locarnini, H. E. Garcia, and A. V. Mishonov. Global ocean heat content 19552008 in light of recently revealedinstrumentation problems. *Geophysical Research Letters*, 36(L07608), 2009.

[57] H. Lindeboom. The coastal zone: an ecosystem under pressure. In *Oceans*, volume 2020, pages 49–84, 2002.

[58] H. F. Lins and J. R. Slack. Streamflow trends in the united states. *Geophysical research letters*, 26(2):227–230, 1999.

[59] J. W. Loder, W. C. Boicourt, and J. H. Simpson. Western ocean boundary shelves coastal segment (w). *The Sea*, 11:3–27, 1998.

[60] K. Lohmann, H. Drange, and M. Bentsen. A possible mechanism for the strong weakening of the North Atlantic subpolar gyre in the mid-1990s. *Geophysical Research Letters*, 36(15), 2009.

[61] M. S. Lozier, V. Roussenov, M. S. C. Reed, and R. G. Williams. Opposing decadal changes for the North Atlantic meridional overturning circulation. *Nature Geoscience*, 3(10):728–734, 2010.

[62] A. LU, S. KANG, D. PANG, T. Wang, et al. Asynchronous temperature variation across china under the background of global warming. *Arid Land Geography*, 32(4):506–511, 2009.

[63] Z. Lu, B. deYoung, and J. Foley. Analysis of Physical Oceanographic Data from Lake Melville, Labrador, July-September 2012. Technical report, Physics and Physical Oceanography Data Report 2013-1, Memorial University, 2013.

[64] H. B. Mann. Nonparametric tests against trend. *Econometrica: Journal of the Econometric Society*, pages 245–259, 1945.

[65] B. Manoha, F. Hendrickx, A. Dupeyrat, C. Bertier, and S. Parey. Impact des évolutions climatiques sur les activités dEDF (projet impec). *La Houille Blanche*, 2:55–60, 2008.

[66] S. R. Marko, D. B. Fissel, P. Wadhams, P. Kelly, and R. D. Brown. Iceberg Severity of Eastern North America: Its Relationship to Sea Ice Variability and Climate Change. *Journal of Climate*, 7(9):1335–1351, 1994.

[67] J. Marshall, F. Dobson, K. Moore, P. Rhines, M. Visbeck, E. d'Asaro, K. Bumke, S. Chang, R. Davis, K. Fischer, et al. The labrador sea deep convection experiment. *Bulletin of the American Meteorological Society*, 79(10):2033–2058, 1998.

[68] J. Marshall and F. Schott. Open-ocean convection: Observations, theory, and models. *Rev. Geophys*, 37(1):1–64, 1999.

[69] R. Modarres and V. de Paulo Rodriguez da Silva. Rainfall trends in arid and semi-arid regions of iran. *Journal of Arid Environments*, 70(2):344–355, 2007.

[70] O. Mohseni, H. G. Stefan, and J. G. Eaton. Global Warming and Potential Changes in Fish Habitat in U.S. Streams. *Climatic Change*, 59(3):389–409, 2003.

[71] M. R. Morgan, K. F. Drinkwater, and R. Pocklington. Temperature trends at coastal stations in eastern Canada. *Climatological Bulletin*, 27(3):135–153, 1993.

[72] T. P. Murat and Küçük. Long-term trend analysis using discrete wavelet components of annual precipitations measurements in marmara region (turkey). *Physics and Chemistry of the Earth, Parts A/B/C*, 31(18):1189–1200, 2006.

[73] R. A. Myers, J. Helbig, D. Holland, and S. Braneh. SEASONAL AND lNTER-ANNUAL VARlABlLlTY OF THE LABRADOR CURRENT AND WEST GREENLAND CURRENT. 1989.

[74] R. G. Najjar, H. A. Walker, P. J. Anderson, E. J. Barron, R. J. Bord, J. R. Gibson, V. S. Kennedy, G. Knight, P. Robert, C. O'Connor, D. Polsky, N. P. Psuty, B. A. Richards, L. G. Sorenson, E. M. Steele, and R. S. Swanson. The potential impacts of climate change on the mid-atlantic coastal region. *Climate Research*, 14(3):219–233, 2000.

[75] N. Ozaki, T. Fukushima, H. Harasawa, T. Kojiri, K. Kawashima, and M. Ono. Statistical analyses on the effects of air temperature fluctuations on river water qualities. *Hydrological Processes*, 17(14):2837–2853, 2003.

[76] T. Partal and E. Kahya. Trend analysis in turkish precipitation data. *Hydrological processes*, 20(9):2011–2026, 2006.

[77] M. C. Peel, B. L. Finlayson, and T. A. McMahon. Updated world map of the koppen-geiger climate classification. *Hydrology and Earth System Sciences*, 4(2):439–473, 2007.

[78] M. C. Peel, B. L. Finlayson, and T. A. McMahon. Updated world map of the K{ö}ppen-Geiger climate classification. *Hydrology and Earth System Sciences Discussions Discussions*, 4(2):439–473, 2007.

[79] T. Peterson, C. Folland, G. Gruza, W. Hogg, A. Mokssit, and N. Plummer. *Report on the activities of the working group on climate change detection and related rapporteurs*. World Meteorological Organization Geneva, 2001.

[80] T. C. Peterson, M. A. Taylor, R. Demeritte, D. L. Duncombe, S. Burton, F. Thompson, A. Porter, M. Mercedes, E. Villegas, R. S. Fils, et al. Recent changes in climate extremes in the caribbean region. *Journal of Geophysical Research: Atmospheres*, 107(D21), 2002.

[81] N. Plummer, M. J. Salinger, N. Nicholls, R. Suppiah, K. J. Hennessy, R. M. Leighton, B. Trewin, C. M. Page, and J. M. Lough. Changes in climate extremes over the Australian region and New Zealand during the twentieth century. In *Weather and Climate Extremes*, pages 183–202. Springer, 1999.

[82] W. Qian and X. Lin. Regional trends in recent temperature indices in china. *Climate Research*, 27(2):119–134, 2004.

[83] T. A. B. Ramaker, A. F. M. Meuleman, L. Bernhardi, and G. Cirkel. Climate change and drinking water production in The Netherlands: a flexible approach. *Water Science and Technology*, 51(5):37–44, 2005.

[84] D. Saunders. The absence of codfish in groswater bay with emphasis on the pack's harbour fishery : interviews with fishermen. Technical Report OREP, Offshore Labrador Biological Studies Program, 1981.

[85] P. K. Sen. Estimates of the regression coefficient based on kendall's tau. *Journal of the American Statistical Association*, 63(324):1379–1389, 1968.

[86] H. A. J. Senhorst and J. J. G. Zwolsman. Climate change and effects on water quality: a first impression. *Water Science and Technology*, 51(5):53–59, 2005.

[87] A. Shabbar, B. Bonsal, and M. Khandekar. Canadian Precipitation Patterns Associated with the Southern Oscillation. *Journal of Climate*, 10(12):3016–3027, 1997.

[88] T. Sheldon and T. Bell. Understanding and responding to the effects of climate change and modernization in nunatsiavut. Technical report, ArcticNet Annual Research Compendium; http://www.arcticnet.ulaval.ca/pdf/compendium2013-14/nunatsiavut_nuluak_2013-14.pdf, 2014.

[89] T. Sheldon and co authors. Lake melville, avativut, kanuittailinnivut. scientific report. Technical report, Nunatsiavut Government; http://makemuskratright.com/wp-content/uploads/2016/04/ScienceReport-low1.pdf, 2016.

[90] R. J. Swart. Impacts of Europe's changing climate2008 indicator-based assessment. Technical report, European Environment Agency (EEA), 2008.

[91] H. Tabari and S. Marofi. Changes of pan evaporation in the west of iran. *Water Resources Management*, 25(1):97–111, 2011.

[92] H. Tabari, B. S. Somee, and M. R. Zadeh. Testing for long-term trends in climatic variables in iran. *Atmospheric Research*, 100(1):132–140, 2011.

[93] A. M. G. K. Tank and G. P. Können. Trends in Indices of Daily Temperature and Precipitation Extremes in Europe, 194699. *Journal of Climate*, 16(22):3665–3680, 2003.

[94] H. Tao, M. Gemmer, Y. Bai, B. Su, and W. Mao. Trends of streamflow in the tarim river basin during the past 50 years: Human impact or climate change? *Journal of Hydrology*, 400:1–9, 2011.

[95] D. W. J. Thompson, S. Lee, and M. P. Baldwin. Atmospheric processes governing the northern hemisphere annular mode/north atlantic oscillation. *Geophysical Monograph-American Geophysical Union*, 134:81–112, 2003.

[96] Q. Tian, Q. Wang, C. Zhan, X. Li, and X. Liu. Analysis of climate change in the coastal zone of eastern china, against the background of global climate change over the last fifty years: Case study of shandong peninsula, china. *International Journal of Geosciences*, 3:379–390, 2012.

[97] D. Tolmazin. Changing coastal oceanography of the black sea. i: Northwestern shelf. *Progress in oceanography*, 15(4):217–276, 1985.

[98] G. K. Vallis, E. P. Gerber, P. J. Kushnir, and B. A. Cash. A mechanism and simple dynamical model of the north atlantic oscillation and annular modes. *Journal of the Atmospheric Sciences*, 61(3):264–280, 2004.

[99] L. A. Vincent and E. Mekis. Changes in daily and extreme temperature and precipitation indices for canada over the twentieth century. *Atmosphere-Ocean*, 44(2):177–193, 2006.

[100] L. A. Vincent, T. C. Peterson, V. R. Barros, M. B. Marino, M. Rusticucci, G. Carrasco, E. Ramirez, L. M. Alves, T. Ambrizzi, M. A. Berlato, et al. Observed trends in indices of daily temperature extremes in south america 1960-2000. *Journal of climate*, 18(23):5011–5023, 2005.

[101] M. Visbeck, E. P. Chassignet, R. G. Curry, T. Delworth, R. R. Dickson, and G. Krahmann. The ocean's response to north atlantic oscillation variability. *Geophysical Monograph-American Geophysical Union*, 134:113–146, 2003.

[102] C. J. Vörösmarty, P. Green, J. Salisbury, and R. B. Lammers. Global Water Resources: Vulnerability from Climate Change and Population Growth. *Science*, 289(5477):284–288, 2000.

[103] B. W. Webb, D. M. Hannah, R. D. Moore, L. E. Brown, and F. Nobilis. Recent advances in stream and river temperature research. *Hydrological Processes*, 22(7):902–918, 2008.

[104] F. C. S. Weiland, L. P. H. van Beek, J. C. J. Kwadijk, and M. F. P. Bierkens. Global patterns of change in discharge regimes for 2100. *Hydrology and Earth System Sciences*, 16(4):1047–1062, 2012.

[105] E. Wolanski. *Estuarine ecohydrology*. Elsevier, 2007.

[106] C. Wood and G. E. McManus. *Atlas of Newfoundland and Labrador*. Breakwater Books Ltd., 1991.

[107] I. Yashayaev. Hydrographic changes in the Labrador Sea, 1960-2005. *Progress in Oceanography*, 73(3):242–276, 2007.

[108] I. Yashayaev and A. Clarke. Recent warming of the Labrador Sea. *AZMP Bulletin PMZA*, 5:12–20, 2006.

[109] S. Yue, P. Pilon, and G. Cavadias. Power of the mann–kendall and spearman's rho tests for detecting monotonic trends in hydrological series. *Journal of hydrology*, 259(1):254–271, 2002.

[110] S. Yue and C. Y. Wang. Applicability of prewhitening to eliminate the influence of serial correlation on the mann-kendall test. *Water Resources Research*, 38(6), 2002.

[111] P. Zhai, X. Zhang, H. Wan, and X. Pan. Trends in total precipitation and frequency of daily precipitation extremes over china. *Journal of Climate*, 18(7):1096–1108, 2005.

[112] X. Zhang, W. D. Hogg, and É. Mekis. Spatial and temporal characteristics of heavy precipitation events over canada. *Journal of Climate*, 14(9):1923–1936, 2001.

[113] J. Zhu and E. Demirov. On the mechanism of interannual variability of the Irminger Water in the Labrador Sea. *Journal of Geophysical Research: Oceans*, 116(C3), 2011.

Appendix A

Seasonal variations in interannual anomalies of temperature

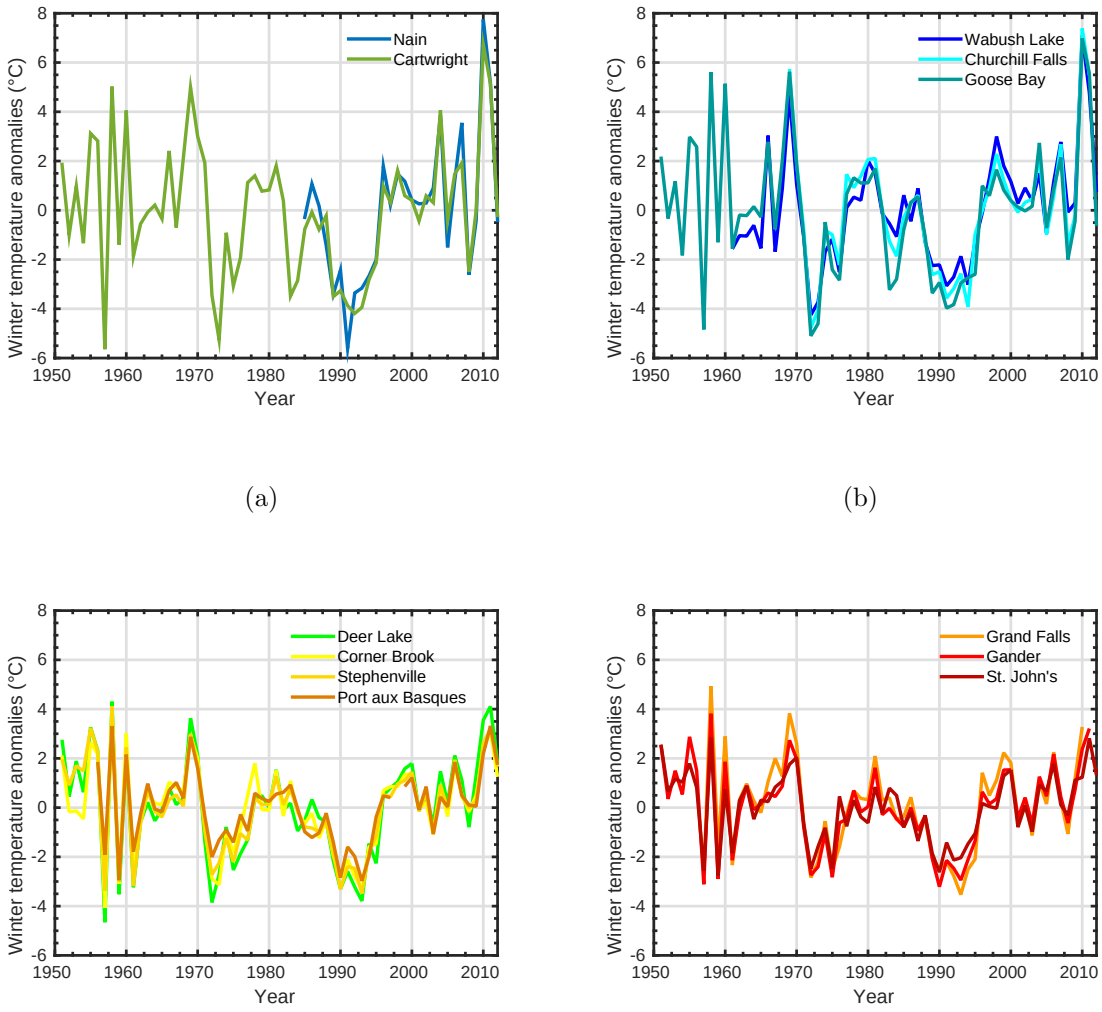

Figure A.1: Interannual anomalies of **winter** mean temperature in (a) Northern and Coastal Labrador; (b) Interior Labrador; (c) West Newfoundland zone; (d) East Newfoundland

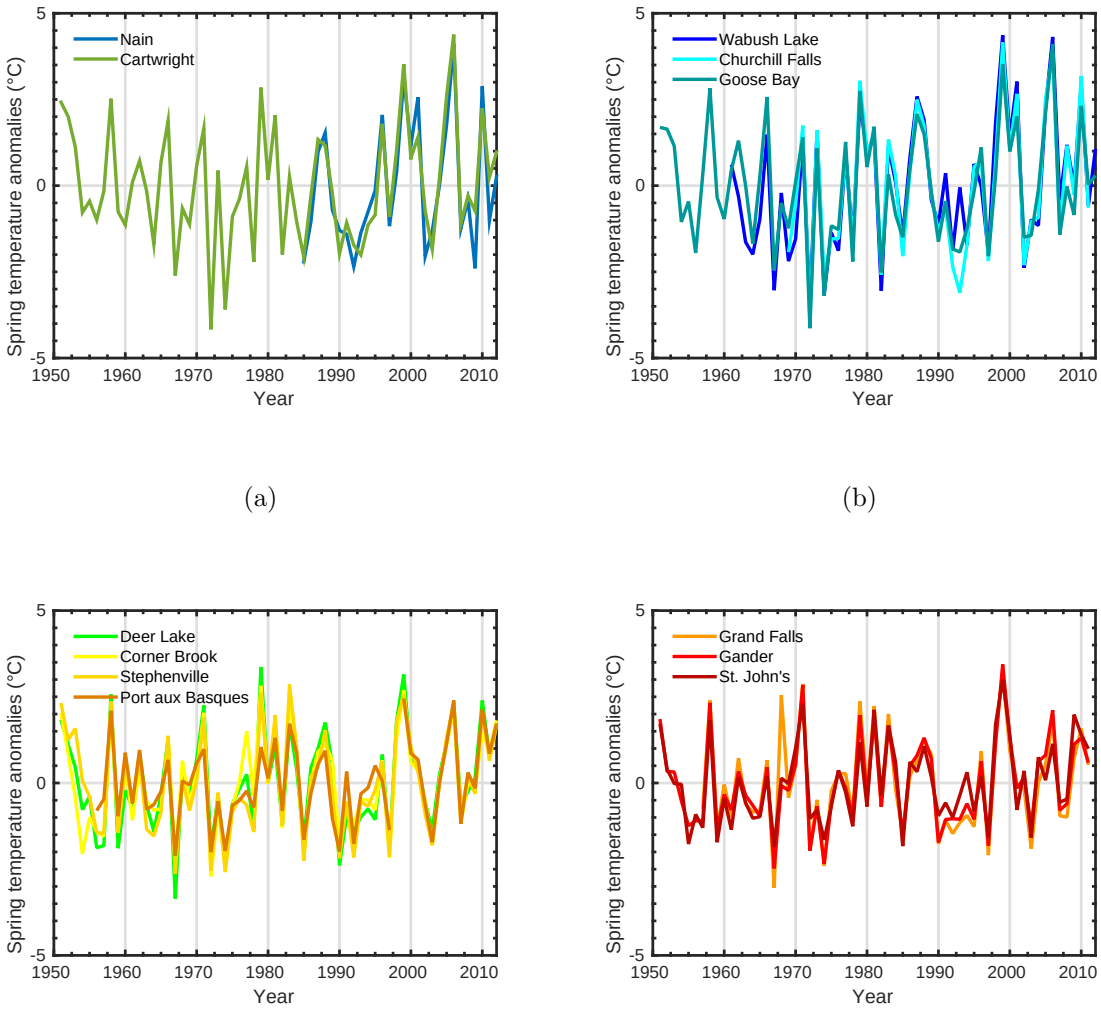

(a) (b)

(c) (d)

Figure A.2: Interannual anomalies of **spring** mean temperature in (a) Northern and Coastal Labrador; (b) Interior Labrador; (c) West Newfoundland zone; (d) East Newfoundland

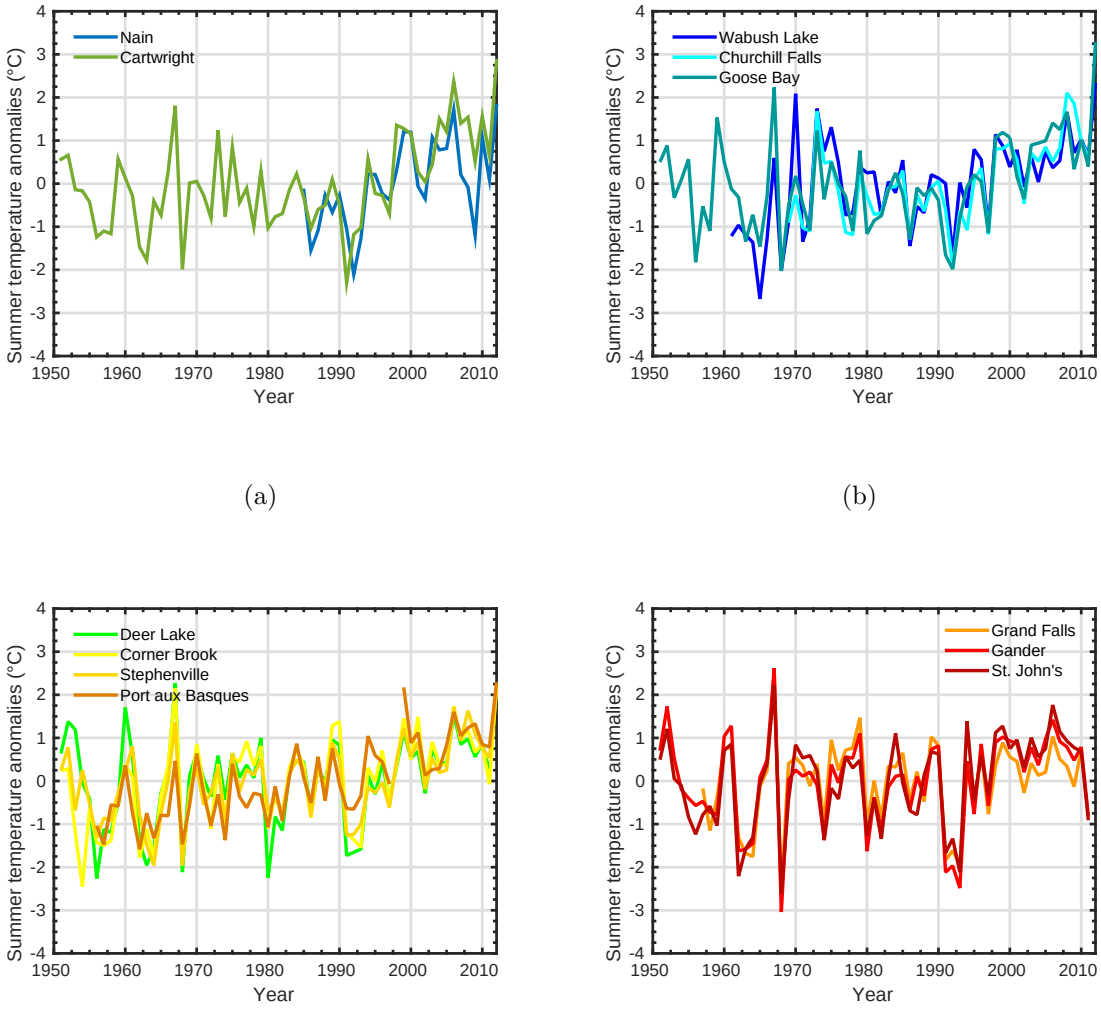

(a) (b)

(c) (d)

Figure A.3: Interannual anomalies of **summer** mean temperature in (a) Northern and Coastal Labrador; (b) Interior Labrador; (c) West Newfoundland zone; (d) East Newfoundland

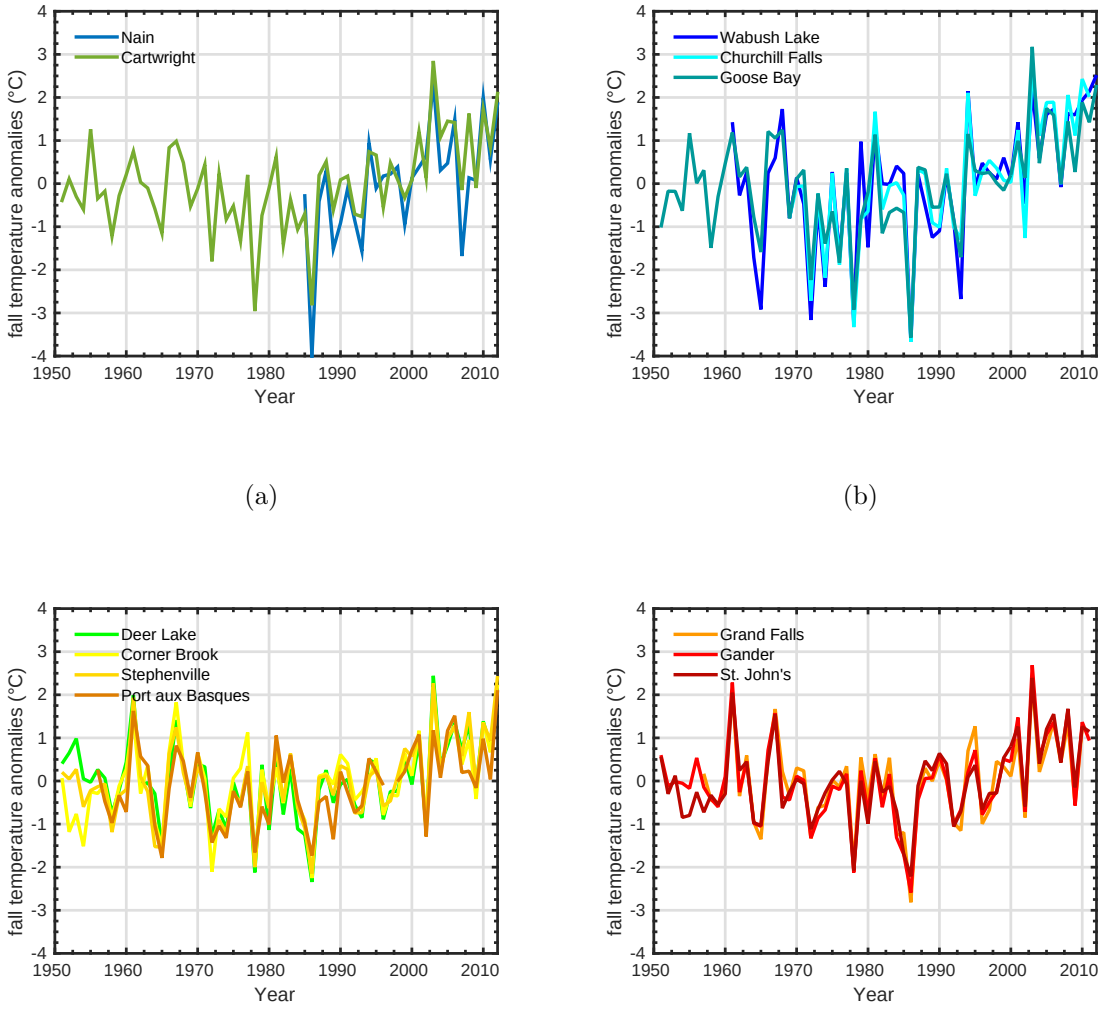

Figure A.4: Interannual anomalies of **autumn** mean temperature in (a) Northern and Coastal Labrador; (b) Interior Labrador; (c) West Newfoundland zone; (d) East Newfoundland

Appendix B

Seasonal variations in multidecadal temperature trends

Climate zone	**Station**	**H 73-92**	**Sen's slope 73-92**	**H 93-12**	**Sen's slope 93-12**
Tundra	Nain	—	—	0	0.1629
Coastal Labrador	Cartwright	0	-0.0768	0	0.1892
Interior Labrador	Goose Bay	0	-0.0657	0	0.1364
Interior Labrador	Churchill Falls	0	-0.0707	1	0.1984
Interior Labrador	Wabush Lake	0	-0.0185	0	0.1487
West Coast	Daniel's Harbour	0	-0.0683	0	0.1488
West Coast	Deer Lake	0	-0.0361	1	0.1612
West Coast	Corner Brook	0	-0.0915	1	0.1243
West Coast	Stephenville	0	-0.0456	1	0.1361
Northeast Coast	Grand Falls	0	-0.0844	1	0.1776
Northeast Coast	Gander	0	-0.0590	1	0.1358
Southwest coast & Avalon	Port aux Basques	0	-0.0593	1	0.1278
Southwest coast & Avalon	St. John's	0	-0.0505	1	0.1347

Table B.1: Trends in **winter** temperature anomalies for the periods 1973-1992 and 1993-2012. Winter season is considered here December-March. H_0 and Sen's slope are presented for each period. (If H_0=1, the null hypothesis is rejected; if H_0=0, there is not enough evidence to reject the null hypothesis). Sen's slope calculated at the 5% significance level.

Climate zone	**Station**	**H 73-92**	**Sen's slope 73-92**	**H 93-12**	**Sen's slope 93-12**
Tundra	Nain	—	—	0	0.0268
Coastal Labrador	Cartwright	0	-0.0083	0	0.0626
Interior Labrador	Goose Bay	0	0.0024	0	0.0647
Interior Labrador	Churchill Falls	0	-0.0324	0	0.0791
Interior Labrador	Wabush Lake	0	0.0363	0	0.0696
West Coast	Daniel's Harbour	0	0.0398	0	0.0632
West Coast	Deer Lake	0	0.0514	0	0.0678
West Coast	Corner Brook	0	0.0402	0	0.0764
West Coast	Stephenville	0	0.0373	0	0.0601
Northeast Coast	Grand Falls	0	0.0383	0	0.0776
Northeast Coast	Gander	0	0.0685	0	0.0761
South Coast & Avalon	Port aux Basques	0	0.0437	0	0.0762
South Coast &	St. John's	0	0.0517	0	0.0590

Table B.2: Trends in **spring** temperature anomalies for the periods 1973-1992 and 1993-2012. Spring season is considered here April-May. H_0 and Sen's slope are presented for each period. (If H_0=1, the null hypothesis is rejected; if H_0=0, there is not enough evidence to reject the null hypothesis).Sen's slope calculated at the 5% significance level.

Climate zone	**Station**	**H 73-92**	**Sen's slope 73-92**	**H 93-12**	**Sen's slope 93-12**
Tundra	Nain	—	—	0	0.0502
Coastal Labrador	Cartwright	0	-0.0517	1	0.1017
Interior Labrador	Goose Bay	1	-0.0741	1	0.1001
Interior Labrador	Churchill Falls	0	-0.0552	1	0.0880
Interior Labrador	Wabush Lake	1	-0.0851	0	0.0592
West Coast	Daniel's Harbour	0	-0.0242	0	0.0401
West Coast	Deer Lake	0	-0.0203	1	0.0557
West Coast	Corner Brook	0	-0.0161	1	0.0664
West Coast	Stephenville	0	-0.0145	1	0.0986
Central Newfoundland	Grand Falls	0	-0.0480	0	0.0303
Central Newfoundland	Gander	0	-0.0241	0	0.0171
South Coast & Avalon	Port aux Basques	0	-0.0516	0	0.0592
South Coast & Avalon	St. John's	0	-0.0165	0	0.0173

Table B.3: Trends in **summer** temperature anomalies for the periods 1973-1992 and 1993-2012. Summer season is considered here June-August. H_0 and Sen's slope are presented for each period. (If H_0=1, the null hypothesis is rejected; if H_0=0, there is not enough evidence to reject the null hypothesis).Sen's slope calculated at the 5% significance level.

Climate zone	**Station**	**H 73-92**	**Sen's slope 73-92**	**H 93-12**	**Sen's slope 93-12**
Tundra	Nain	—	—	0	0.0597
Coastal Labrador	Cartwright	0	0.0174	1	0.0785
Interior Labrador	Goose Bay	0	0.0256	1	0.1066
Interior Labrador	Churchill Falls	0	0.0206	1	0.1315
Interior Labrador	Wabush Lake	0	-0.0031	1	0.1311
West Coast	Daniel's Harbour	0	0.0150	0	0.0588
West Coast	Deer Lake	0	0.0056	1	0.0802
West Coast	Corner Brook	0	0.0140	1	0.0805
West Coast	Stephenville	0	0.0341	1	0.1033
Northeast Coast	Grand Falls	0	0.0163	0	0.0659
Northeast Coast	Gander	0	0.0159	1	0.0892
South Coast & Avalon	Port aux Basques	0	0.0185	0	0.0313
South Coast & Avalon	St. John's	0	0.0235	1	0.1008

Table B.4: Trends in **autumn** temperature anomalies for the periods 1973-1992 and 1993-2012. Autumn season is considered here September-November. H_0 and Sen's slope are presented for each period. (If H_0=1, the null hypothesis is rejected; if H_0=0, there is not enough evidence to reject the null hypothesis). Sen's slope calculated at the 5% significance level.

Appendix C

Variations in extreme temperature and precipitation

The extreme characteristics of precipitation

Figures C.5,C.6 depict the $90th$ percentiles of total precipitation, rain and snow.

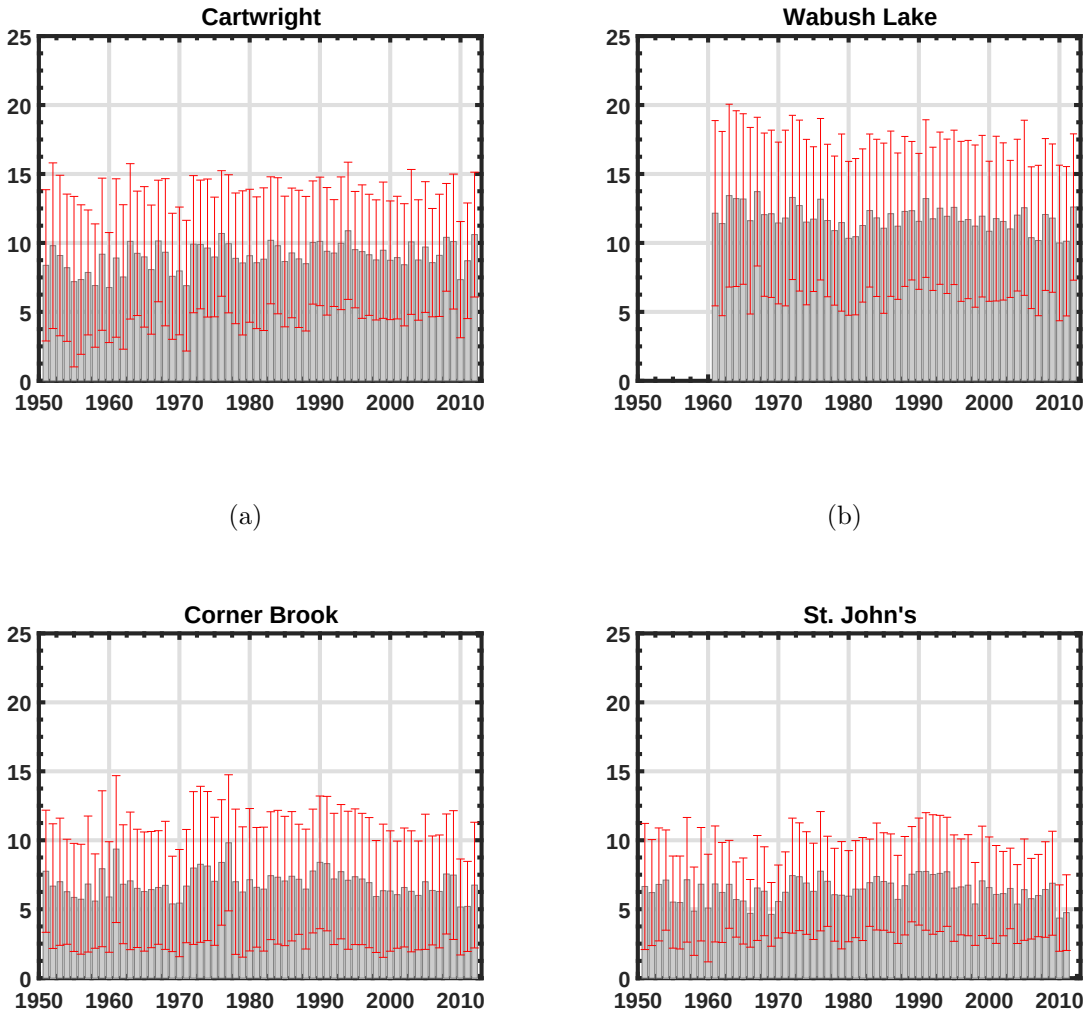

(a) (b)

(c) (d)

Figure C.1: Diurnal ranges of temperature in (a) Northern and Coastal Labrador; (b) Interior Labrador; (c) West Newfoundland zone; (d) East Newfoundland

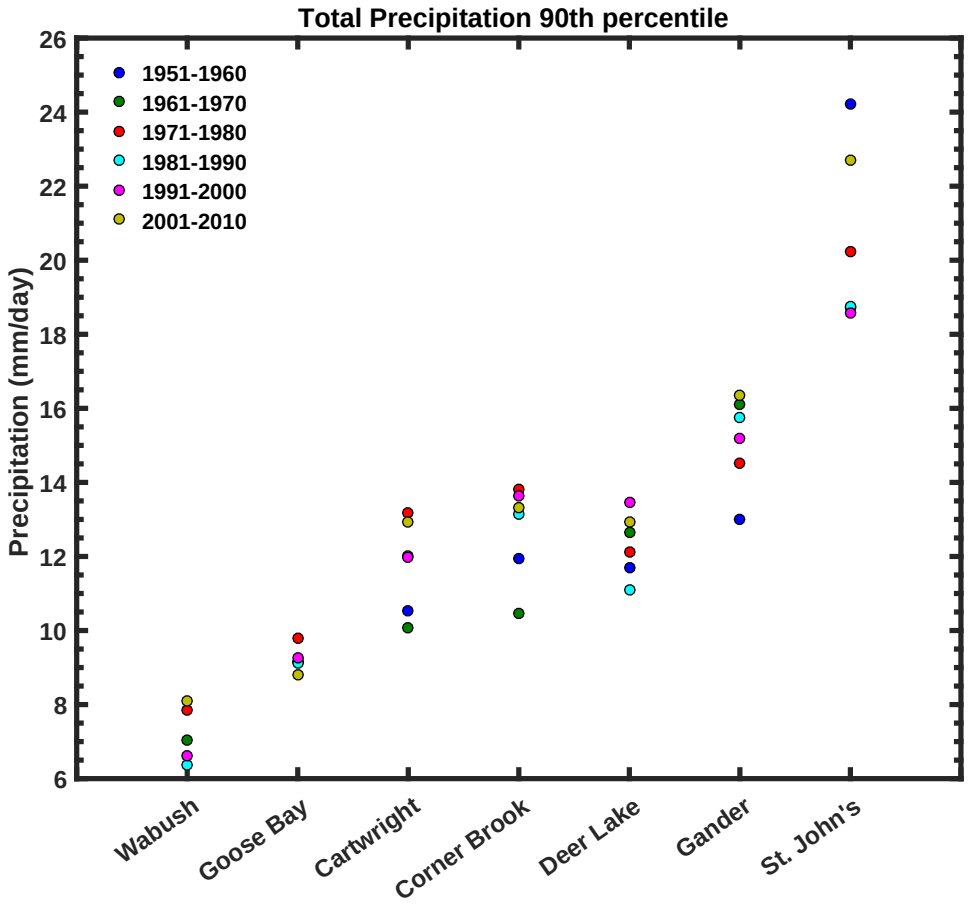

Figure C.2: Regional upper threshold for precipitation for each period and station, calculated as the $90th$ percentile, for total daily precipitation.

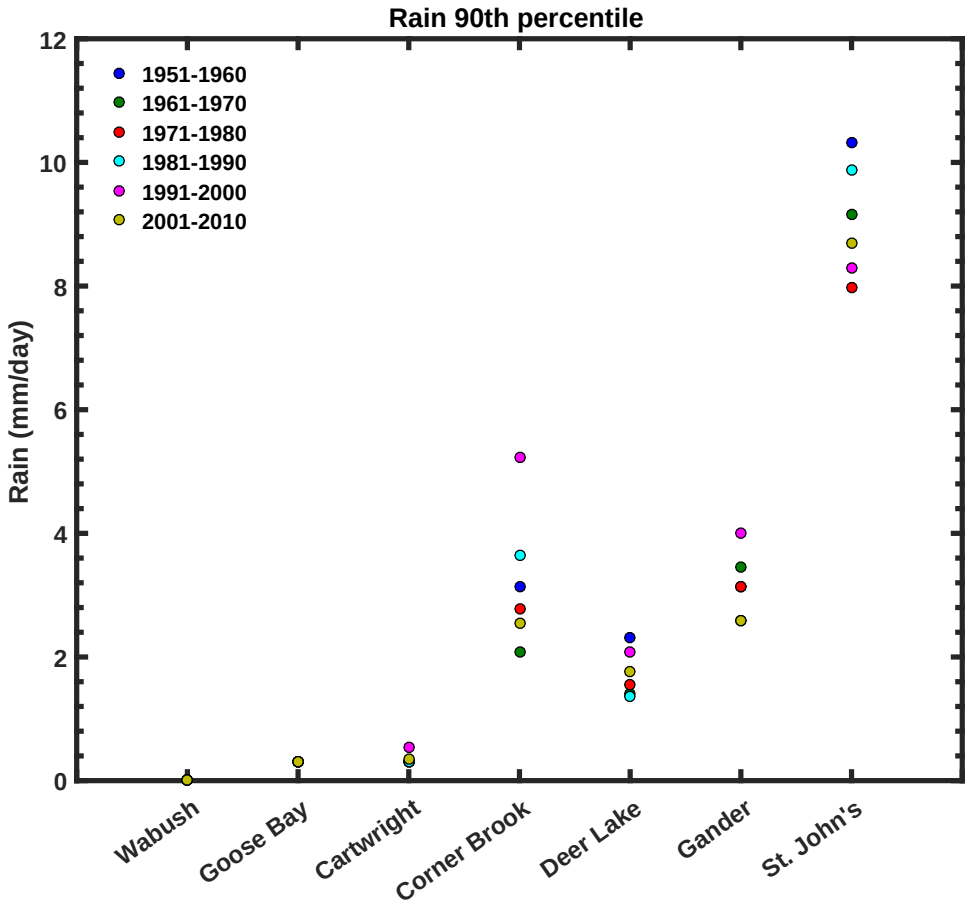

Figure C.3: Regional upper threshold for precipitation for each period and station, calculated as the $90th$ percentile, for daily rain.

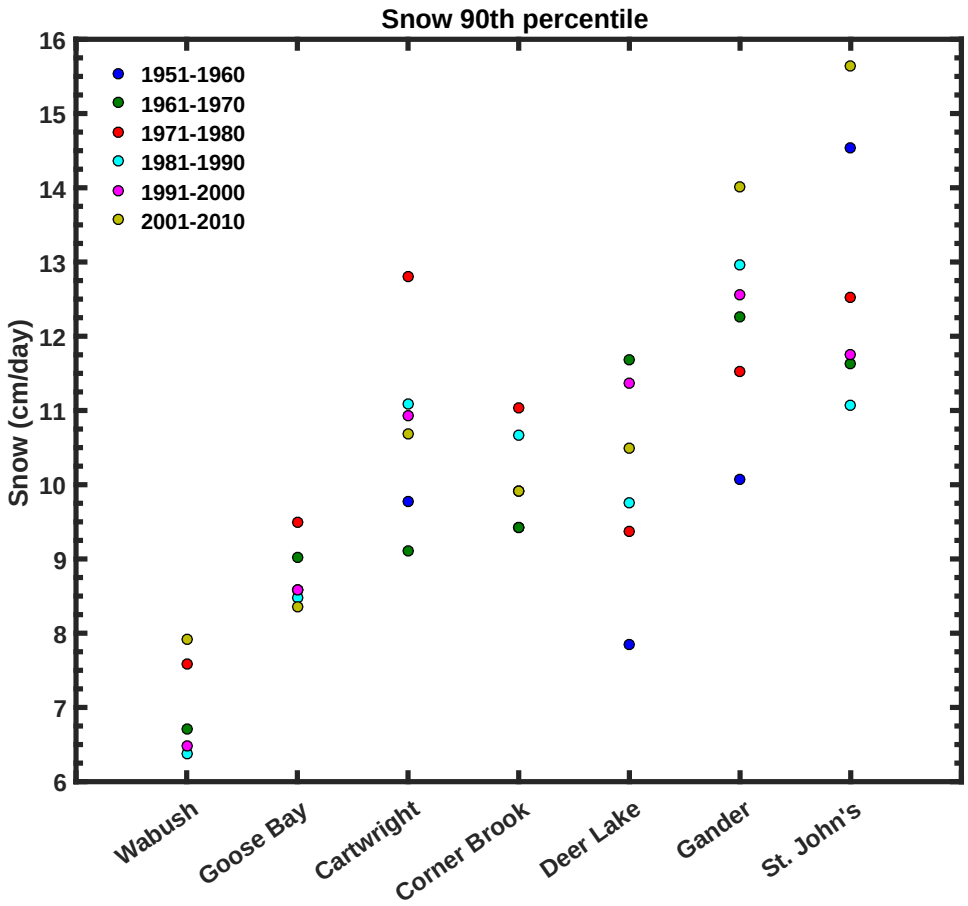

Figure C.4: Regional upper threshold for precipitation for each period and station, calculated as the $90th$ percentile, for daily snow.

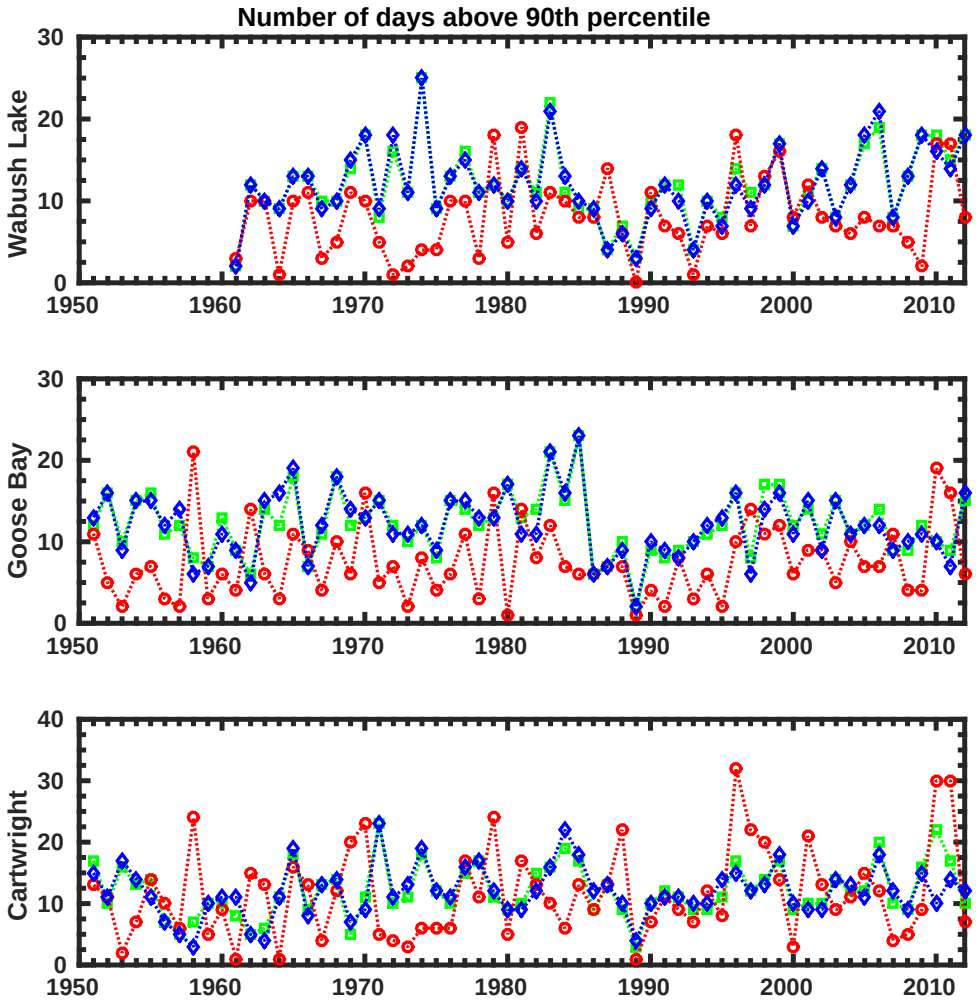

Figure C.5: Number of annual extreme precipitation events in Labrador. Total precipitation is depicted in green, rain is in red and blue represents snow.

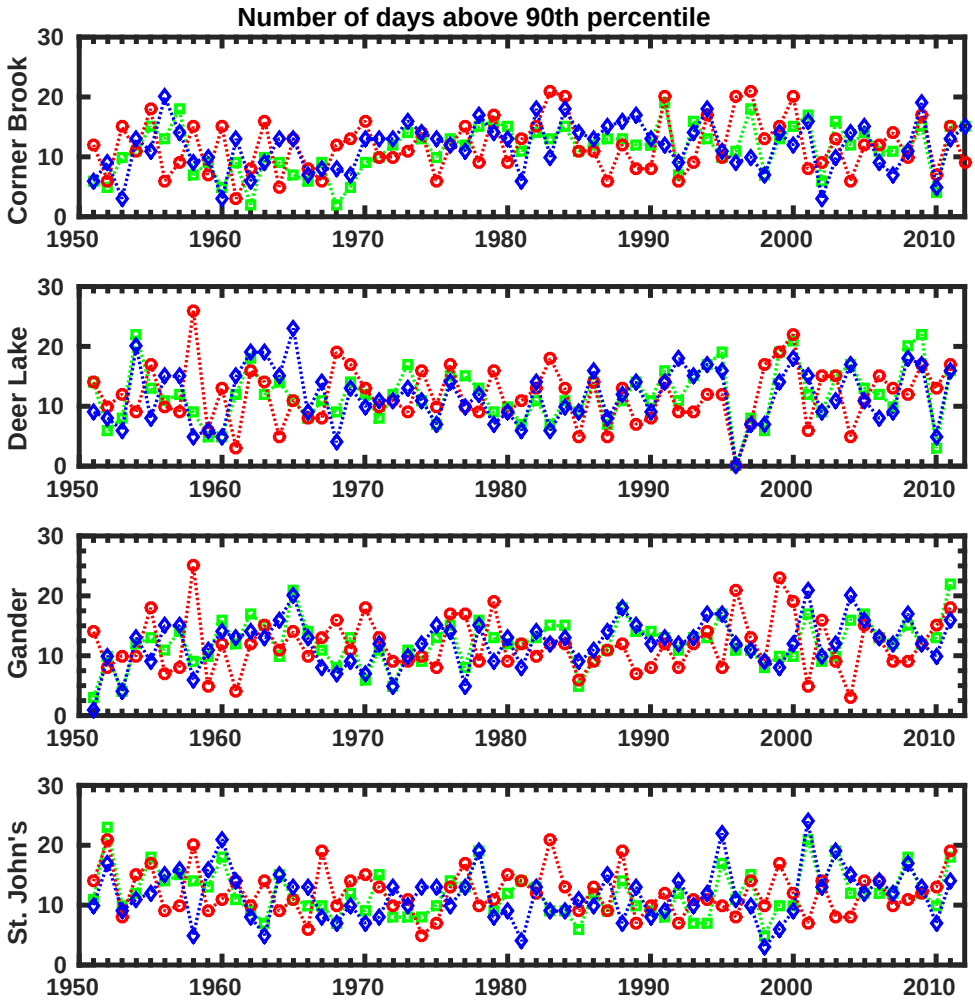

Figure C.6: Number of annual extreme precipitation events in Newfoundland. Total precipitation is depicted in green, rain is in red and blue represents snow.

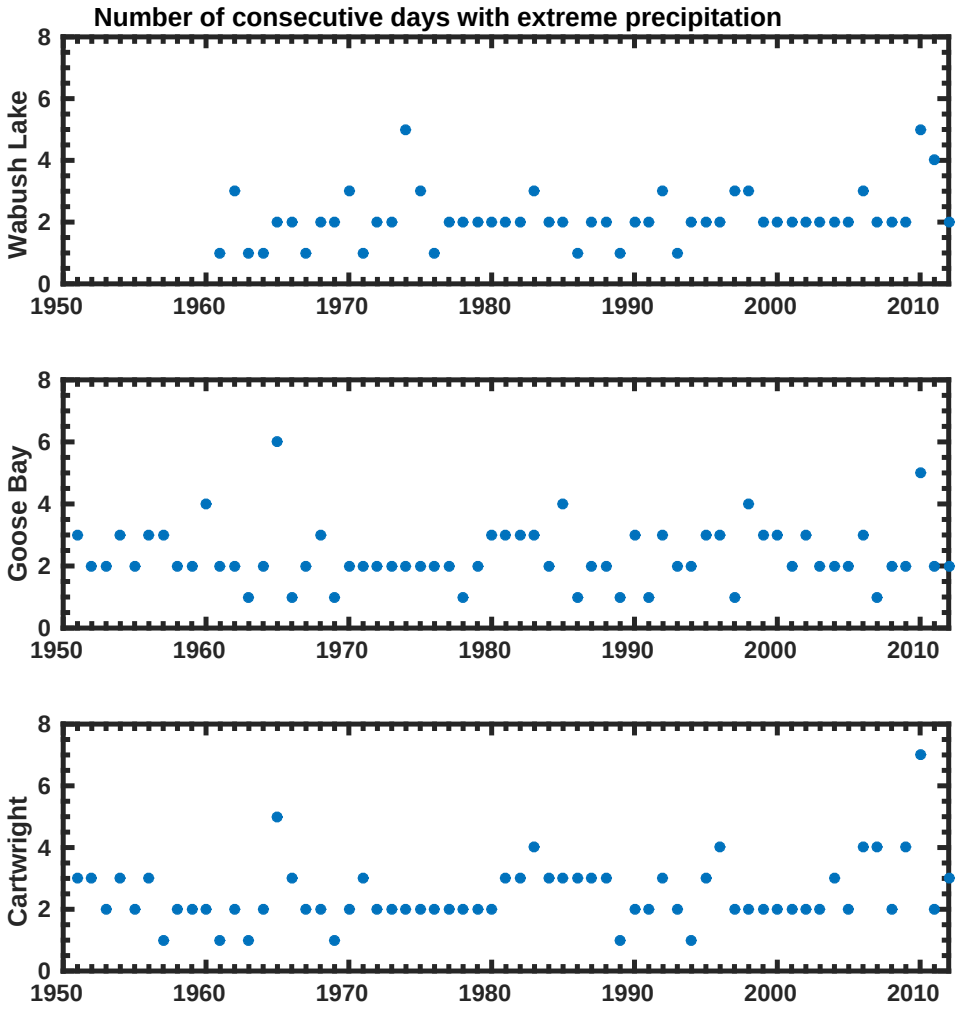

Figure C.7: Annual number of consecutive days with extreme precipitation (over 90th percentile) in Labrador

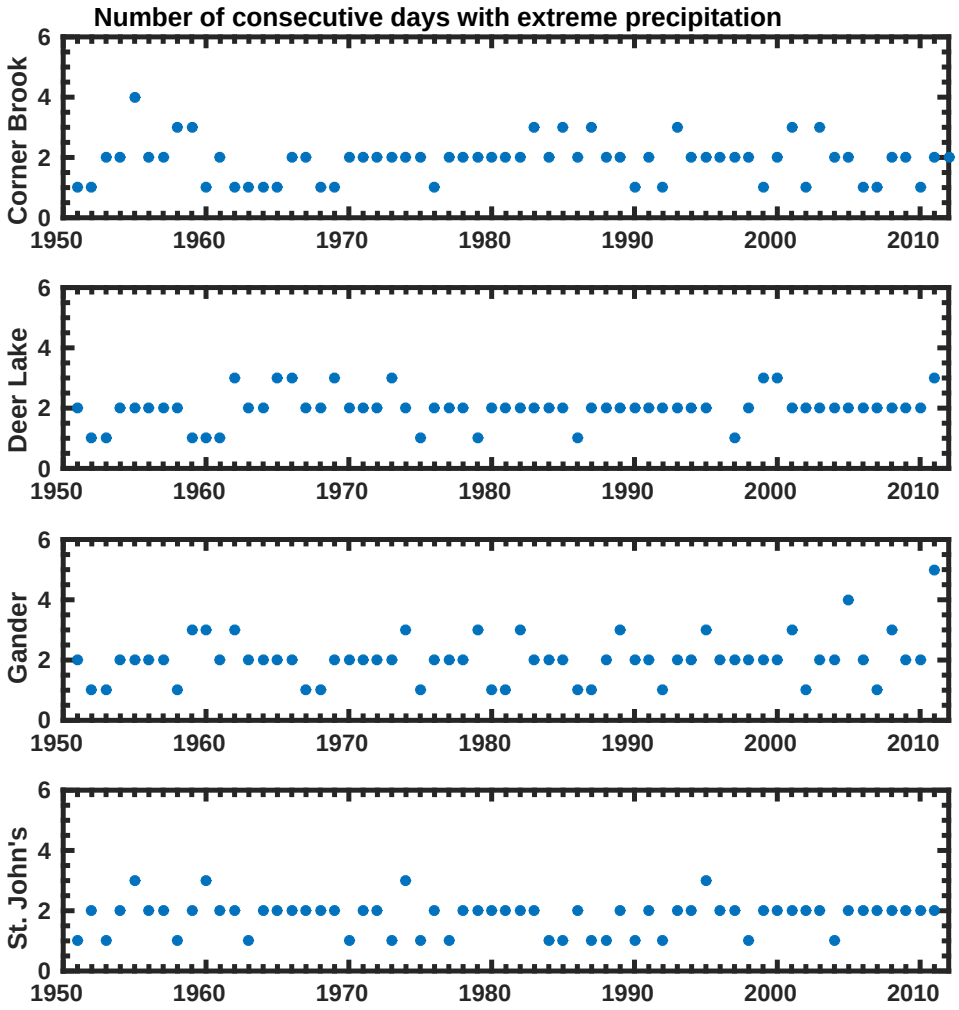

Figure C.8: Annual number of consecutive days with extreme precipitation (over 90th percentile) in Newfoundland

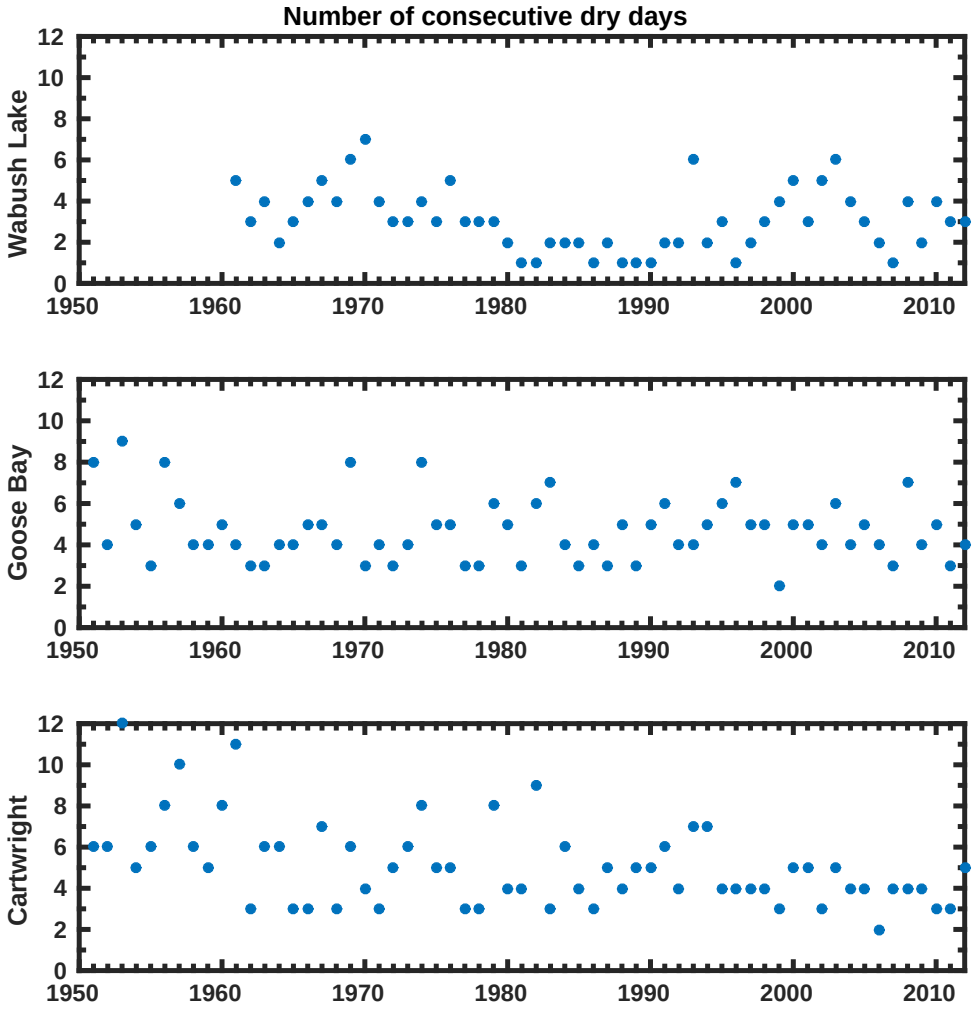

Figure C.9: Annual number of consecutive days without precipitation in Labrador.

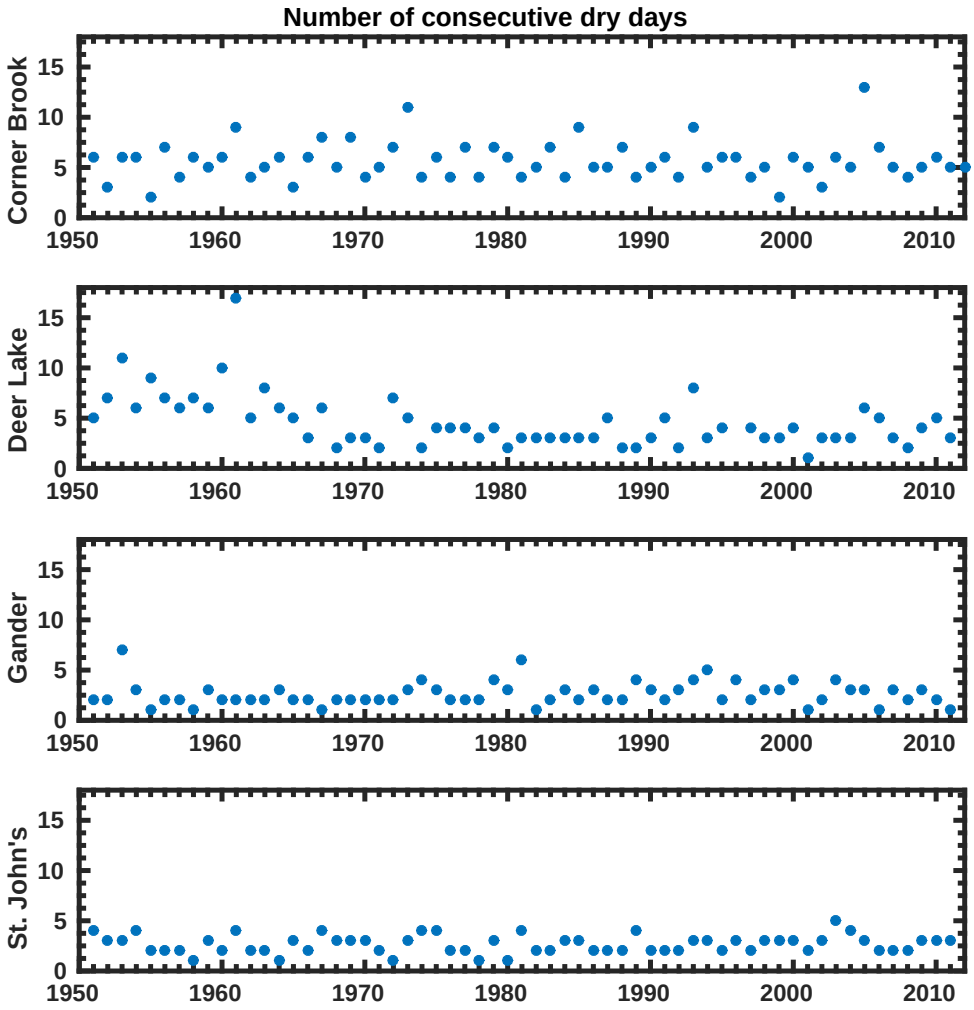

Figure C.10: Annual number of consecutive days without precipitation in Newfoundland

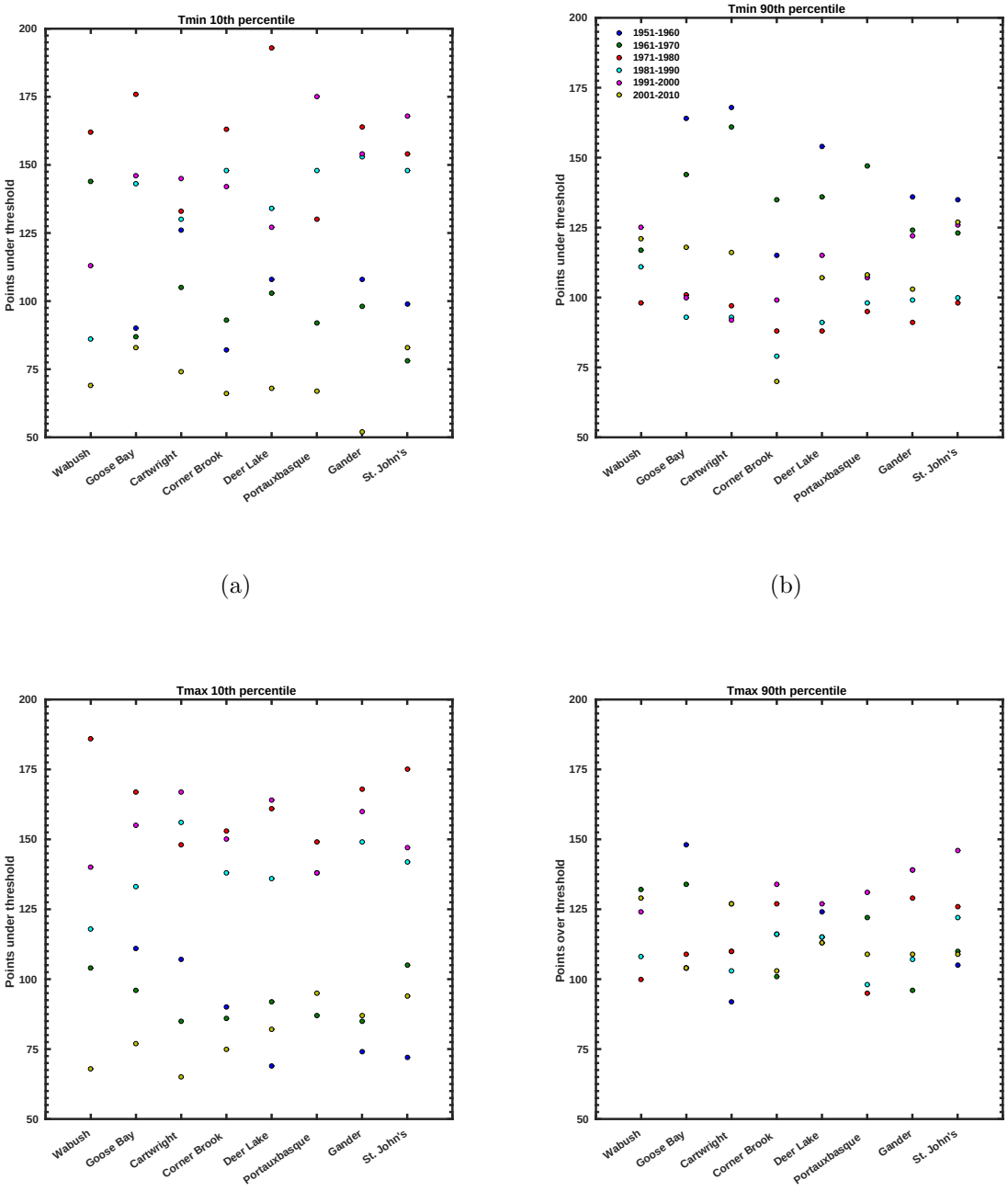

Figure C.11: Number of extreme cold temperature events in (a) minimum temperature and (c) maximum temperature, and extreme warm temperature events in (b) minimum temperature and (d) maximum temperature in each station and decade. Upper and lower thresholds are calculated as the 90th and 10th percentiles, respectively.

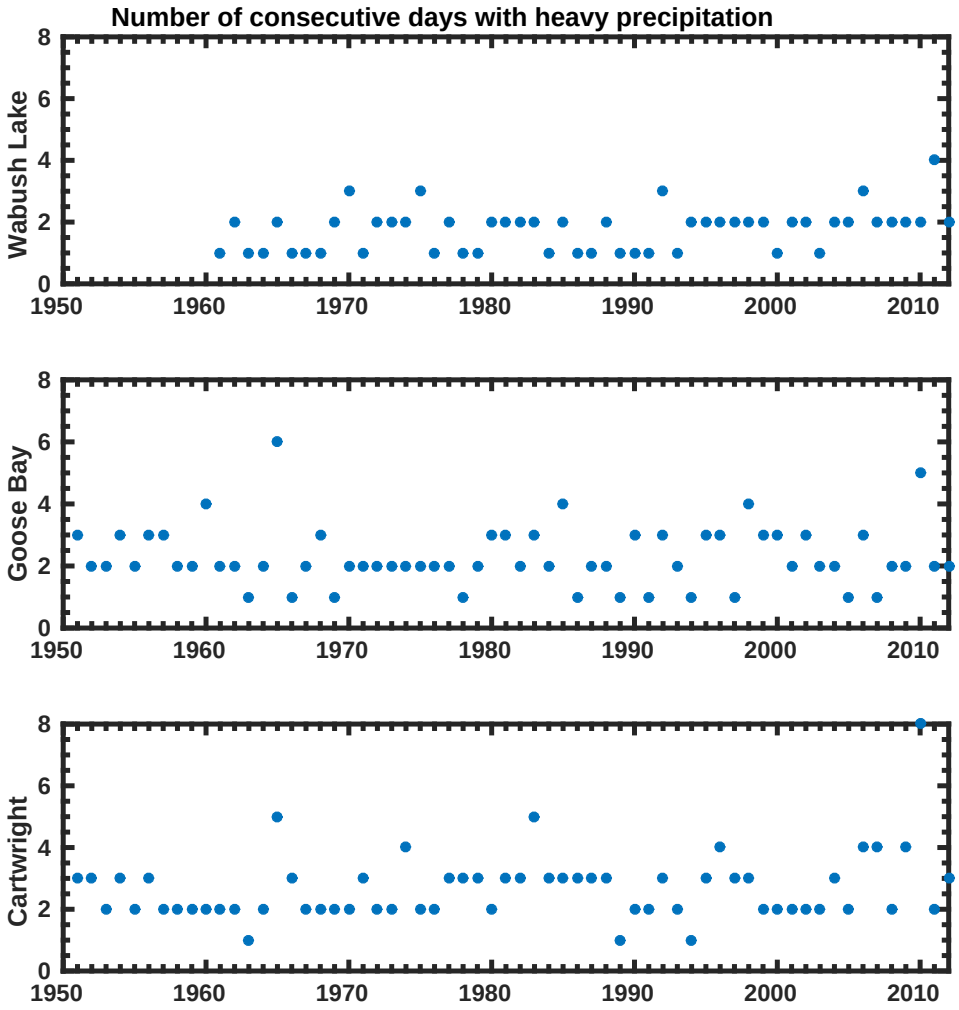

Figure C.12: Annual number of consecutive days with total precipitation over 10mm in Labrador

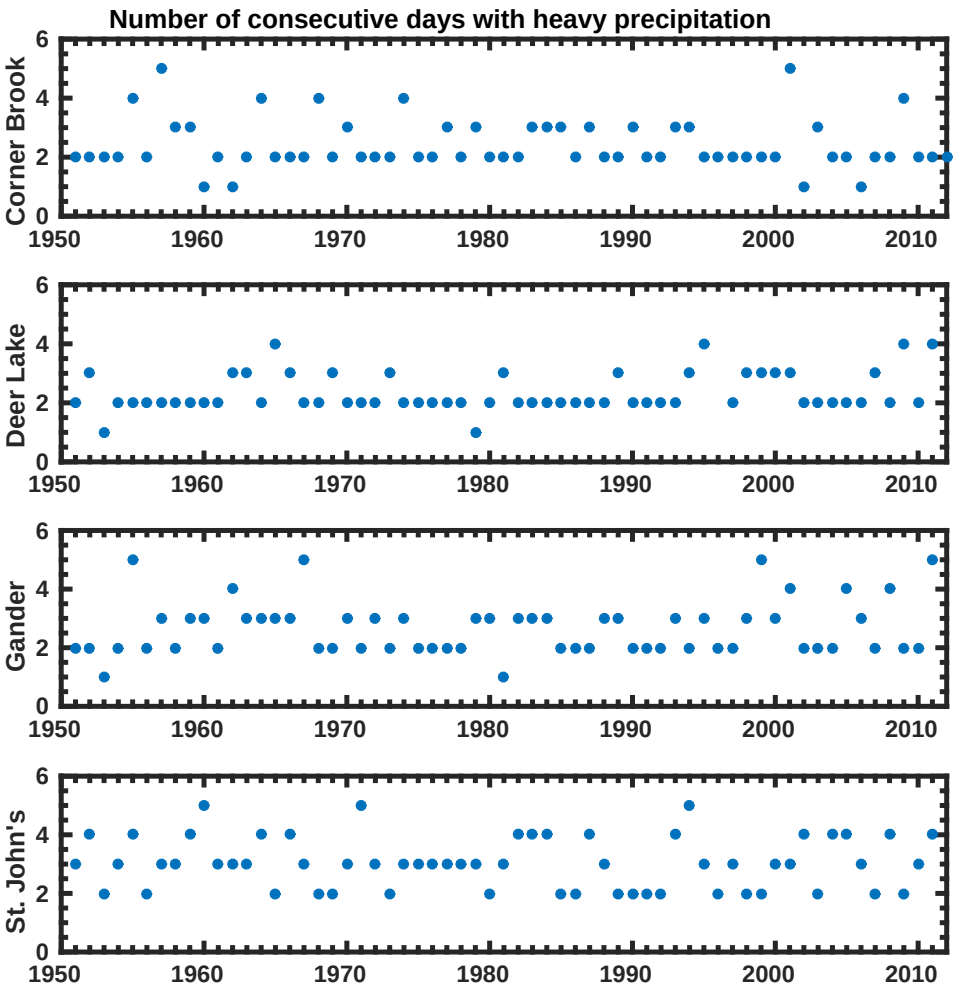

Figure C.13: Annual number of consecutive days with total precipitation over 10mm in Newfoundland